Measurement of $t\bar{t}$ multi-differential cross sections in dilepton channel at 13 TeV and extraction of m_t^{pole}, α_s, and PDF constraints [TOP-18-004 approval]

Olaf Behnke, Mykola Savitskyi, Oleksandr Zenaiev
(DESY)

TOP PAG meeting
13.11.2018

Introduction

- Measurements of $t\bar{t}$ production provide precision tests of pQCD:
  - $t\bar{t}$ cross sections can be used to extract PDFs: constrain high-x gluon
  - constrain fundamental SM parameters: α_s, m_t^{pole}
- Goal of this analysis: measure multi-differential $t\bar{t}$ cross sections
  - e.g. for PDFs 2D $t\bar{t}$ cross sections $M(t\bar{t})$ vs $y(t\bar{t})$ provide more information than total and single-differential cross sections: at LO $x_{1,2} = (M(t\bar{t})/\sqrt{s})\exp\left[\pm y(t\bar{t})\right]$
- 1st QCD analysis of 2D $t\bar{t}$ data done in CMS with 8 TeV data: TOP-14-013 [EPJ C77 (2017) 459]

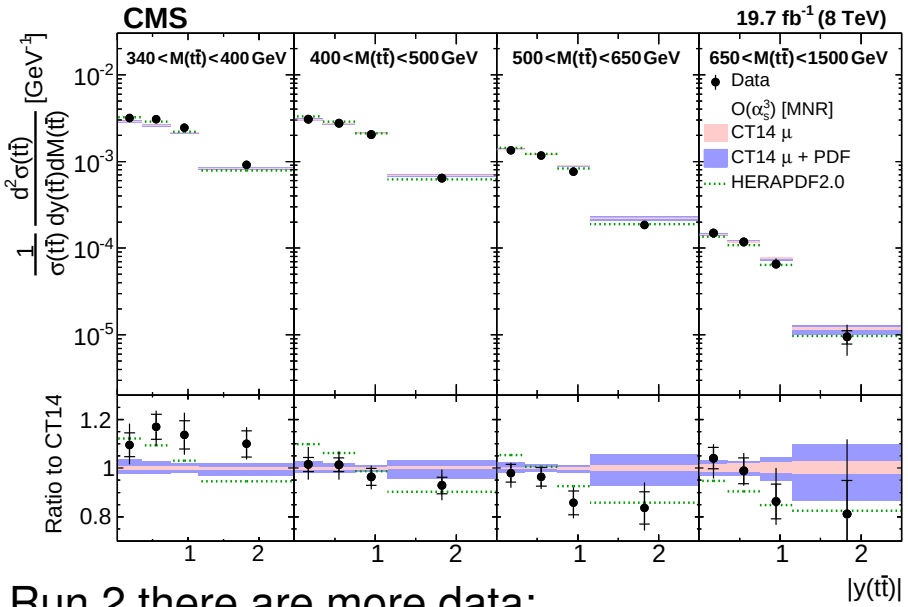

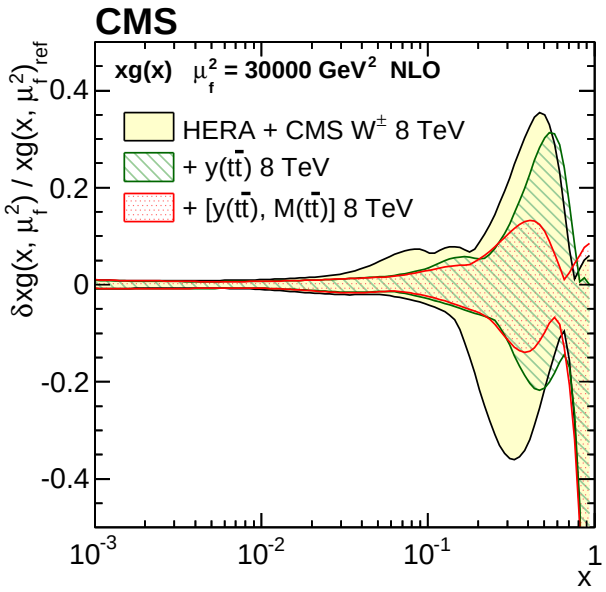

- In Run 2 there are more data:
  - more precise measurements can be done
  - multi-differential cross sections can be measured, e.g. $M(t\bar{t})$ vs $y(t\bar{t})$ in bins of extra jet multiplicity (N_{jet}) are additionally sensitive to α_S
  - for first time, sensitivity of $M(t\bar{t})$ to m_t^{pole} is exploited $\rightarrow$ simultan. PDF+α_s +m_t^{pole} fit

Measured cross sections

- normalised 2D cross sections as in TOP-14-013:
  [parton level]
  (1) $[p_T(t), y(t)]$
  (2) $[M(t\bar{t}), y(t)]$
  (3) $[M(t\bar{t}), y(t\bar{t})]$
  (4) $[M(t\bar{t}), \Delta\eta(t, \bar{t})]$
  (5) $[M(t\bar{t}), \Delta\phi(t, \bar{t})]$
  (6) $[M(t\bar{t}), p_T(t\bar{t})]$
  (7) $[M(t\bar{t}), p_T(t)]$ (not in TOP-14-013, but this one is interesting for NNLO)
  $\rightarrow$ compare them to MC predictions
  $\rightarrow$ keep reference to what was measured in Run-I
  $\rightarrow$ to facilitate comparison with upcoming NNLO calculations for 2D (theorists promised NNLO predictions soon)
- normalised 3D cross sections:
  [particle level + derived corrections particle$\rightarrow$parton level]
  (1) $[N_{\text{jet}}, M(t\bar{t}), y(t\bar{t})]$, 2 and 3 N_{jet} bins (maximum 48 bins measured)
  $\rightarrow$ compare to MC predictions
  $\rightarrow$ compare to NLO predictions with different PDFs, α_S, m_t^{pole}
  $\rightarrow$ extract PDFs, α_S, m_t^{pole}

Logistics

- CADI: TOP-18-004
- Documentation:
  - paper draft: TOP-18-004 (v8) Nov 4 (style of plots in this talk is updated compared to paper at CADI)
  - analysis note: AN-18-043 (v16)
- Related analysis:
  - TOP-17-014 (1D cross sections): same event and object selection
  - TOP-14-013 (2D x-sections @ 8 TeV): similar QCD analysis
- Many thanks to ARC (Michael Henry Schmitt, Klaus Rabbertz, Jan Kieseler, Regina Demina) for very efficient review of analysis and help to improve documentation!
  - **no changes to the analysis,** apart from updating NLO fits with improved precision
  - updates to figures in paper
  - many extra information and checks in AN
- Many thanks to Hannes Jung for joining as CCLE!

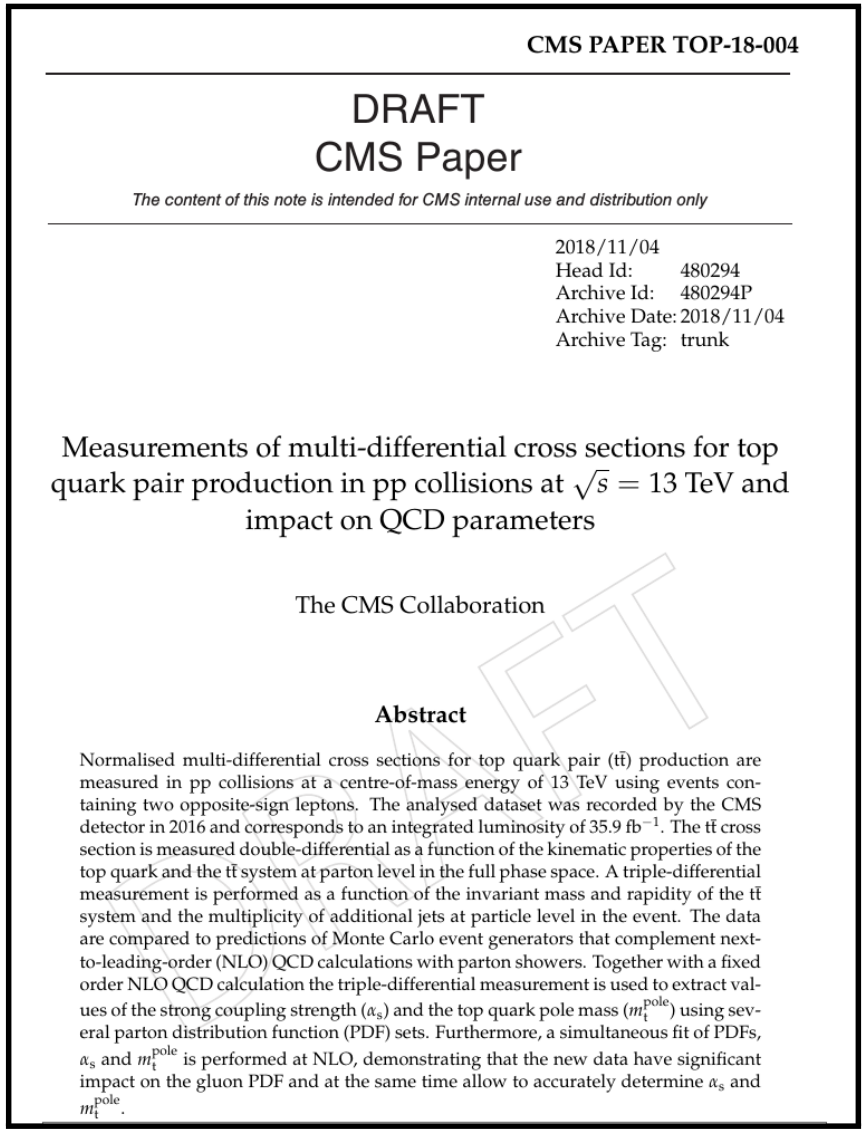

CMS PAPER TOP-18-004

DRAFT
CMS Paper

The content of this note is intended for CMS internal use and distribution only

2018/11/04
Head Id: 480294
Archive Id: 480294P
Archive Date: 2018/11/04
Archive Tag: trunk

Measurements of multi-differential cross sections for top quark pair production in pp collisions at $\sqrt{s} = 13$ TeV and impact on QCD parameters

The CMS Collaboration

Abstract

Normalised multi-differential cross sections for top quark pair ($\mathrm{t\bar{t}}$) production are measured in pp collisions at a centre-of-mass energy of 13 TeV using events containing two opposite-sign leptons. The analysed dataset was recorded by the CMS detector in 2016 and corresponds to an integrated luminosity of 35.9 fb^{-1}. The $\mathrm{t\bar{t}}$ cross section is measured double-differential as a function of the kinematic properties of the top quark and the $\mathrm{t\bar{t}}$ system at parton level in the full phase space. A triple-differential measurement is performed as a function of the invariant mass and rapidity of the $\mathrm{t\bar{t}}$ system and the multiplicity of additional jets at particle level in the event. The data are compared to predictions of Monte Carlo event generators that complement next-to-leading-order (NLO) QCD calculations with parton showers. Together with a fixed order NLO QCD calculation the triple-differential measurement is used to extract values of the strong coupling strength (α_s) and the top quark pole mass ($m_\mathrm{t}^\mathrm{pole}$) using several parton distribution function (PDF) sets. Furthermore, a simultaneous fit of PDFs, α_s and $m_\mathrm{t}^\mathrm{pole}$ is performed at NLO, demonstrating that the new data have significant impact on the gluon PDF and at the same time allow to accurately determine α_s and $m_\mathrm{t}^\mathrm{pole}$.

Analysis overview

1. Event selection (same as in 1D $t\bar{t}$ analysis)

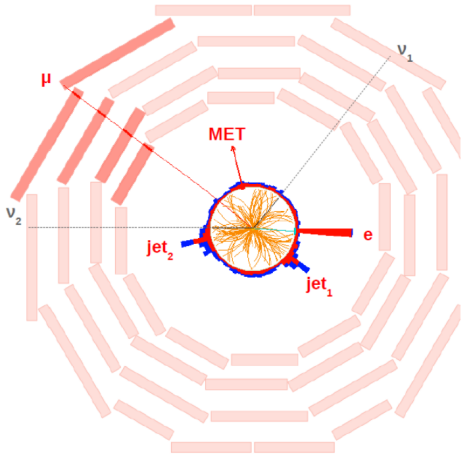

2. Kinematic reconstruction (same as in 1D $t\bar{t}$ analysis + loose)

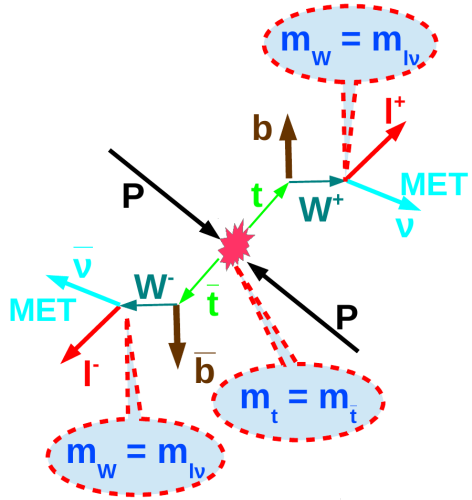

3. Unfolding and results

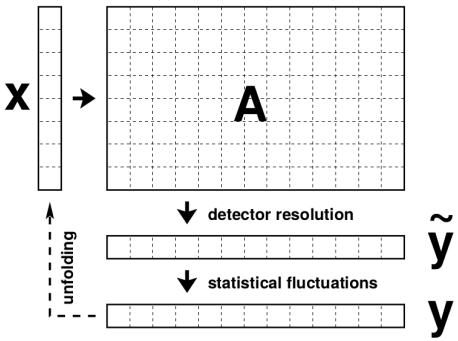

4. Data interpretation

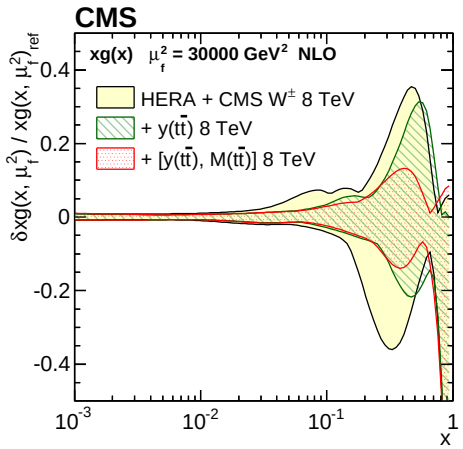

Analysis overview

1. Event selection (same as in 1D $t\bar{t}$ analysis)

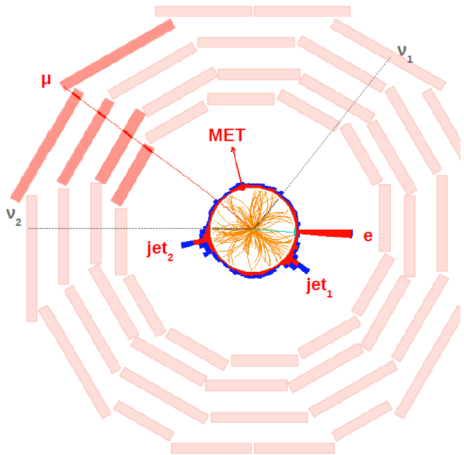

2. Kinematic reconstruction (same as in 1D $t\bar{t}$ analysis + loose)

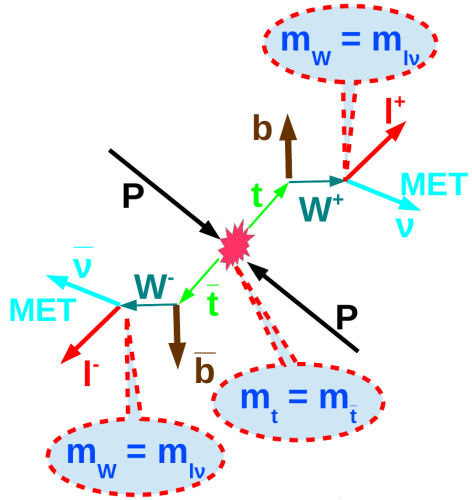

3. Unfolding and results

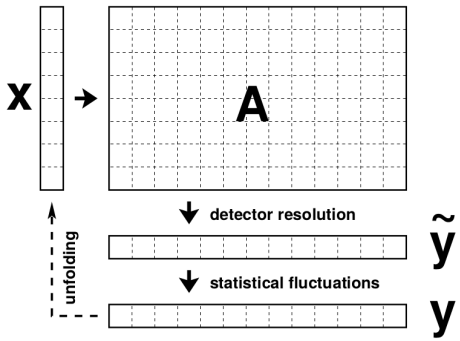

4. Data interpretation

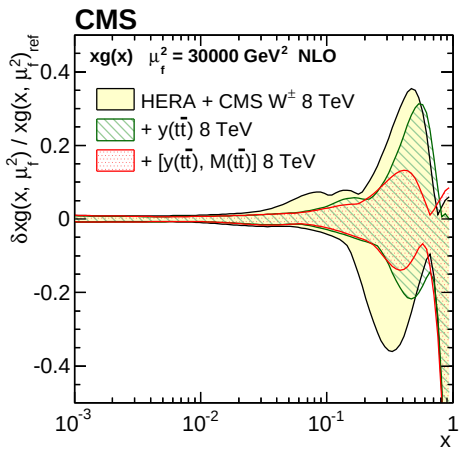

Data and MC samples

Data and MC following 1D analysis [TOP-17-014]:

- Run2016 B-H data, 35.9 fb^{-1} (Feb17 ReReco)
- Summer16 MC production for Moriond17:
  - signal sample ($t\bar{t}$):
    - ★ POWHEGv2+PYTHIA8 [CUETP8M2T4] + modelling systematic variations (each sample has $\sim$ 150M $\sim \times 5$ data statistics: extra samples were requested for this analysis to reduce statistical fluctuations in systematic uncertainties)
    - ★ for comparison with measured x-sections: POWHEGv2+HERWIG++ [EE5C]
    - ★ for comparison with measured x-sections: MG5_aMC@NLO(FXFX)+PYTHIA8
  - background samples:
    - ★ single t [POWHEGv1+PYTHIA8]
    - ★ Z+jets [MG5_aMC@NLO MLM]
    - ★ W+jets [MG5_aMC@NLO MLM]
    - ★ diboson [PYTHIA8]

Event selection

Event selection following 1D analysis [TOP-17-014]:

- $l^{\pm}l^{\mp}$, 2 jets:
  - combination of single- and dilepton triggers (details in backup)
  - leptons: $p_T(l) > 25(20)$ GeV, $|\eta(l)| < 2.4$ (cut based ID, tight isolat.), $M(ll) > 20$ GeV
  - ee, $\mu\mu$ channels: MET > 40 GeV, excluded $76 < M(ll) < 106$ GeV
  - jets: anti-kT $R = 0.4$ PF CHS, $p_T(\text{jet}) > 30$ GeV, $|\eta(\text{jet})| < 2.4$, $\Delta R(\text{jet}, l) > 0.4$, at least 1 b-tagged jet (CSVv2 loose WP)
  - solution of kinematic reconstruction (full or loose)
- Corrections and scale factors:
  - pileup reweighting: weights derived for $\sigma = 69.2$ mb using official tools
  - triggers: efficiencies derived using unprescaled MET triggers as in TOP-17-001, TOP-17-014 [described in AN-16-392]
  - lepton ID/ISO: official SFs from TopMUO, TopEGM applied
  - JES: official SFs applied [Summer16_23Sep2016 V4 for AK4PFchs]
  - JER: official SFs applied [Summer16_25nsV1_MC_SF_AK4PFchs.txt]
  - b-tagging: official SFs applied [CSVv2_Moriond17_B_H.csv, “mujets” for c and b, “incl” for light jets]

Analysis overview

1. Event selection (same as in 1D $t\bar{t}$ analysis)

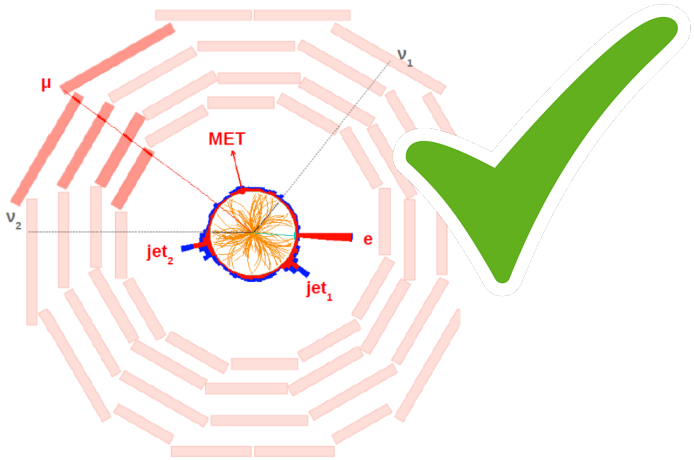

2. Kinematic reconstruction (same as in 1D $t\bar{t}$ analysis + loose)

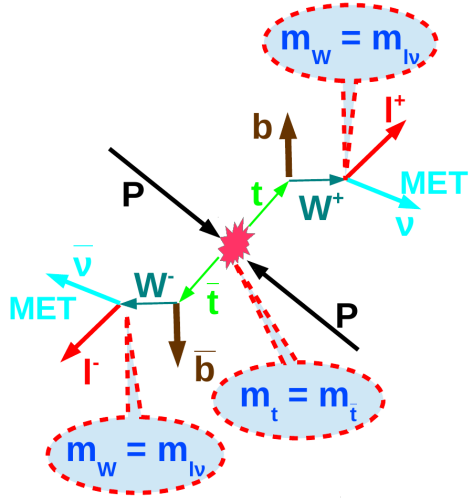

3. Unfolding and results

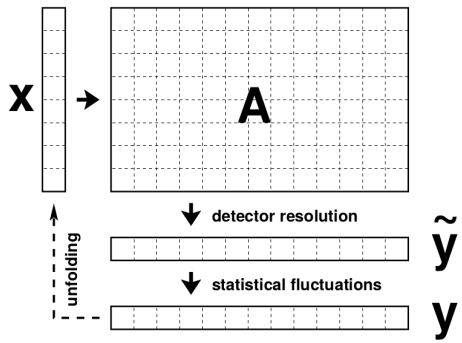

4. Data interpretation

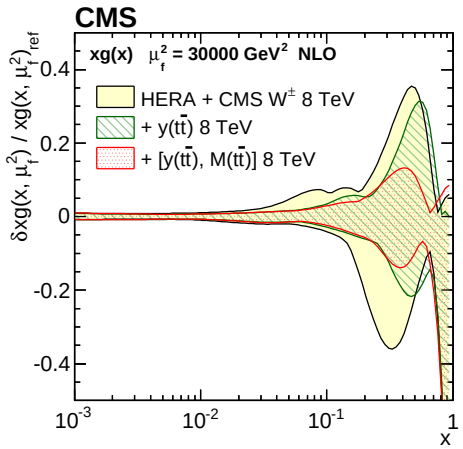

Kinematic reconstruction (KR)

Problem: reconstruct t, $\bar{t}$ from visible objects

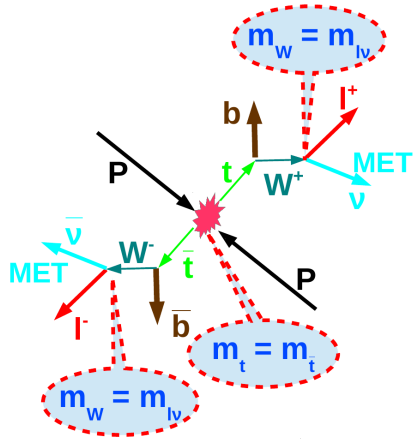

- Input for kinematic reconstruction: leptons, jets, MET
  - exactly two leptons in event, one MET: no ambiguity
  - ≥ 2 jets (at least one b tagged)
    - require $M(lb) < 180$ GeV
    - rank jets according to b tags
    - among equal b-tags, rank jets in p_T
- Full KR: use 6 constraints to find 6 unknowns by solving a system of equations
  - unknowns: momenta of ν (3), $\bar{\nu}$ (3)
  - constraints: MET (2), m_t (2), m_W (2)
  - recover all unknowns $\rightarrow$ recover t, $\bar{t}$
  - same method used in TOP-17-014 and earlier measurements
  - detector level $M(t\bar{t})$ distribution has low sensitivity to generator level m_t, but to m_t kinematic constraint:
    - significant dependence of unfolded $M(t\bar{t})$ on MC m_t
    - to avoid bias, loose KR is exploited for $[M(t\bar{t}), y(t\bar{t}), N_{\text{jet}}]$ used to extract m_t^{pole}
- Loose KR: recover $t\bar{t}$ only, no m_t constraint
  - $p_{x,y}(\nu\bar{\nu}) = \text{MET}_{x,y}$
  - $p_z(\nu\bar{\nu}) = p_z(l\bar{l})$, $E(\nu\bar{\nu}) = E(l\bar{l})$
  - require $M(\nu\bar{\nu}) \geq 0$, $M(l\bar{l}\nu\bar{\nu}) \geq 2M_W$ by adjusting $p_z(\nu\bar{\nu})$ and $E(\nu\bar{\nu})$: tiny effect

Control plots, after full KR

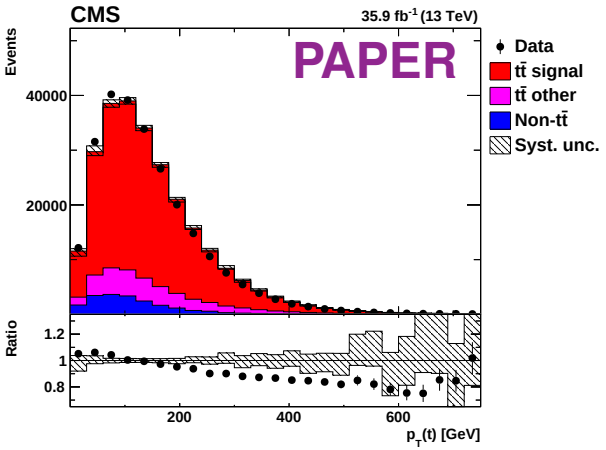

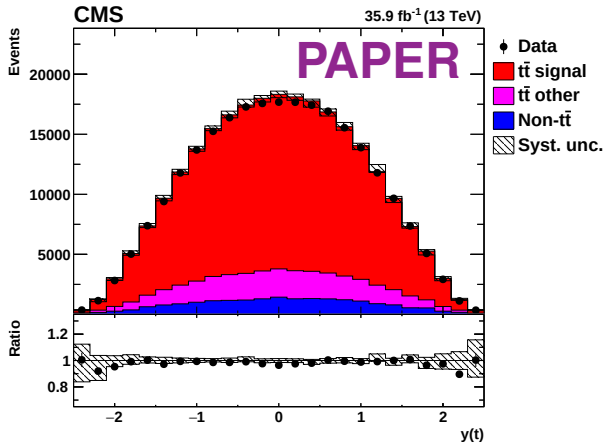

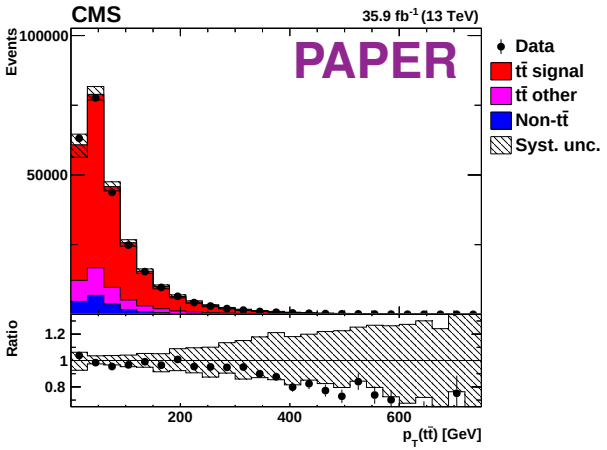

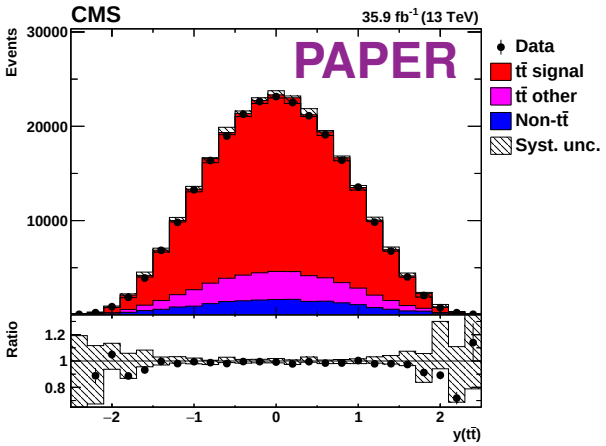

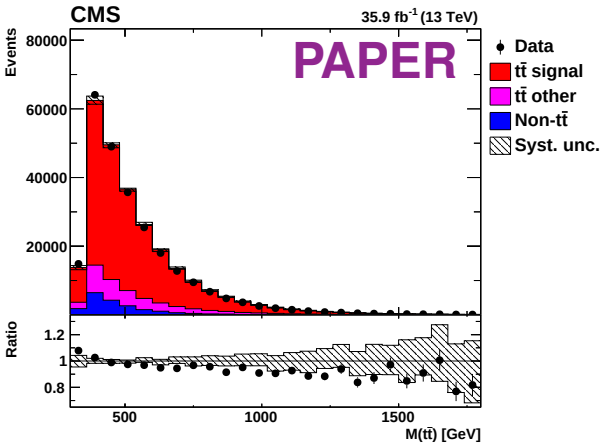

- small non-$t\bar{t}$ background ($\approx$ 8%), '$t\bar{t}$ other' is dominated by decays via τ
- in general, good description of all distributions within uncertainties
- softer $p_T(t)$, $p_T(t\bar{t})$, $M(t\bar{t})$ in data than nominal MC (seen earlier and/or in other analyses)

Control plots, after loose KR

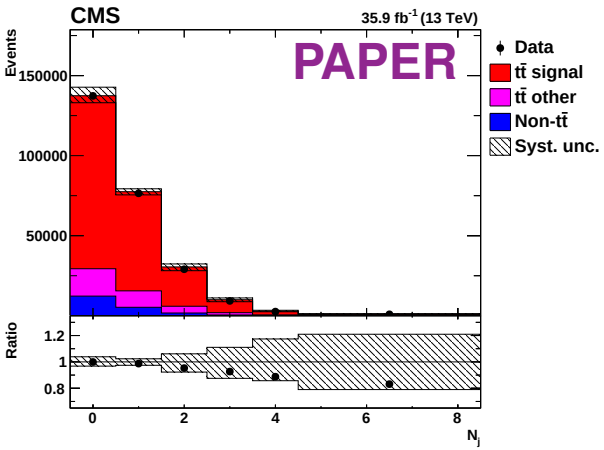

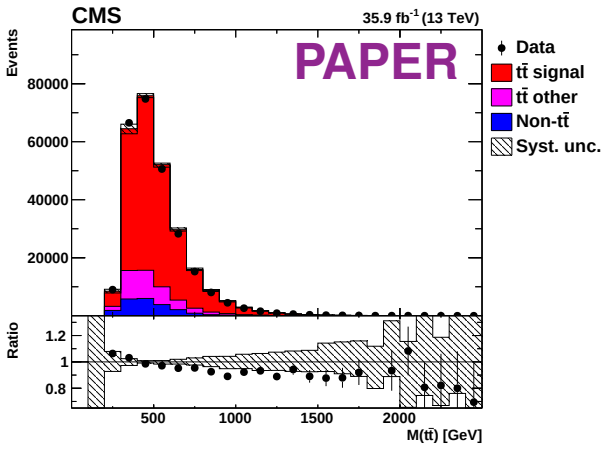

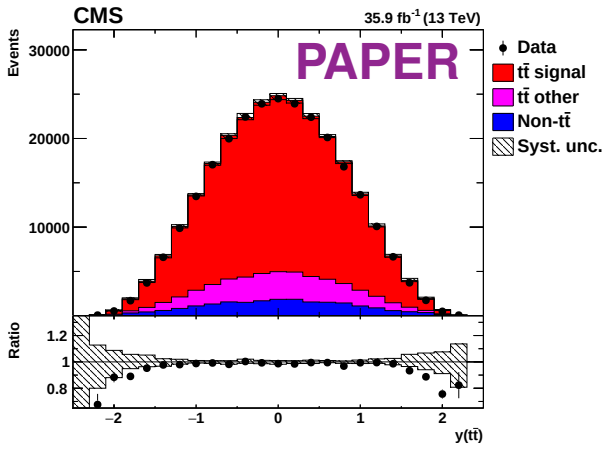

- N_{jet} is multiplicity of additional [extra] jets (not from $t\bar{t}$ decay)
- $M(t\bar{t})$, $y(t\bar{t})$ after loose KR are similar to the ones after full KR
- in general, good description of all distributions within uncertainties
- softer N_{jet} in data than nominal MC (seen earlier and/or other analyses)

Analysis overview

1. Event selection (same as in 1D $t\bar{t}$ analysis)

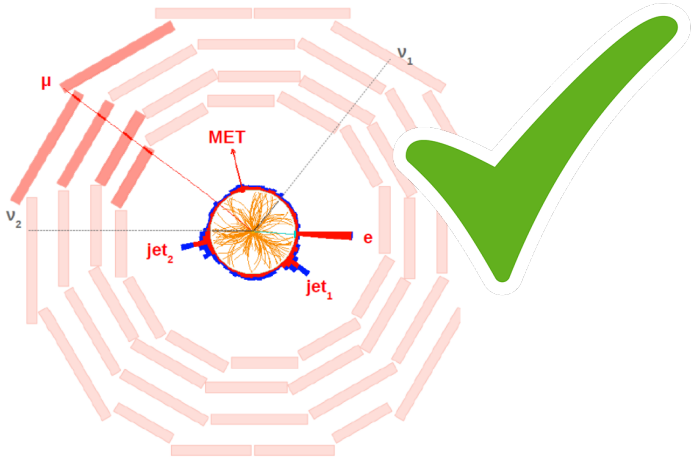

2. Kinematic reconstruction (same as in 1D $t\bar{t}$ analysis + loose)

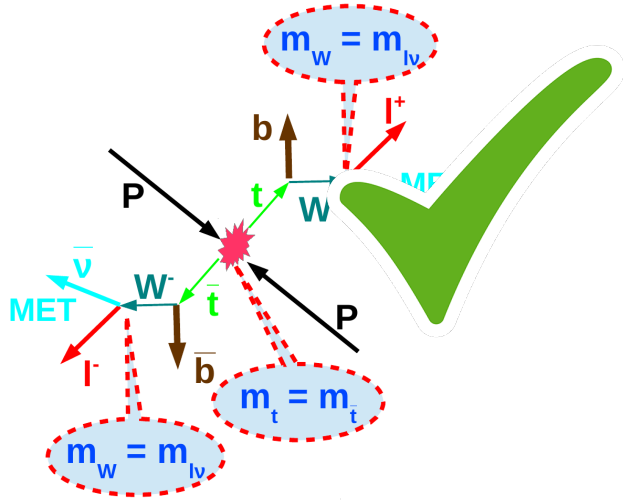

3. Unfolding and results

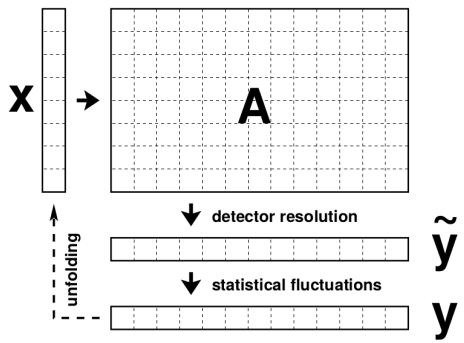

4. Data interpretation

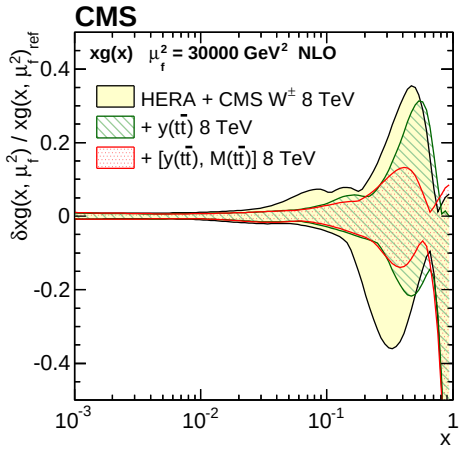

Cross section determination

Background subtraction: $y = D - B$

D: data, B: background ('$t\bar{t}$ other' + 'non-$t\bar{t}$')
('$t\bar{t}$ other' is normalised consistently with signal '$t\bar{t}$')

Unfolding problem: $\mu = Ax$

μ: detector expectation (observation and its covariance: y and V_{yy}), M_y bins
A: response matrix (taken from MC)
x: unknown truth, M_x bins ($M_x \leq M_y$)
x_0: bias vector for regularisation (taken from MC)

$$\mathcal{L} = (y - Ax)^T V_{yy}^{-1} (y - Ax) + \tau^2 (x - x_0)^T (L^T L)(x - x_0)$$

Solution:

$$\frac{\partial \mathcal{L}}{\partial x} = 0 \quad \Rightarrow \quad x = x(y, V_{yy}, x_0) \text{ and } V_{xx} = V_{xx}(y, V_{yy}, x_0)$$

Solution obtained using regularised multidimensional unfolding with TUnfold (as in TOP-14-013):

- damp bin-to-bin correlations by biasing curvature to MC ("bias vector")
- regularised strength determined by minimising global correlation coefficient ('MinRhoAvg')
- finer binning at detector level, limited only by Gaussian stat. $\rightarrow$ reduce "wide bins" problem
- coarser binning at generator level, limited by resolution
- verified by closure tests (BACKUP)

Response matrix, purity, stability, efficiency: exemplary 2D plots

Exemplary plots for $[p_T(t), y(t\bar{t})]$:

Purity, stability, efficiency

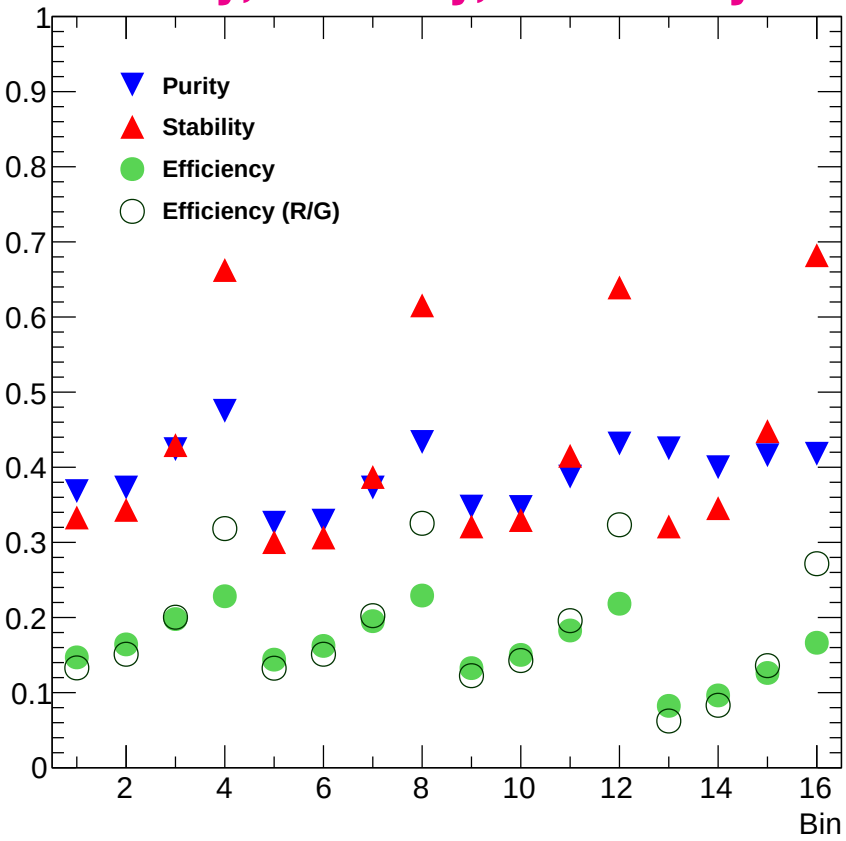

Response matrix

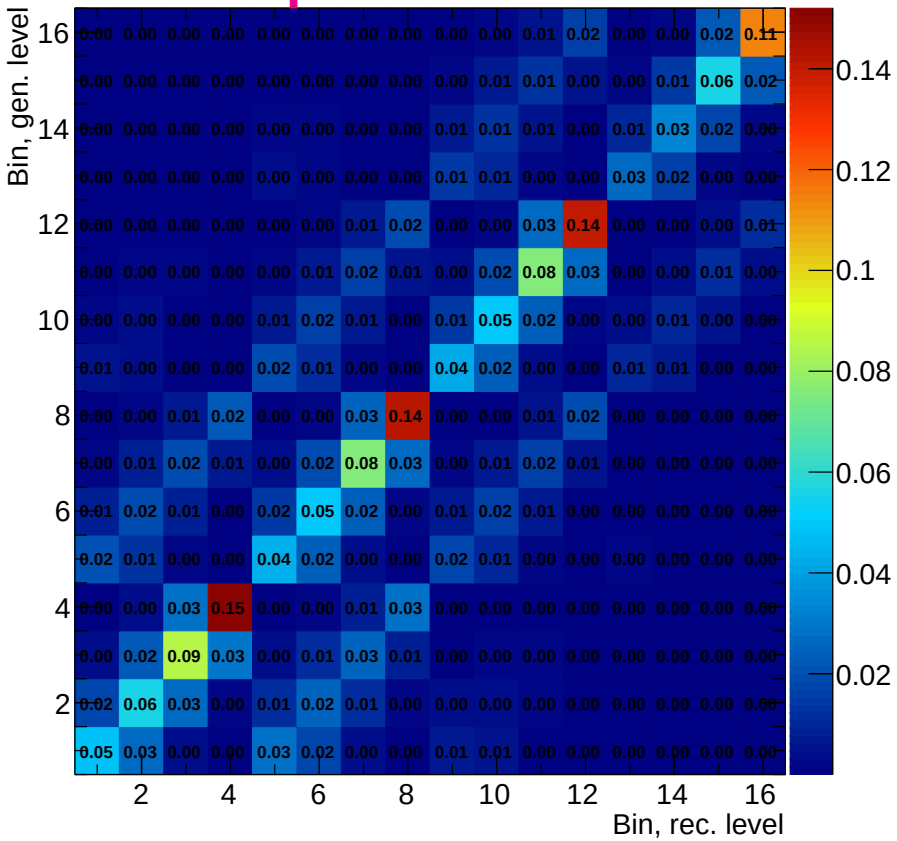

- Efficiency definition includes kinematic acceptance
- Response matrix is not the one used in unfolding (TUnfold allows finer detector level bins)
- Purity, stability > 30% for 2D x-sections

Response matrix, purity, stability, efficiency: exemplary 3D plots

Exemplary plots for $[N_{\text{jet}}^{0,1,2+}, M(t\bar{t}), y(t\bar{t})]$:

Purity, stability, efficiency

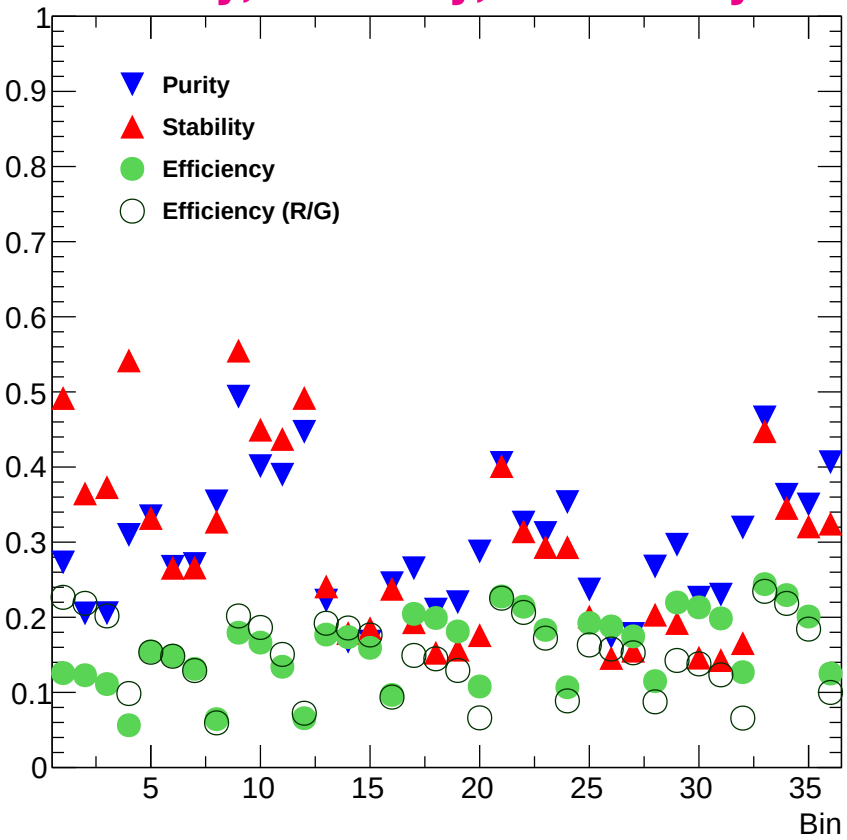

Response matrix

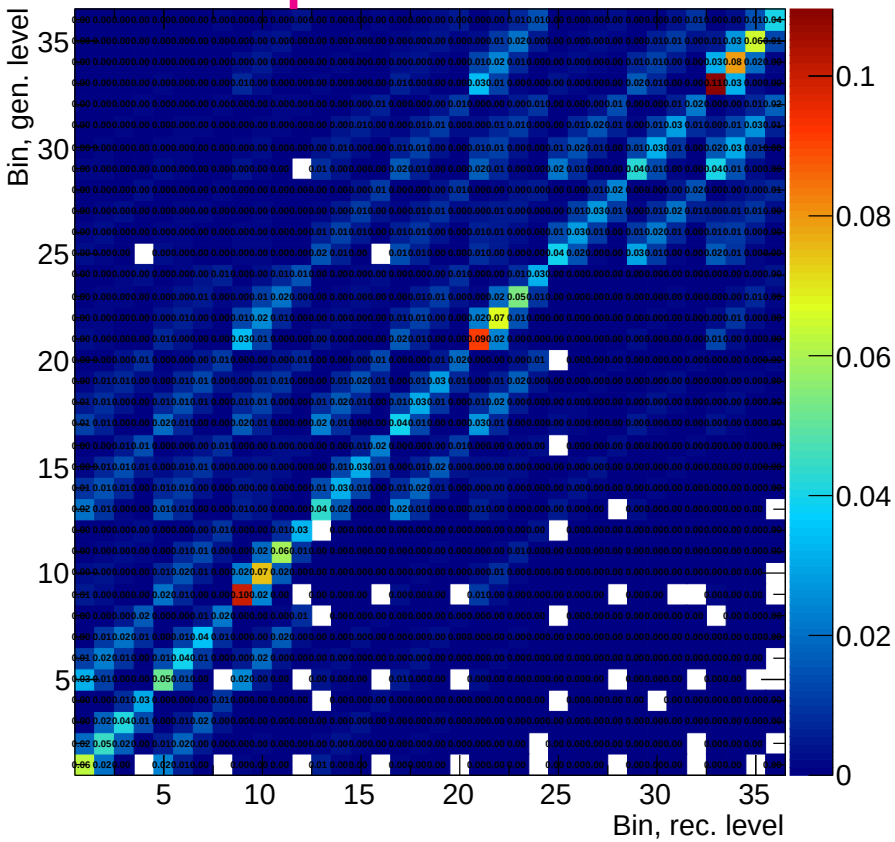

- Efficiency definition includes kinematic acceptance
- Response matrix is not the one used in unfolding (TUnfold allows finer detector level bins)
- Purity, stability generally > 20% for 3D x-sections

Systematic uncertainties

Experimental (everything follows official recommendations):

- JES (splitted in sources, also propagated to MET)
- JER
- b-tagging SFs
- lepton ID/ISO SFs
- triggers SFs
- pileup reweighting
- non-$t\bar{t}$ background normalisation varied by 30%
- lumi and branching ratios cancel for normalised cross section

Model uncertainties (everything follows official recommendations):

- based on weights ('mod w'):
  - ME scales (envelope of 6 variations dominated by simultaneous μ_r,μ_f var.)
  - PDFs and α_s (CT14 eigenvectors)
  - b-quark fragmentation (envelope of varied Bowler-Lund and Peterson funct.)
  - b-hadron branching ratios
- based on independent samples ('mod i')
  - $m_t \pm 1$ GeV (using samples with ± 3 GeV $\rightarrow$ rescaled by $1/3$)
  - h_{damp}
  - ISR μ, FSR μ (latter rescaled by $1/\sqrt{2}$)
  - color reconnection: envelope of 3 samples with different tunes
  - underlying event tune

Data uncertainties: 2D x-sections

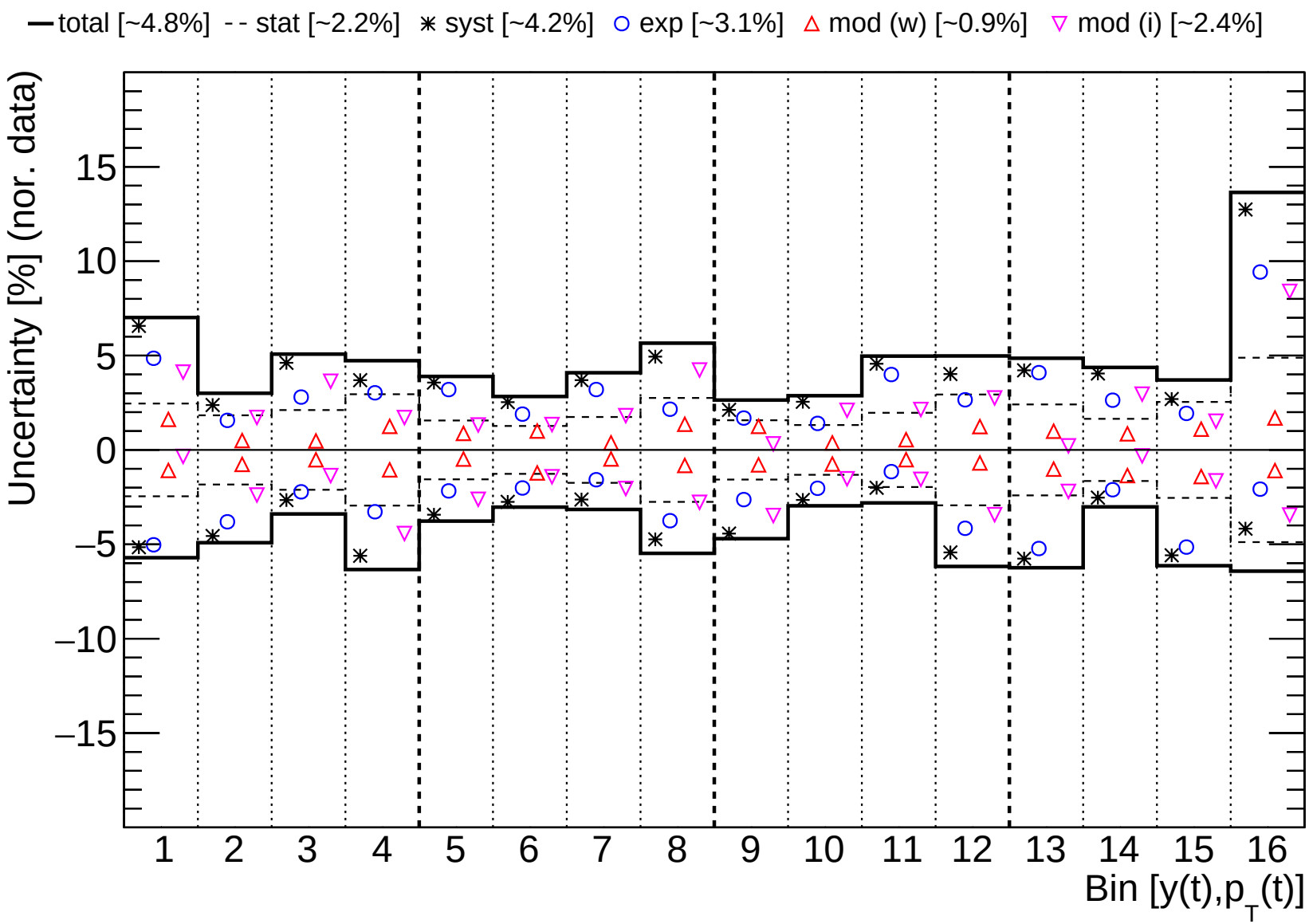

Data uncertainties: 3D x-sections

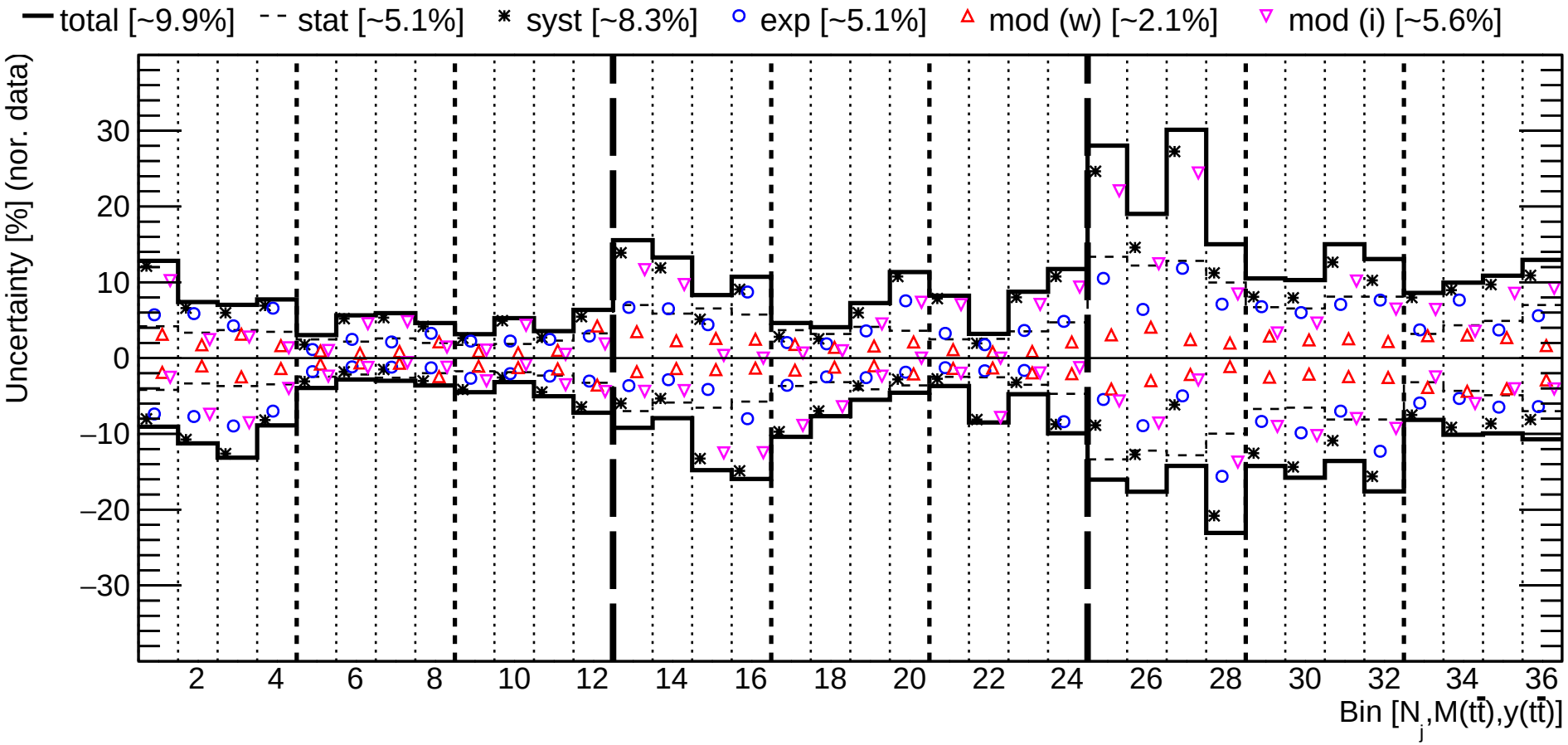

- total uncertainties are typically 5–10% for 2D and 5–20% for 3D x-sections
- dominated by systematics, with about equal contribution from experim. and model sources
  - more detailed breakdown of uncertainties in backup
  - experimental systematics are dominated by JES
  - model systematics receive similar contributions from several variations
  - both are to some extend affected by limited MC statistics (extra MC was generated)

Results

- Measured seven 2D and two 3D cross sections
- All cross sections are provided at parton level for $t\bar{t}$ (before t decay) but particle level for jets
  - corrections particle$\rightarrow$ parton level (e.g. fixed-order predictions) derived and provided
- 2D and 3D x-sections are compared to MC predictions:
  - POWHEGV2 + PYTHIA8 ('POW-PYT')
  - POWHEGV2 + HERWIG++ ('POW-HER')
  - MG5_AMC@NLO + PYTHIA8 ('FXFX-PYT')
- Each comparison is quantified by χ^2 which takes into account data bin-by-bin correlations and cross section normalisation:

$$\chi^2 = \mathbf{R}_{N-1}^T \mathbf{Cov}_{N-1}^{-1} \mathbf{R}_{N-1},$$

$$\mathbf{Cov} = \mathbf{Cov}^{\text{unf}} + \mathbf{Cov}^{\text{syst}},$$

$$\mathbf{Cov}_{ij}^{\text{syst}} = \sum_{k,l} \frac{1}{N_k} C_{j,k} C_{i,k}, \quad 1 \leq i \leq N, \quad 1 \leq j \leq N,$$

  $\rightarrow$ resulted χ^2 are translated into p-values and compared on one plot
  [caveat: no theory unc. $\rightarrow$ p-value have limited sense
- Planning to compare 2D x-sections to NNLO predict. (if provided by theor. within $\sim$ 1 week)
- Further, 3D cross sections are exploited for PDF+α_s +m_t extraction using NLO calculations

Results: 2D x-sections $[y(t), p_T(t)]$

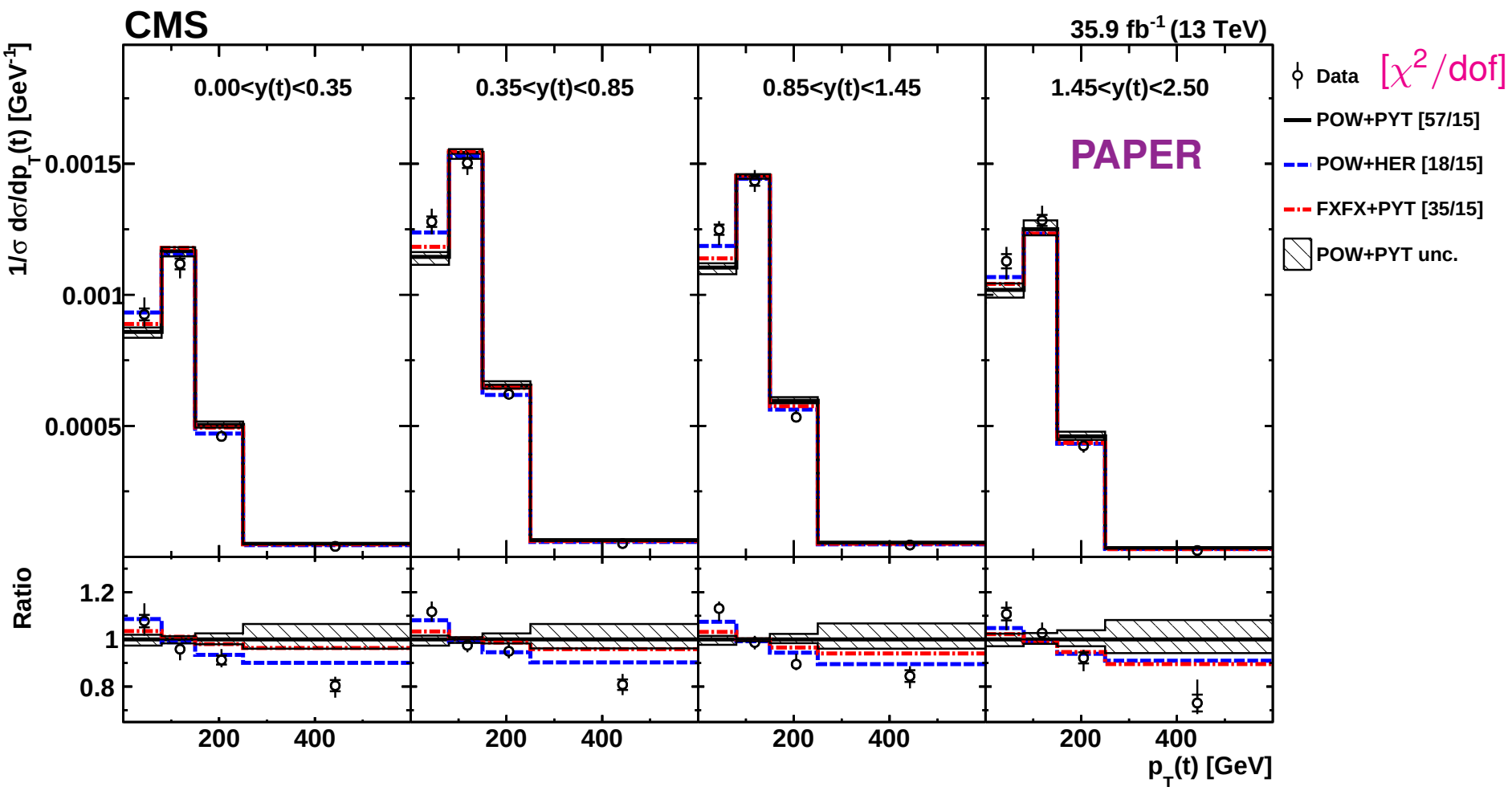

→ 'POW-PYT' and 'FXFX-PYT' predict softer $p_T(t)$ in entire $y(t)$ range

→ better description by 'POW-HER'

Results: 2D x-sections $[M(t\bar{t}),y(t)]$

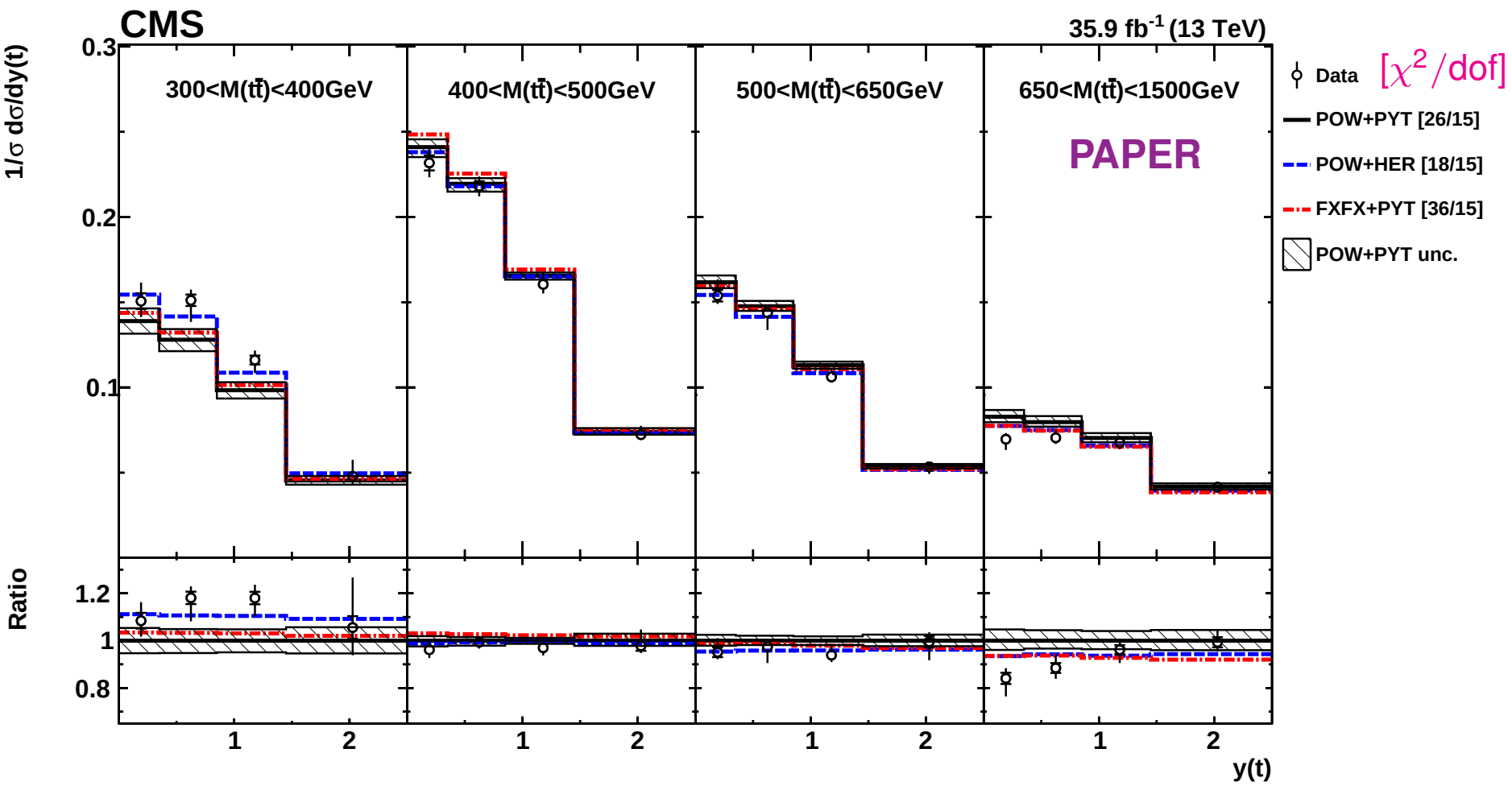

→ MC is more central than data at largest $M(t\bar{t})$

→ best description by 'POW-HER' (mainly $M(t\bar{t})$ slope)

Results: 2D x-sections $[M(t\bar{t}),y(t\bar{t})]$

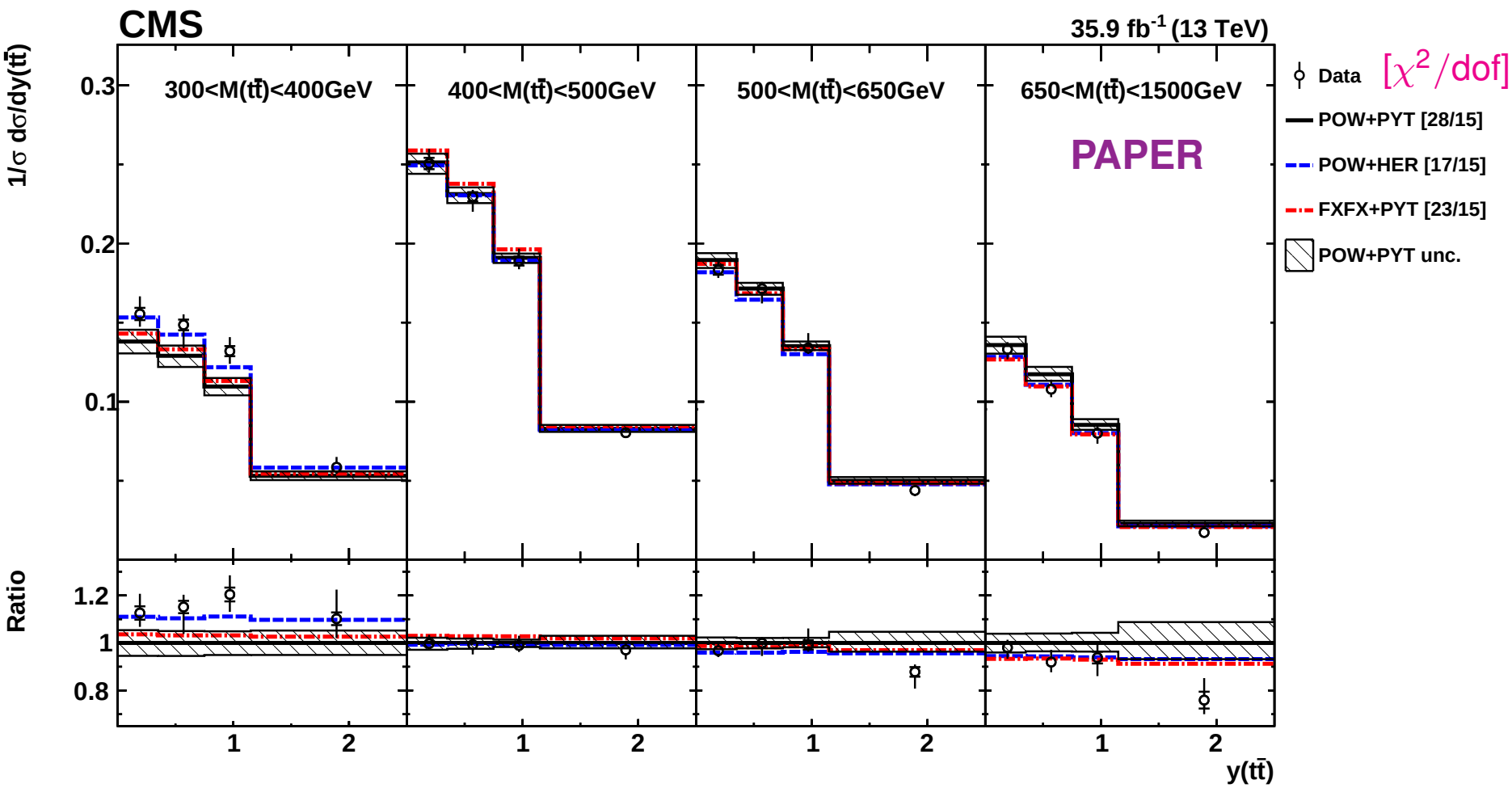

→ MC is (somewhat) less central than data at largest $M(t\bar{t})$

→ best description by 'POW-HER' (mainly $M(t\bar{t})$ slope)

Results: 2D x-sections $[M(t\bar{t}),\Delta\eta(t,\bar{t})]$

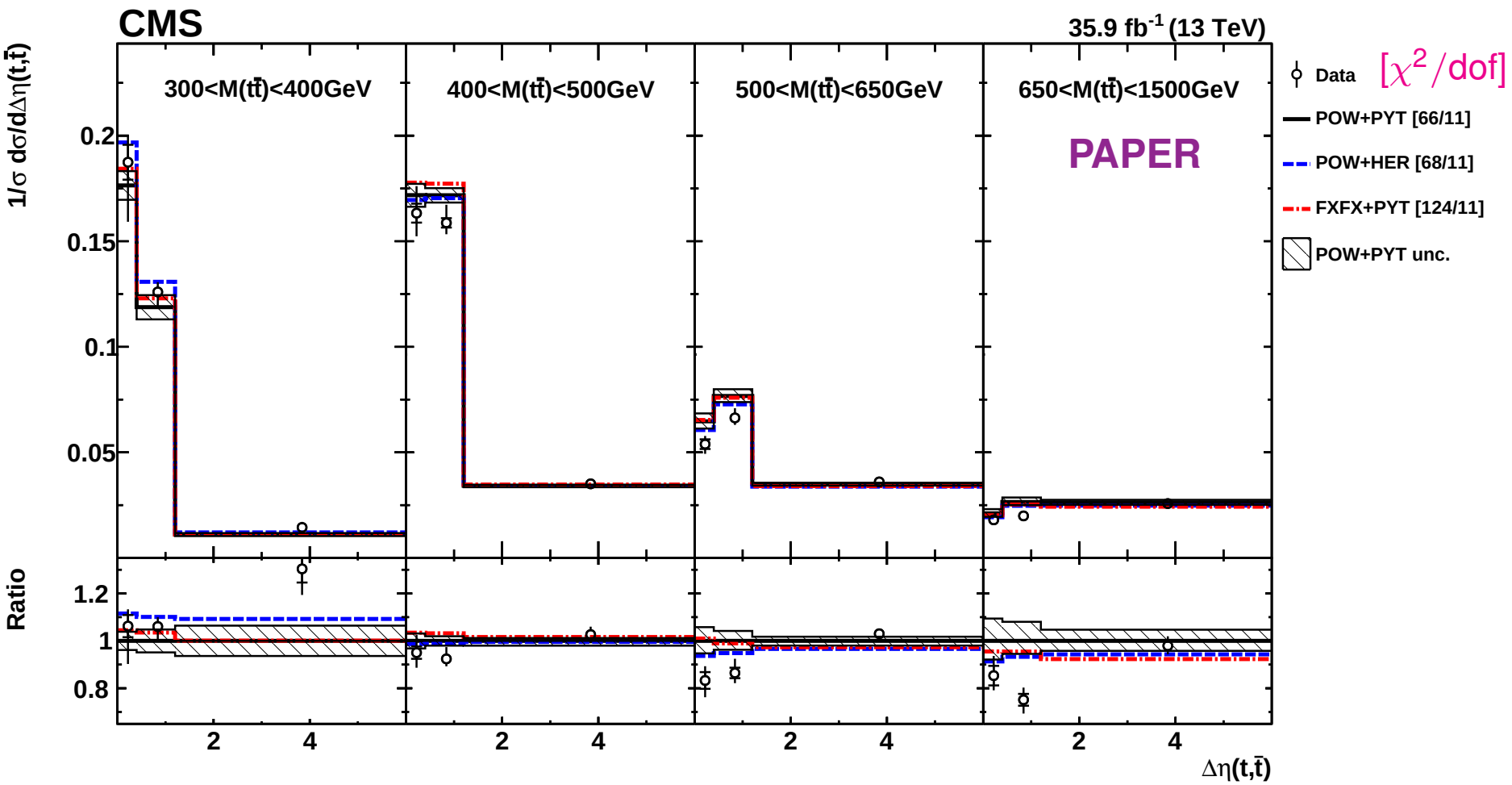

→ predicted $\Delta\eta(t,\bar{t})$ are too low at medium and high $M(t\bar{t})$

→ at large $M(t\bar{t})$, t and $\bar{t}$ have a larger η separation than in MC: correlated with a lower $p_T(t)$

→ bad description by all MC, strongest disagreement for 'FXFX-PYT'

Results: 2D x-sections $[M(t\bar{t}),\Delta\phi(t,\bar{t})]$

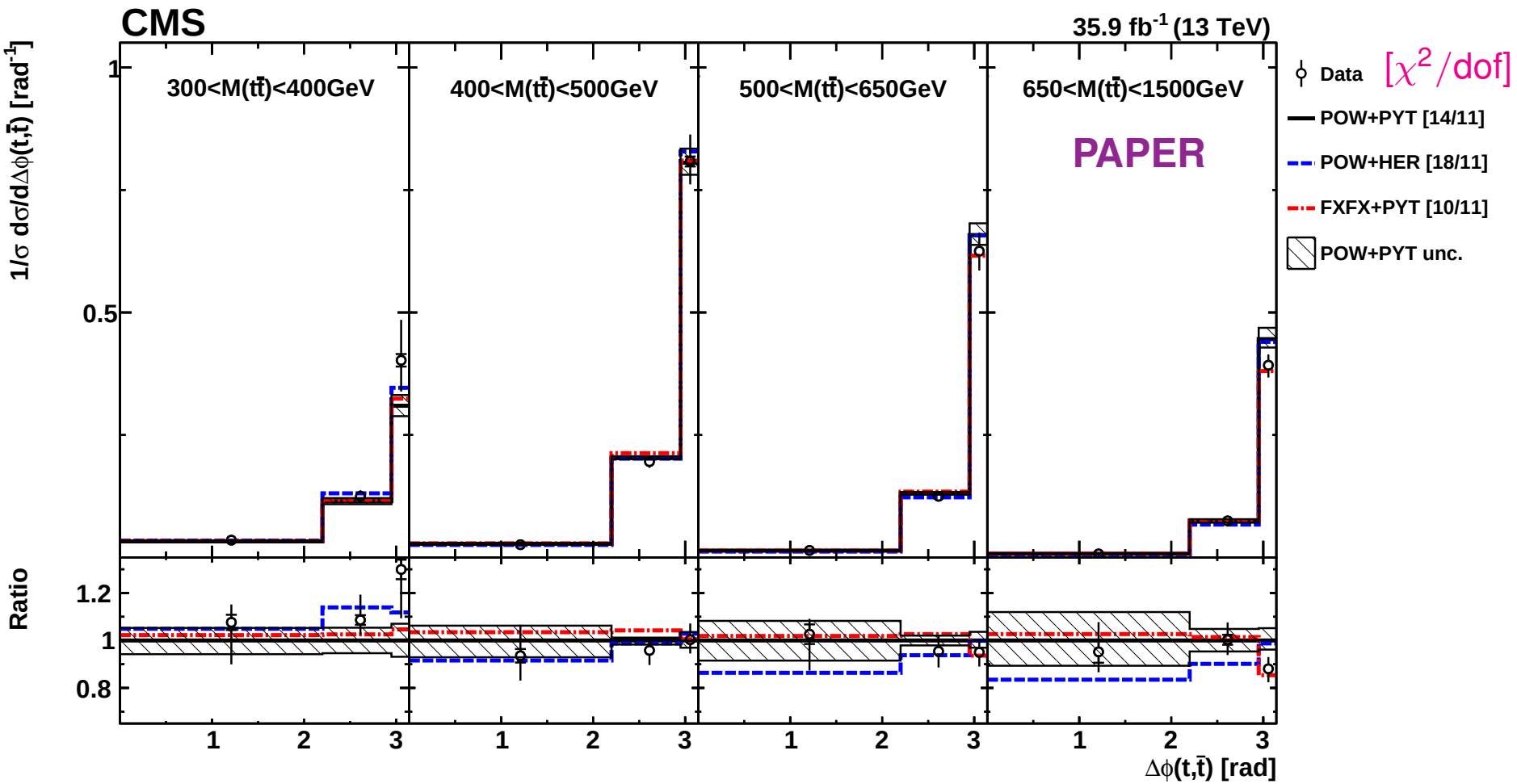

→ all MC describe data well

Results: 2D x-sections $[M(t\bar{t}),p_T(t\bar{t})]$

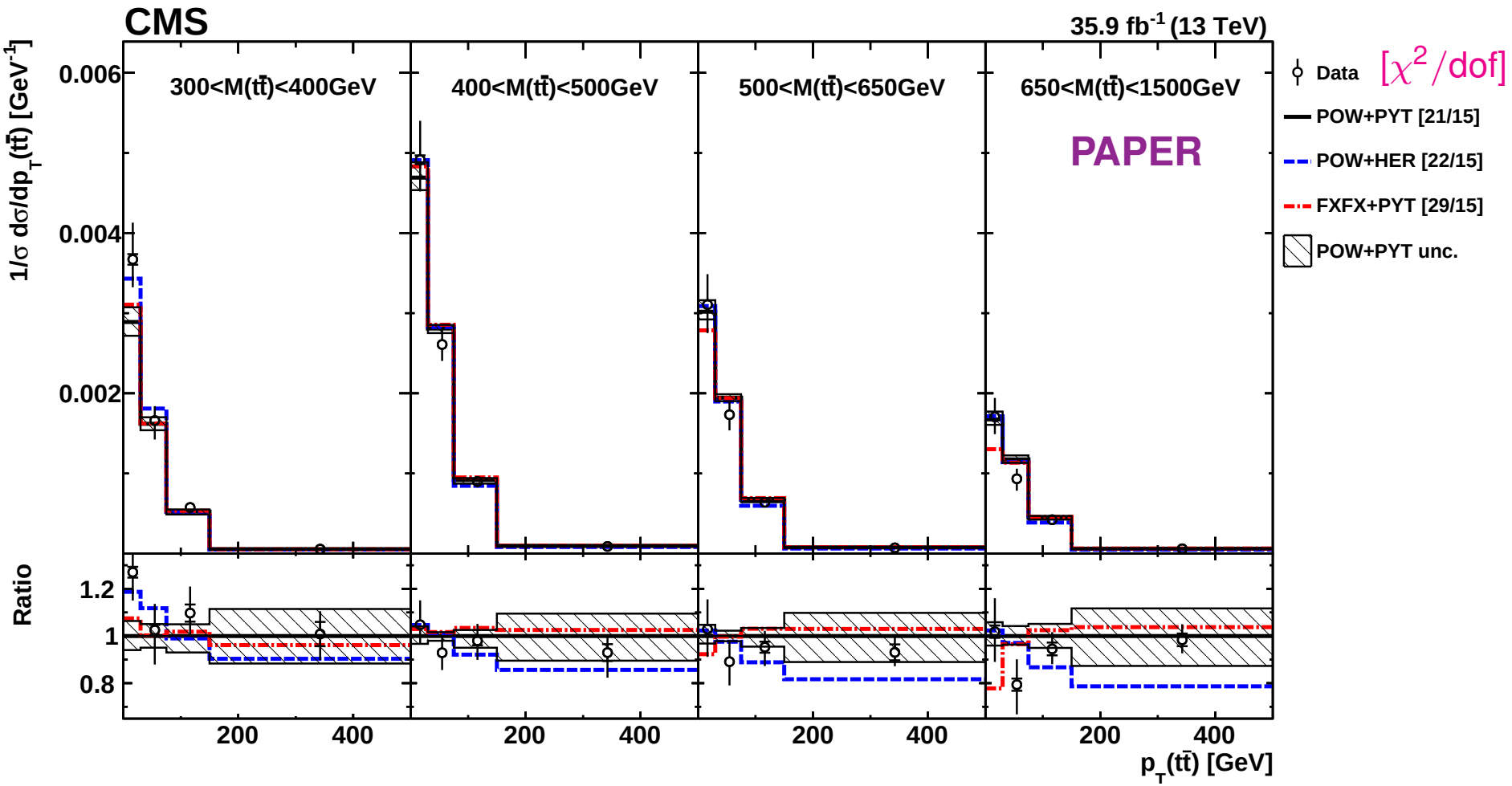

→ all MC describe data well, but 'FXFX-PYT' predicts too hard $p_T(t\bar{t})$ at highest $M(t\bar{t})$

Results: 2D x-sections $[M(t\bar{t}),p_T(t)]$

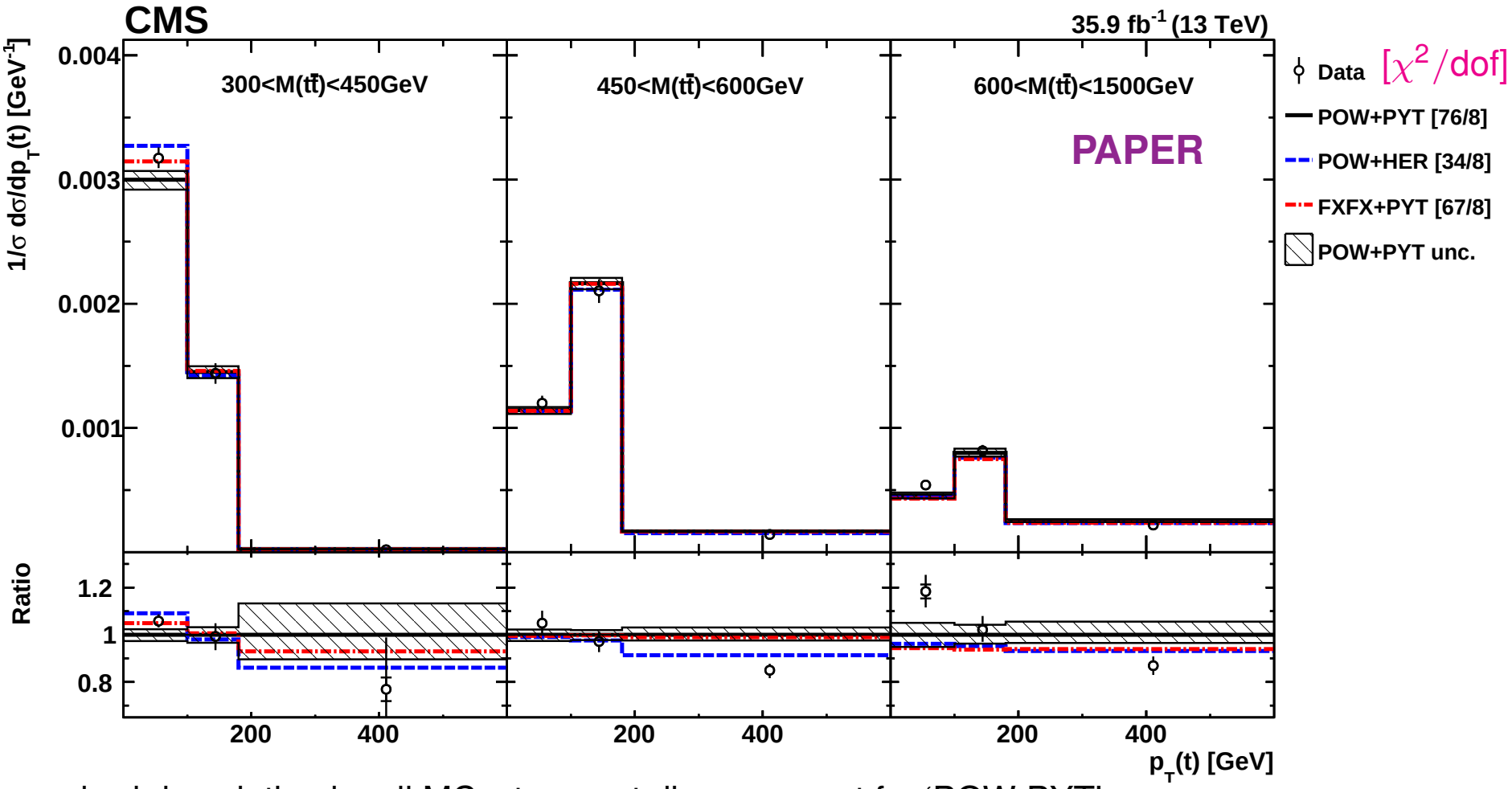

→ bad description by all MC, strongest disagreement for 'POW-PYT'

→ notice: 'POW-HER' describes $p_T(t)$ in entire $y(t)$ range well, but predicts too hard $p_T(t)$ at high $M(t\bar{t})$

Results: 3D x-sections $[N_{\text{jet}}^{0,1+}, M(t\bar{t}), y(t\bar{t})]$

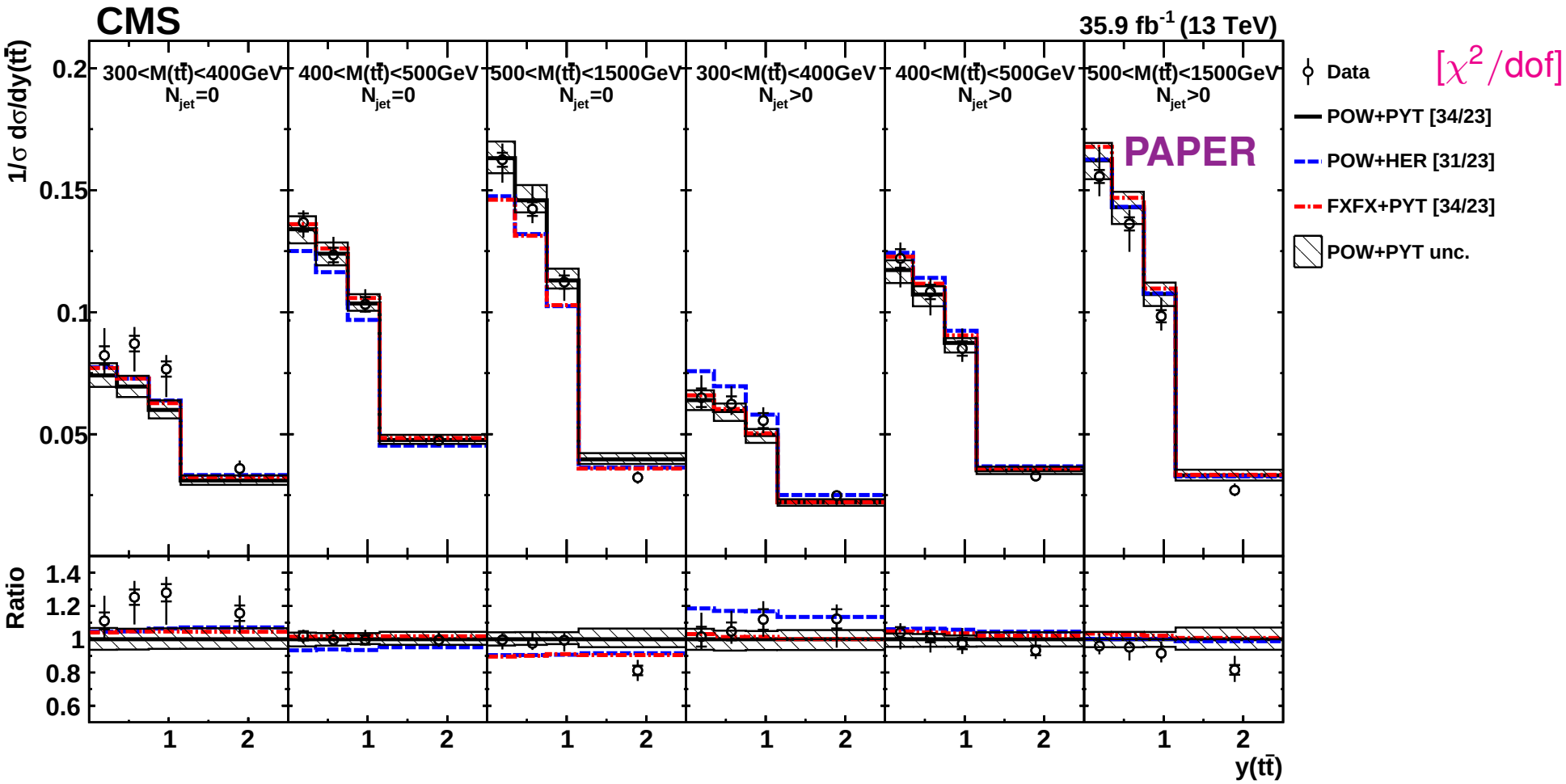

→ all MC describe data well

Results: 3D x-sections $[N_{\text{jet}}^{0,1,2+}, M(t\bar{t}), y(t\bar{t})]$

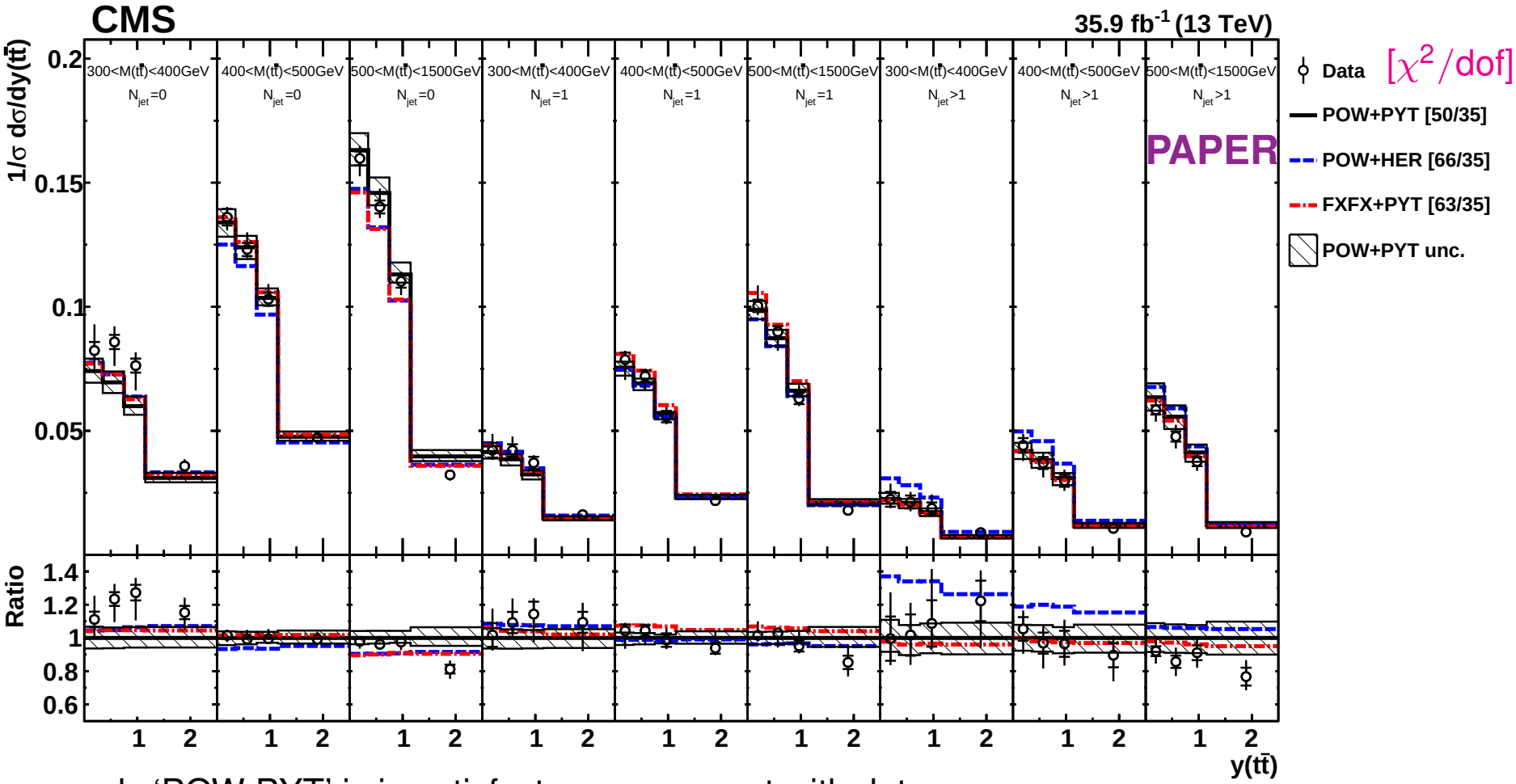

→ only 'POW-PYT' is in satisfactory agreement with data

→ 'POW-HER' predicts too high cross section at $N_{\text{jet}} > 1$

→ 'FXFX-PYT' describes worse $M(t\bar{t})$ at $N_{\text{jet}} = 1$

Results: summary of comparison to MC models

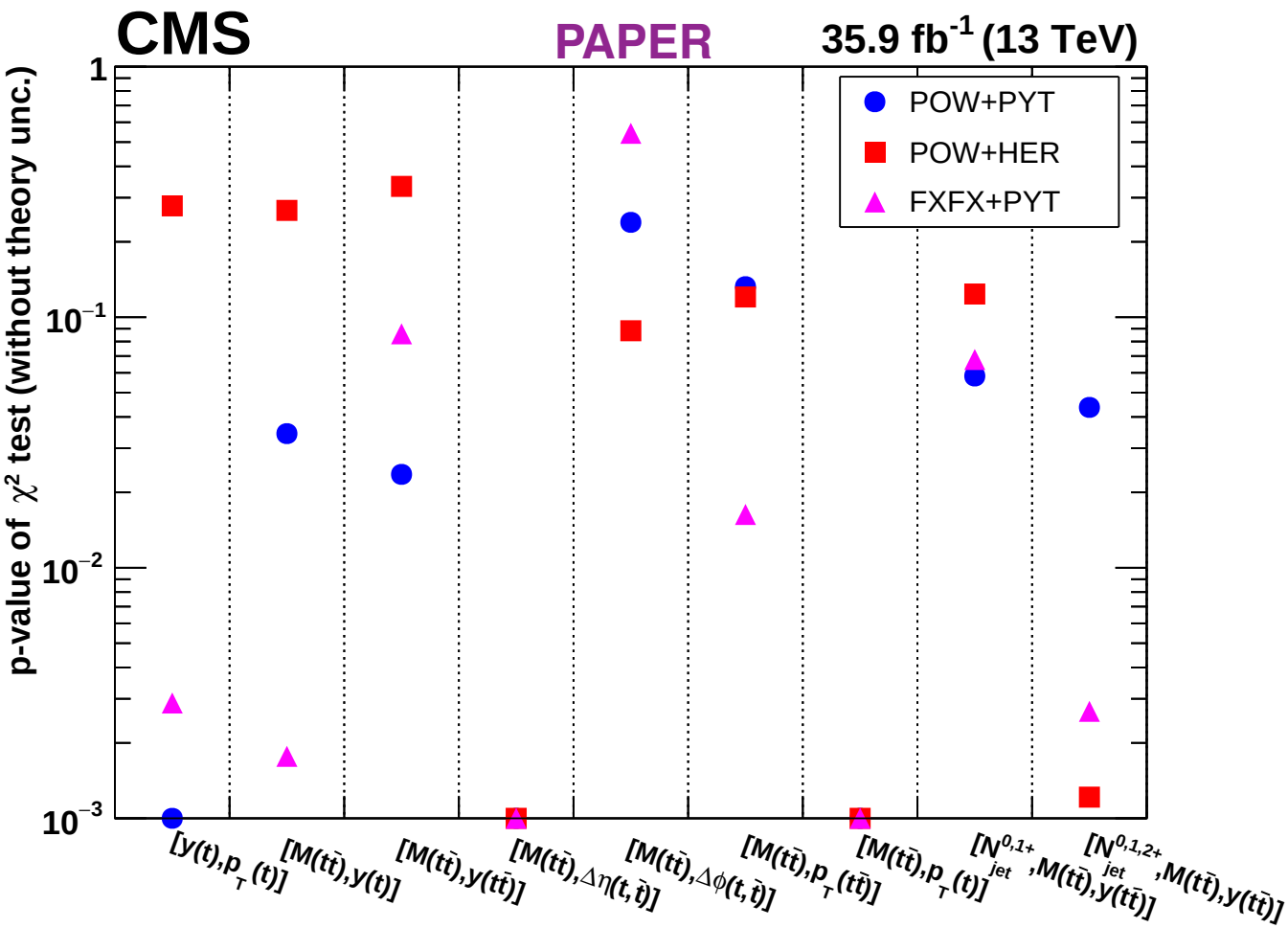

- none of central MC predictions is able to describe all distributions, in particular $[M(t\bar{t}), \Delta\eta(t,\bar{t})]$, $[M(t\bar{t}), p_T(t)]$
- overall, best description is provided by 'POW-PYT' and 'POW-HER':
  - 'POW-HER' describes better distributions probing $p_T(t)$
  - 'POW-PYT' describes better distributions probing N_{jet} and radiation

Analysis overview

1. Event selection (same as in 1D $t\bar{t}$ analysis)

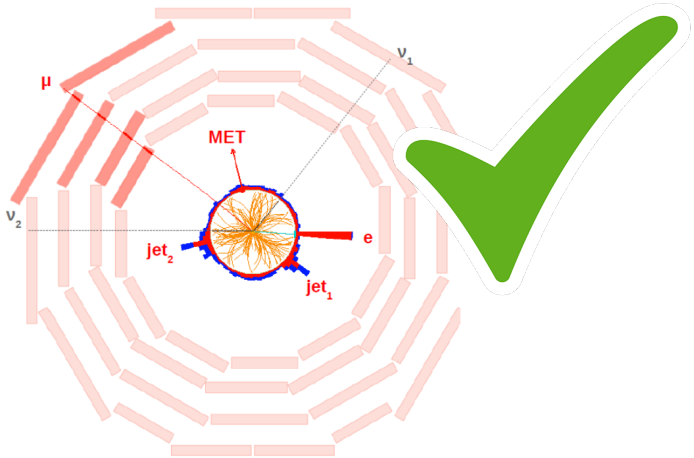

2. Kinematic reconstruction (same as in 1D $t\bar{t}$ analysis + loose)

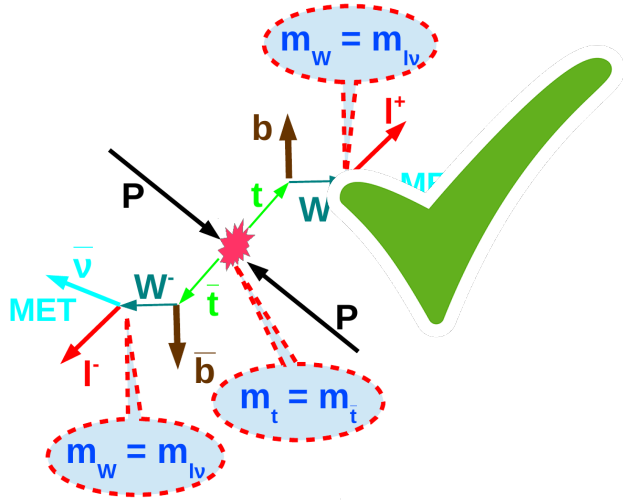

3. Unfolding and results

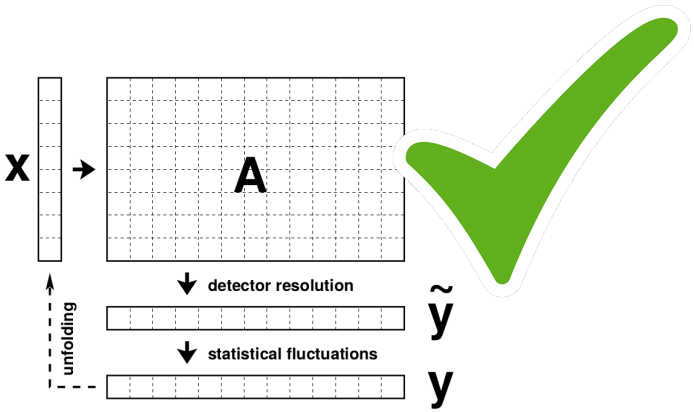

4. Data interpretation

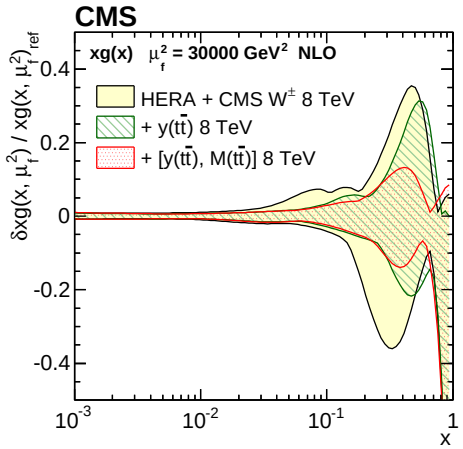

Data interpretation

Data interpretation consists of two parts:

(1) comparison theory vs data using external PDF sets:

- extracting α_s keeping m_t^{pole} fixed
- extracting m_t^{pole} keeping α_s fixed

$\rightarrow$ this presents α_s, m_t^{pole} extraction from $t\bar{t}$ data only

(2) simultaneous fit of PDFs, α_s and m_t^{pole} using $t\bar{t}$ and HERA DIS:

$\rightarrow$ this presents fully unbiased extraction of α_s, m_t^{pole} and PDFs, but using also HERA data

$\rightarrow$ important as exercise to understand $t\bar{t}$ data, providing baseline for future global fits

NLO calculations (1)

NLO is highest order available for $t\bar{t}$ + jets. Consistent NLO for all N_{jet} values:

- $[N_{\text{jet}}^{0,1+}, M(t\bar{t}), y(t\bar{t})]$ with 2 N_{jet} bins:
  - $\sigma^{\text{NLO}}(N_{\text{jet}} = 0) = \sigma^{\text{NLO}}(t\bar{t}) - \sigma^{\text{NLO}}(t\bar{t} + 1\text{jet})$
  - $\sigma^{\text{NLO}}(N_{\text{jet}} > 0) = \sigma^{\text{NLO}}(t\bar{t} + 1\text{jet})$
- $[N_{\text{jet}}^{0,1,2+}, M(t\bar{t}), y(t\bar{t})]$ with 3 N_{jet} bins:
  - $\sigma^{\text{NLO}}(N_{\text{jet}} = 0) = \sigma^{\text{NLO}}(t\bar{t}) - \sigma^{\text{NLO}}(t\bar{t} + 1\text{jet})$
  - $\sigma^{\text{NLO}}(N_{\text{jet}} = 1) = \sigma^{\text{NLO}}(t\bar{t} + 1\text{jet}) - \sigma^{\text{NLO}}(t\bar{t} + 2\text{jets})$
  - $\sigma^{\text{NLO}}(N_{\text{jet}} > 1) = \sigma^{\text{NLO}}(t\bar{t} + 2\text{jets})$

Focused on cross sections with 2 N_{jet} bins, using 3 N_{jet} bins as cross check:

- larger scale unc. for 3 N_{jet} bins, while no significant gain in sensitivity to PDF,α_s,m_t^{pole}
- NLO predictions for 3 N_{jet} bins ($t\bar{t}$ + 2 jets) are much more time expensive to get:
  - sufficient for cross check

NLO calculations (2)

- NLO predictions for inclusive $t\bar{t}$, $t\bar{t}$ + 1 jet and $t\bar{t}$ + 2 jets are computed and compared to data using MadGraph5_aMC@NLO + aMCfast + ApplGrid + xFitter
- $\mu_r = \mu_f = H'/2, H' = \sum_i m_{T,i}$ where the sum runs over all final-state partons (t, $\bar{t}$ and up to three light partons in the $t\bar{t}+2$ jets calculations) and $m_T = \sqrt{m^2 + p_T^2}$ (study of scale dependence in backup). Uncertainties:
  - μ_r, μ_f are varied by factor 2 (6 variations in total)
  - alternative functional form $\mu_r = \mu_f = H/2, H = \sum_i m_{T,i}$ with the sum runs over t and $\bar{t}$
- $m_t^{\text{pole}} = 172.5 \pm 1$ GeV (sometimes ± 5 GeV for presentation purposes)
- PDFs and α_s from several groups via LHAPDF, $\alpha_s \pm 0.001$ for uncertainties (sometimes ± 0.005 for presentation purposes)
- multiplied with NP corrections ($< 5\%$) from parton to particle jet level (BACKUP)

On technical side, this exercise was not always easy (done for the 1st time!):

- $\sim$ 100 years of CPU time, or a few months of real time
  - expected a few ‰ numerical unc. on theory predictions in individual bins [negligible]
  - once the paper is public, plan to release NLO grids and data in xFitter format, such that re-interpretation can be done using ready tools by anyone
- a number of problems/bugs was fixed and reported to MadGraph5_aMC@NLO (backup)
  - one severe problem for $t\bar{t}$ + jets was fixed in aMCfast + ApplGrid interface
  - many new features were implemented in xFitter specially for this analysis

Data and theory uncertainties $[N_{\text{jet}}^{0,1+}, M(t\bar{t}), y(t\bar{t})]$

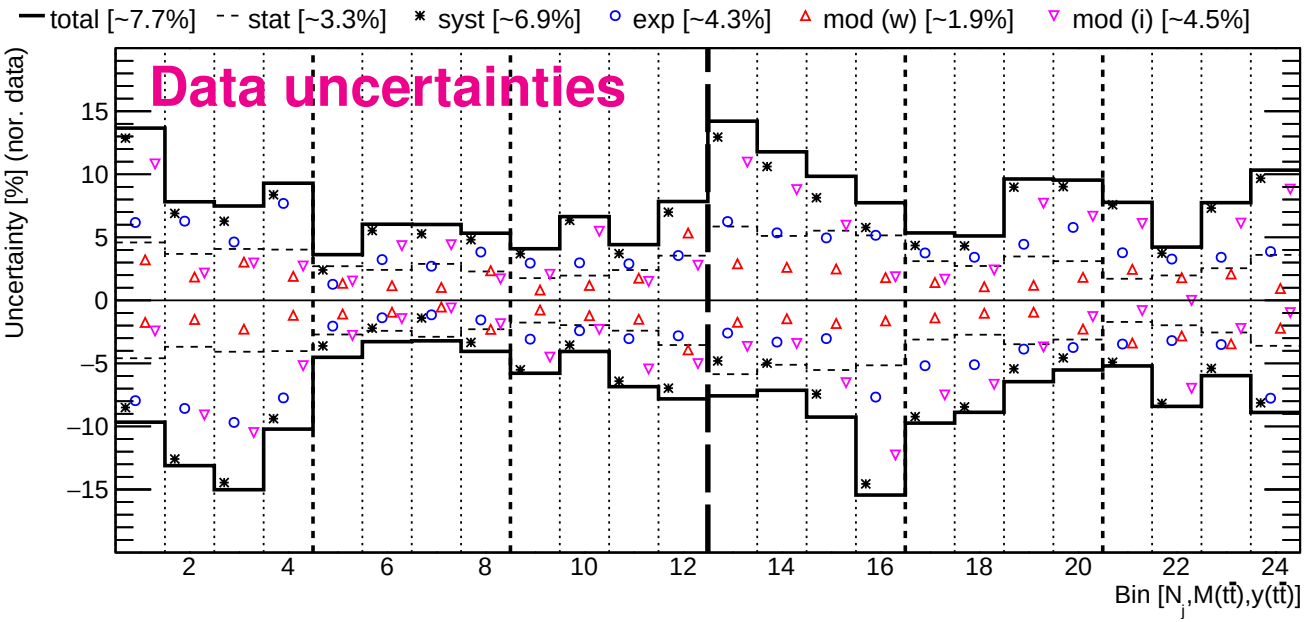

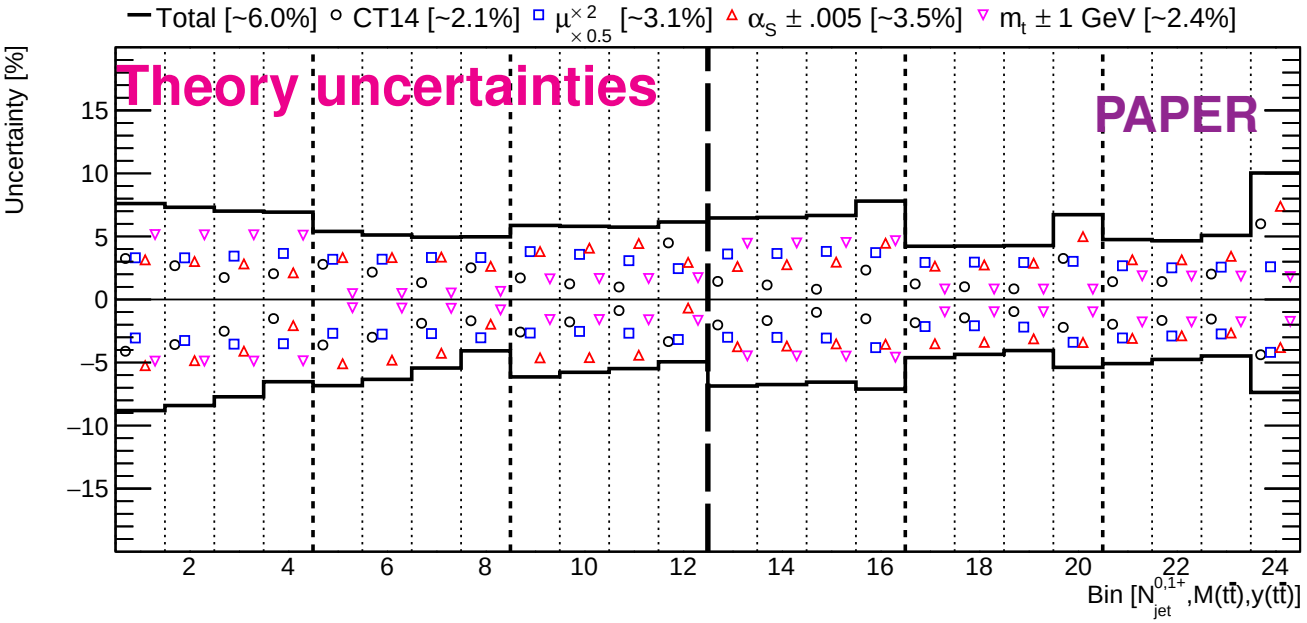

- Data and theory uncertainties are comparable
- Theory scale uncertainties are comparable to PDF, α_s and m_t unc.

$\rightarrow$ Data can constrain PDF, α_s and m_t

Results: $[N_{\text{jet}}^{0,1+}, M(t\bar{t}), y(t\bar{t})]$ compared to NLO pred. with diff. PDFs

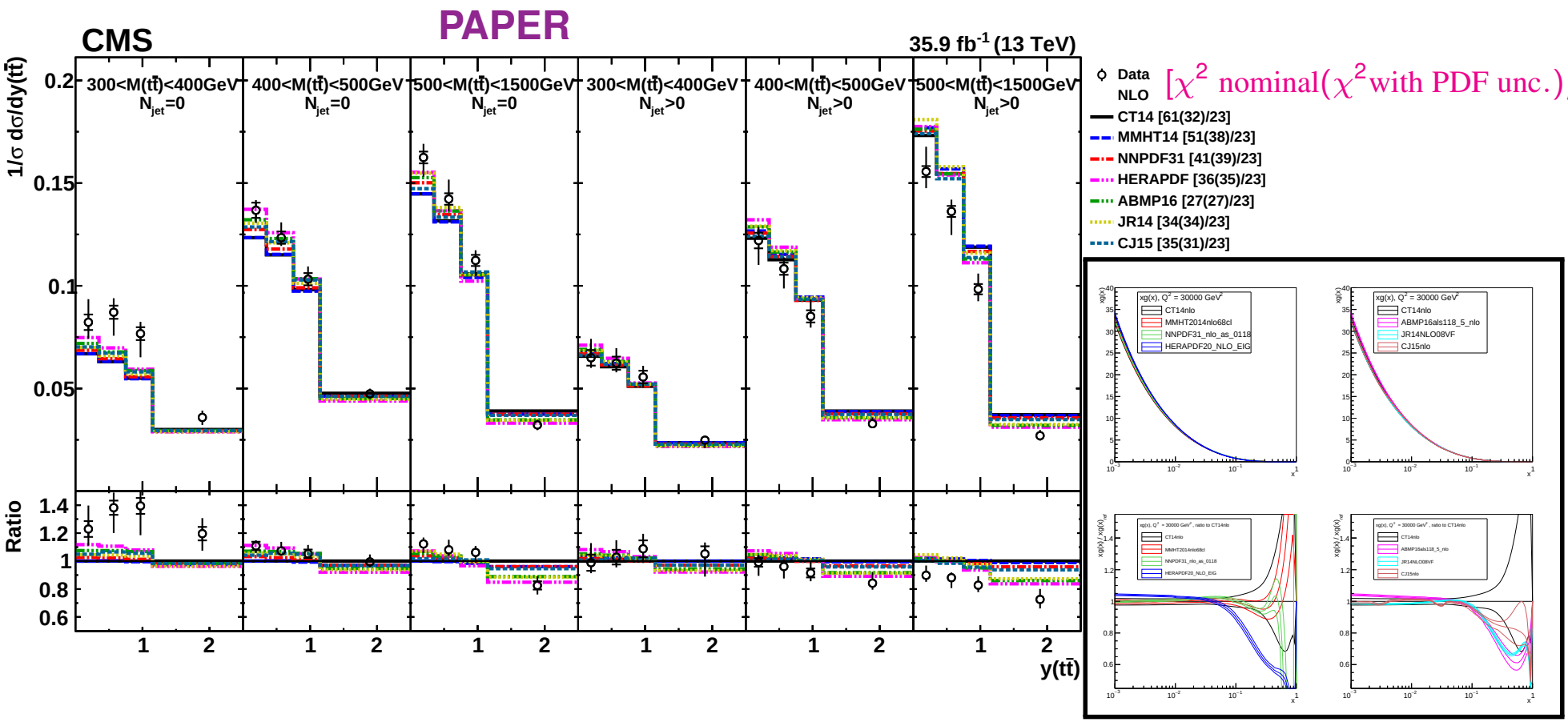

- description depends on PDFs (seven modern PDF sets considered)
- MMHT2014, ABMP16: total $\sigma(t\bar{t})$ data, NNPDF3.1: total and differential (Run-I) $\sigma(t\bar{t})$ data, other PDFs: no $t\bar{t}$ data

Results: $[N_{\text{jet}}^{0,1+}, M(t\bar{t}), y(t\bar{t})]$ compared to NLO pred. with diff. α_s

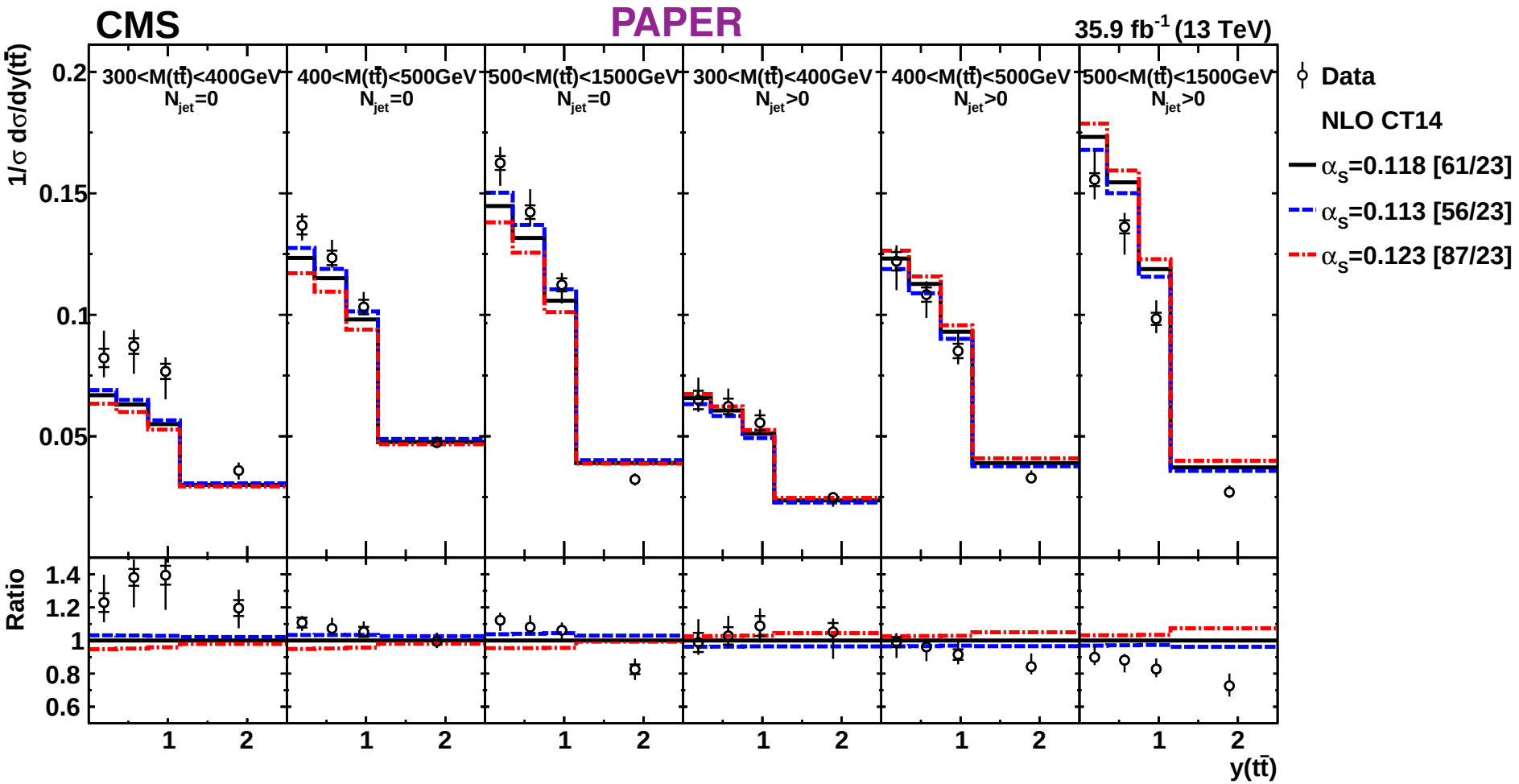

- α_s sensitivity comes from different N_{jet} bins
- also (indirect) sensitivity comes from $[M(t\bar{t}), y(t\bar{t})]$ via sensitivity to PDFs

Results: $[N_{\text{jet}}^{0,1+}, M(t\bar{t}), y(t\bar{t})]$ compared to NLO pred. with diff. m_t^{pole}

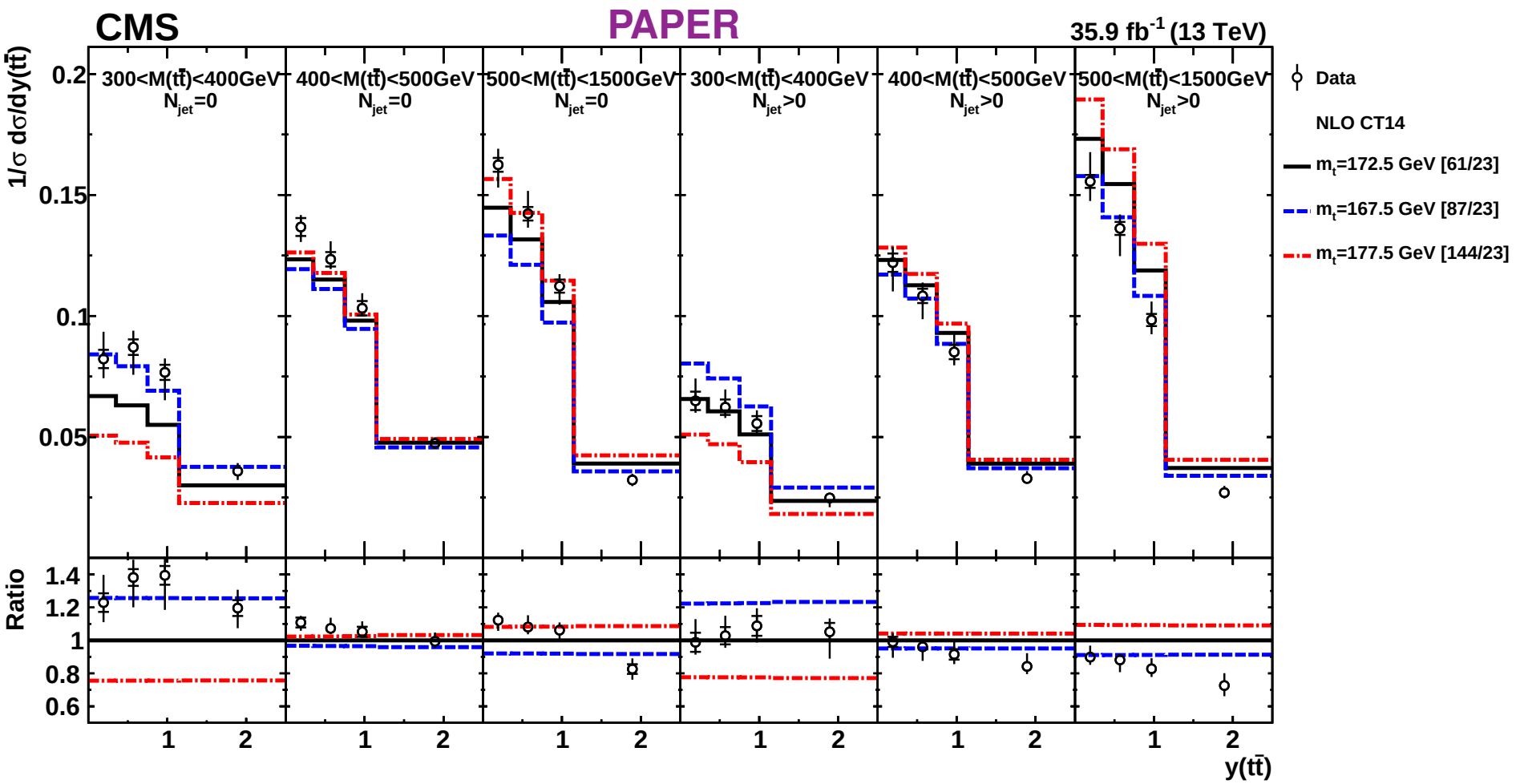

- m_t sensitivity comes from $M(t\bar{t})$, mainly 1st bin
- this method is rather different from extracting m_t^{pole} from total $t\bar{t}$ x-section, and more similar to extracting m_t^{pole} from $t\bar{t}j$ diff. x-section [CMS-PAS-TOP-13-006, ATLAS JHEP 1510 (2015) 121]
- previous determination using this method: prelim. D0 results [FERMILAB-CONF-16-383-PPD]

Results: extraction of α_s from $[N_{\text{jet}}^{0,1+}, M(t\bar{t}), y(t\bar{t})]$

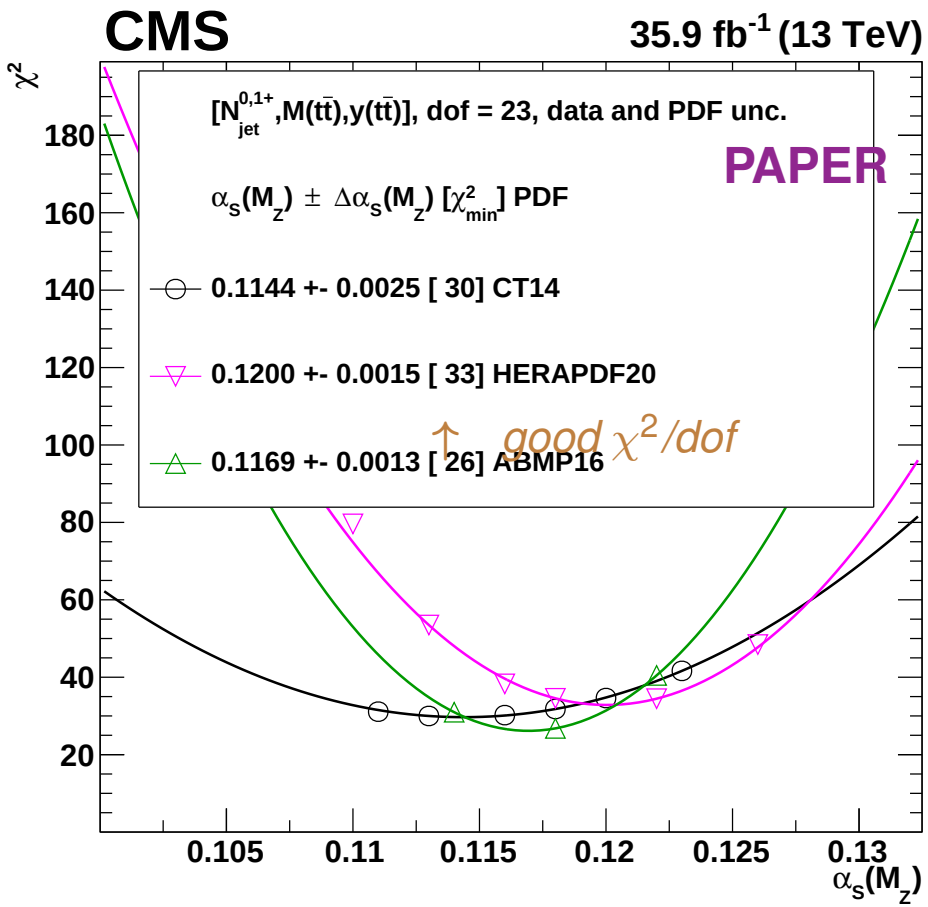

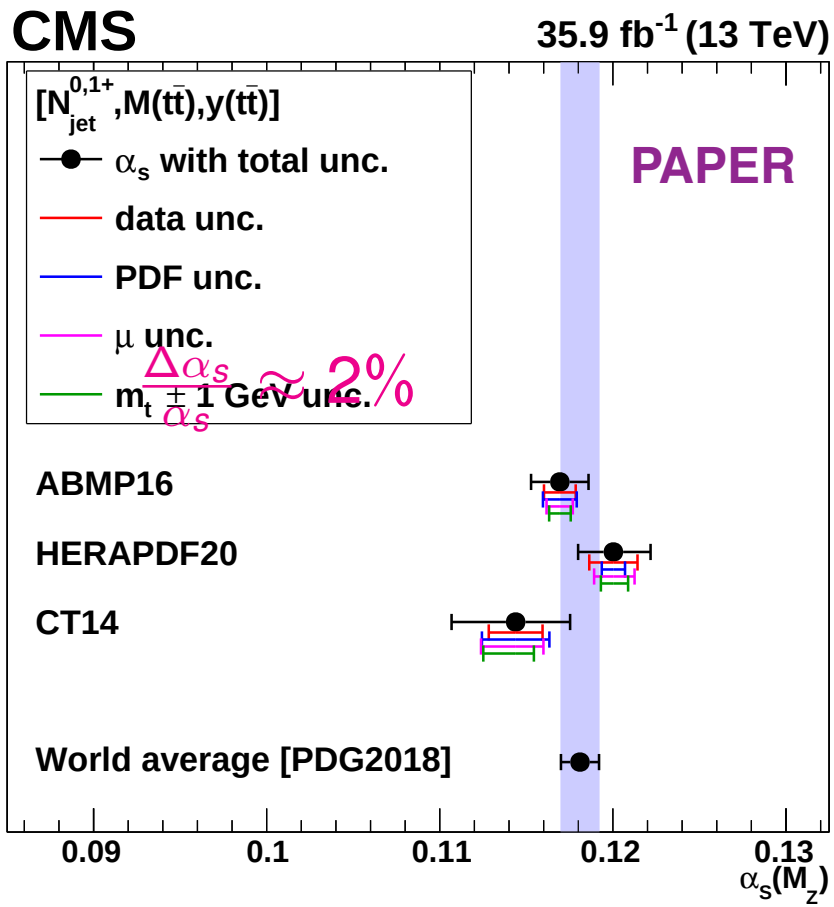

- used $m_t^{\text{pole}} = 172.5$ GeV in ME for all PDF sets (ABMP16 fitted $m_t^{\text{pole}} = 171.44$ GeV)
- precise determination of α_s is possible using these data
- significant dependence on PDF set observed (correlation between g and α_s)

Results: extraction of m_t^{pole} from $[N_{\text{jet}}^{0,1+}, M(t\bar{t}), y(t\bar{t})]$

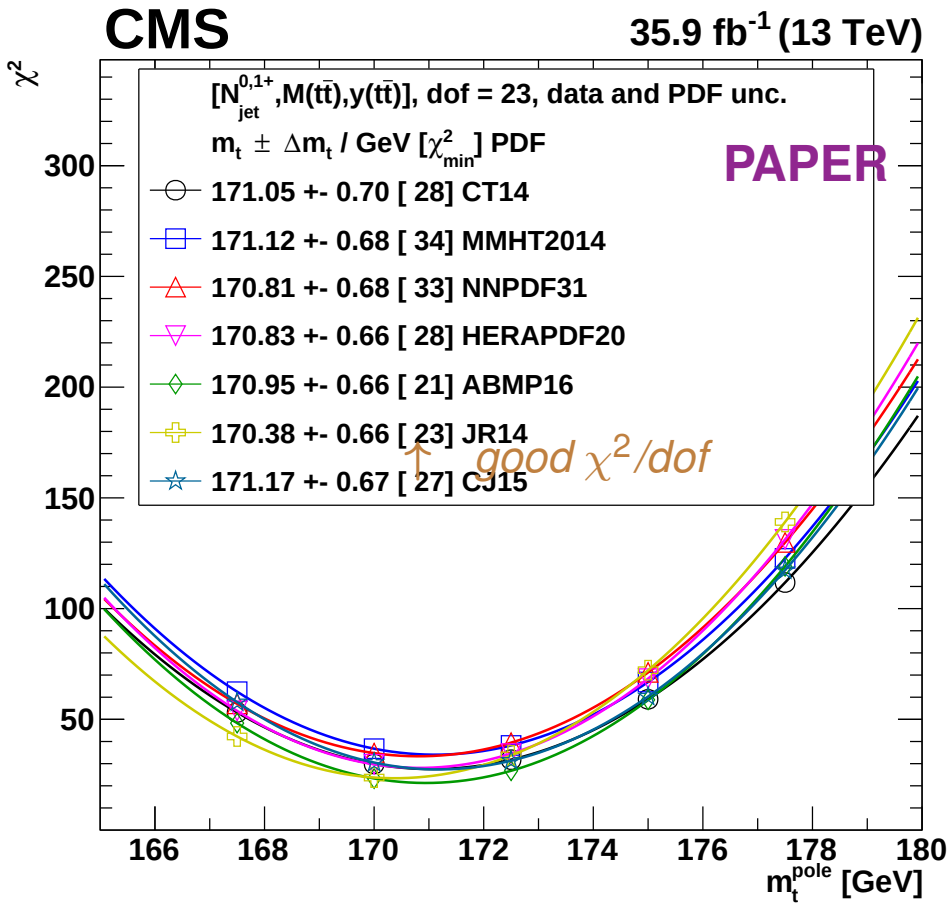

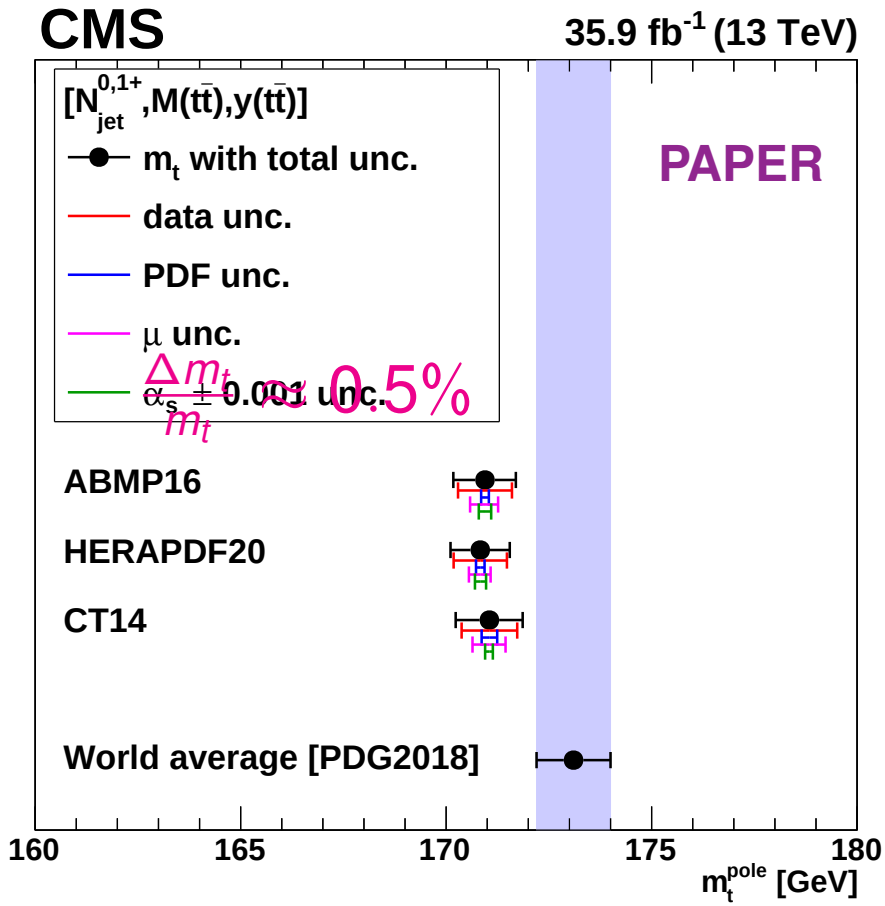

- used α_s from each PDF set ($\alpha_s = 0.118$ in CT and HERAPDF, $\alpha_s = 0.119$ in ABMP)
- precise determination of m_t^{pole} is possible using these data
- no significant dependence on PDF set

Cross checks

Cross checks for α_s and m_t^{pole} extraction (results in backup):

- using $[N_{\text{jet}}^{0,1,2+}, M(t\bar{t}), y(t\bar{t})]$
- using single-differential N_{jet}, $M(t\bar{t})$ or $y(t\bar{t})$ cross sections
- using $[p_T(t\bar{t}), M(t\bar{t}), y(t\bar{t})]$ cross sections with 2 $p_T(t\bar{t})$ bins
- extra checks requested by the ARC:
  - using unnormalised cross sections
  - using ratios of cross sections for 1+ to 0+ jets (R_j) in bins of $M(t\bar{t})$ and $y(t\bar{t})$ (similar to 3/2 jet ratio in p_T or η bins)

$\rightarrow$ consistent results obtained in all cross checks

$\rightarrow$ in this analysis, observables ($\frac{1}{\sigma}\frac{\mathrm{d}\sigma}{\mathrm{d}\ldots}$) have been chosen to have **maximum sensitivity to QCD paramaters and minimum experimental and scale uncertainties**

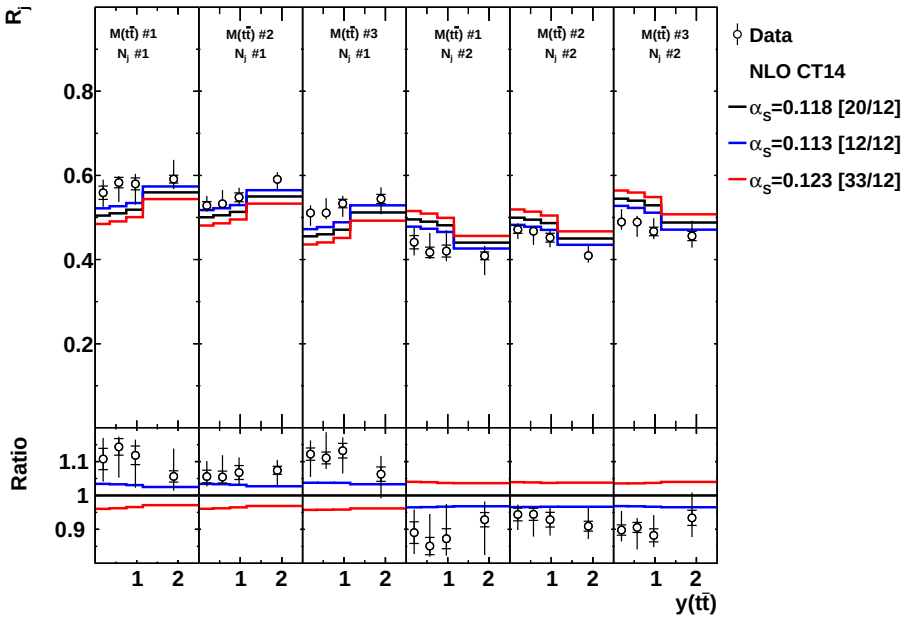

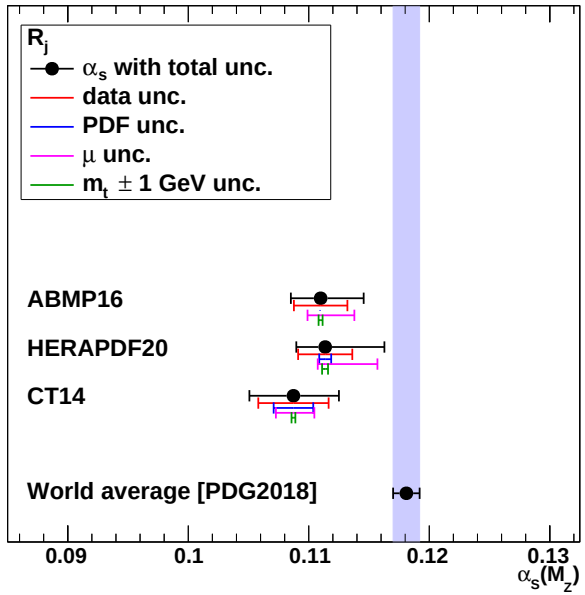

Remark on limitations in theory calculations

NLO is the only available theory publicly available today, but there are limitations:

- impact of missing threshold resummation is $\Delta m_t \sim 0.7$ GeV [Eur.Phys.J. C60 (2009) 375]
- impact of missing FSR resummation is $\Delta m_t \sim 0.5$ GeV [Eur. Phys. J. C73 (2013) 2438]
  - in general, good agreement between NLO and NLO+PS [Fig. 1 in Eur. Phys. J. C73 (2013) 2438]
- EW corrections could be a few % near threshold [Phys. Rev. D91 (2015) 014020] [JHEP10 (2017) 186]
- **most wanted is NNLO QCD (not exist for $t\bar{t}$ +jets)**

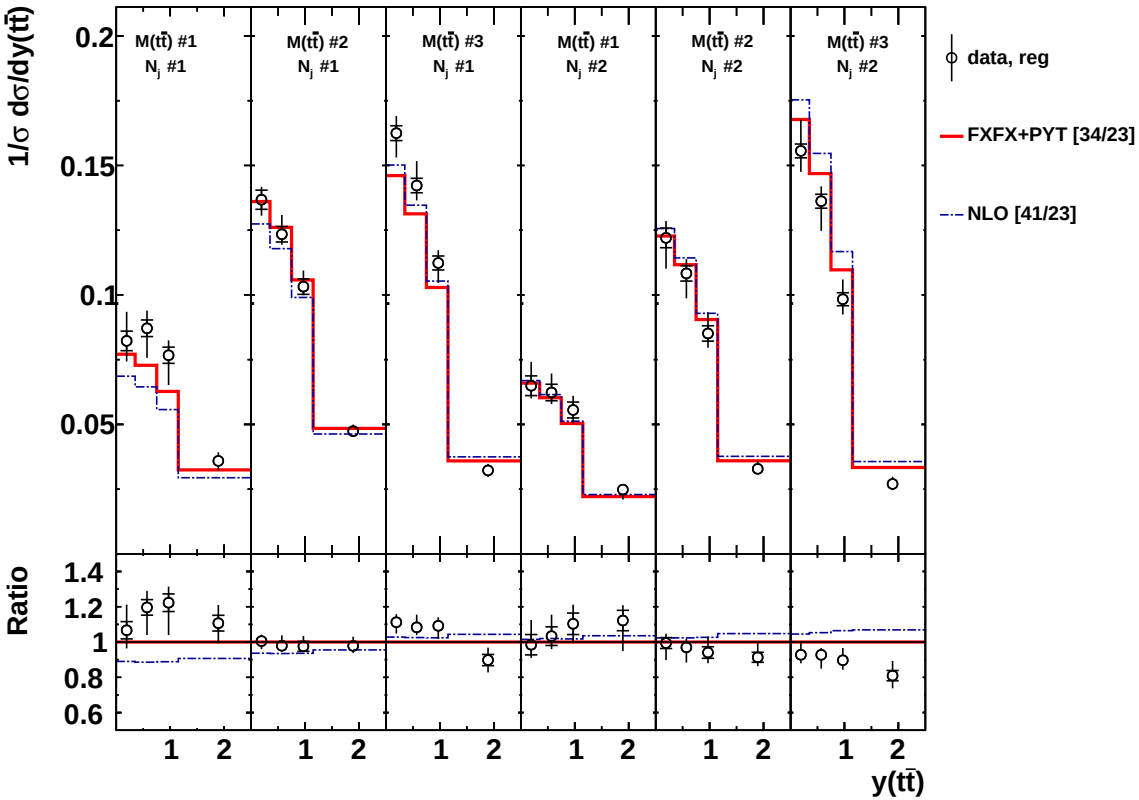

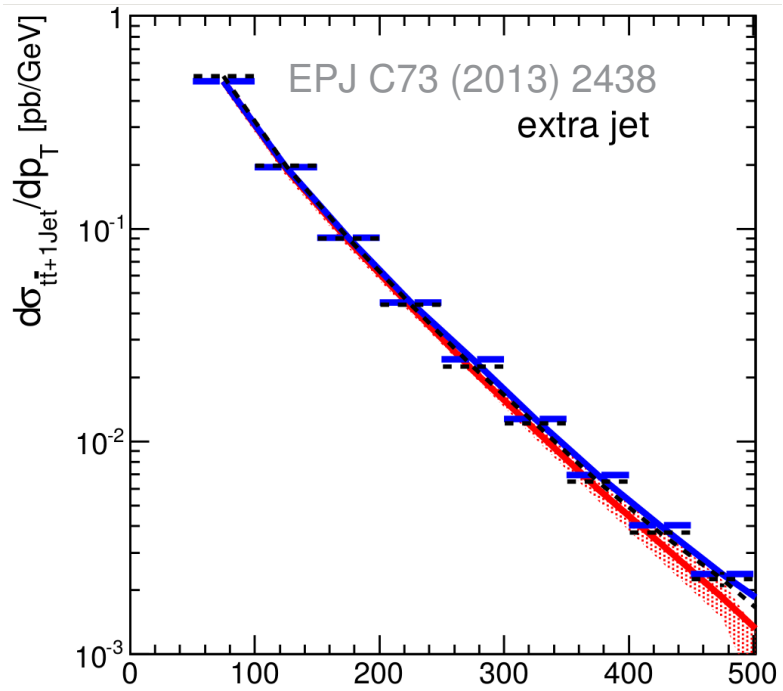

Simultaneous PDF + α_s + m_t^{pole} fit: results

- followed standard approach: using HERA DIS data only, or HERA + $t\bar{t}$ data to demonstrate added value from $t\bar{t}$ on PDF and α_s determination
- settings follow HERAPDF2.0 fit (very similar to TOP-14-013), use xFitter-2.0.0
- input data: combined HERA DIS [1506.06042] + $t\bar{t}$
- (further details in BACKUP)

Data sets	χ^2/dof	
	Nominal fit	$+[N_{\text{jet}}, y(t\bar{t}), M(t\bar{t})]$
CMS $t\bar{t}$		10/23
HERA CC e^-p, $E_p = 920$ GeV	55/42	55/42
HERA CC e^+p, $E_p = 920$ GeV	38/39	39/39
HERA NC e^-p, $E_p = 920$ GeV	218/159	217/159
HERA NC e^+p, $E_p = 920$ GeV	438/377	448/377
HERA NC e^+p, $E_p = 820$ GeV	70/70	71/70
HERA NC e^+p, $E_p = 575$ GeV	220/254	222/254
HERA NC e^+p, $E_p = 460$ GeV	219/204	220/204
Correlated χ^2	82	90
Log-penalty χ^2	+2	−7
Total χ^2/dof	1341/1130	1364/1151

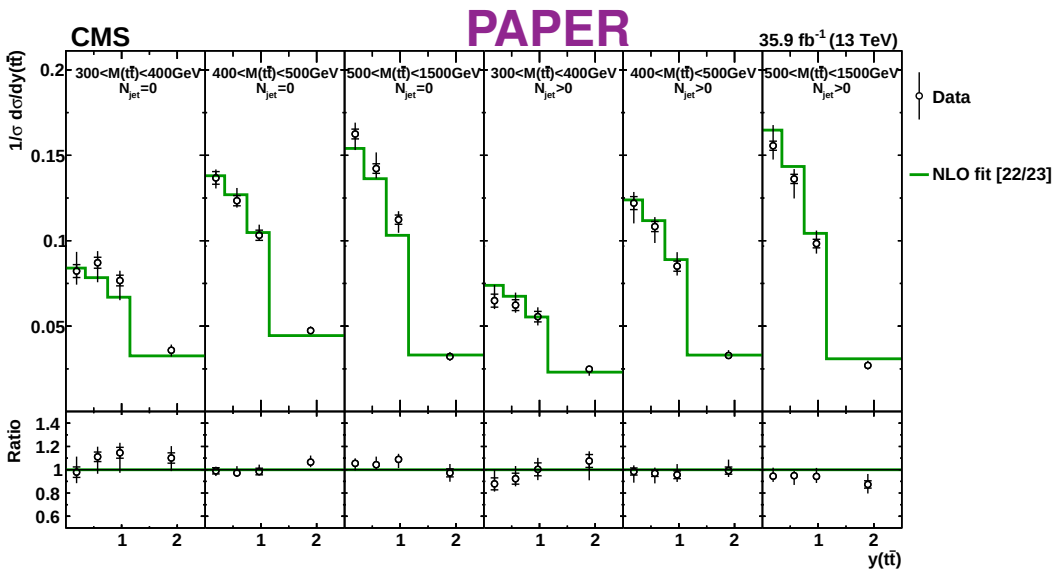

$$\alpha_s(M_Z) = 0.1135 \pm 0.0016(\text{fit})^{+0.0002}_{-0.0004}(\text{mod})^{+0.0008}_{-0.0001}(\text{par})^{+0.0011}_{-0.0005}(\text{scale}) = 0.1135^{+0.0021}_{-0.0017}(\text{total})$$

$$m_t^{\text{pole}} = 170.5 \pm 0.7(\text{fit})^{+0.1}_{-0.1}(\text{mod})^{+0.0}_{-0.1}(\text{par})^{+0.3}_{-0.3}(\text{scale})\ \text{GeV} = 170.5 \pm 0.8(\text{total})\ \text{GeV}$$

→ two SM parameters can be simultaneously determined from these data to high precision with only weak correlation between them ($\rho = 0.3$) + constraints on PDFs (next slides)

Simultaneous PDF + α_s + m_t^{pole} fit: correlation between α_s and gluon

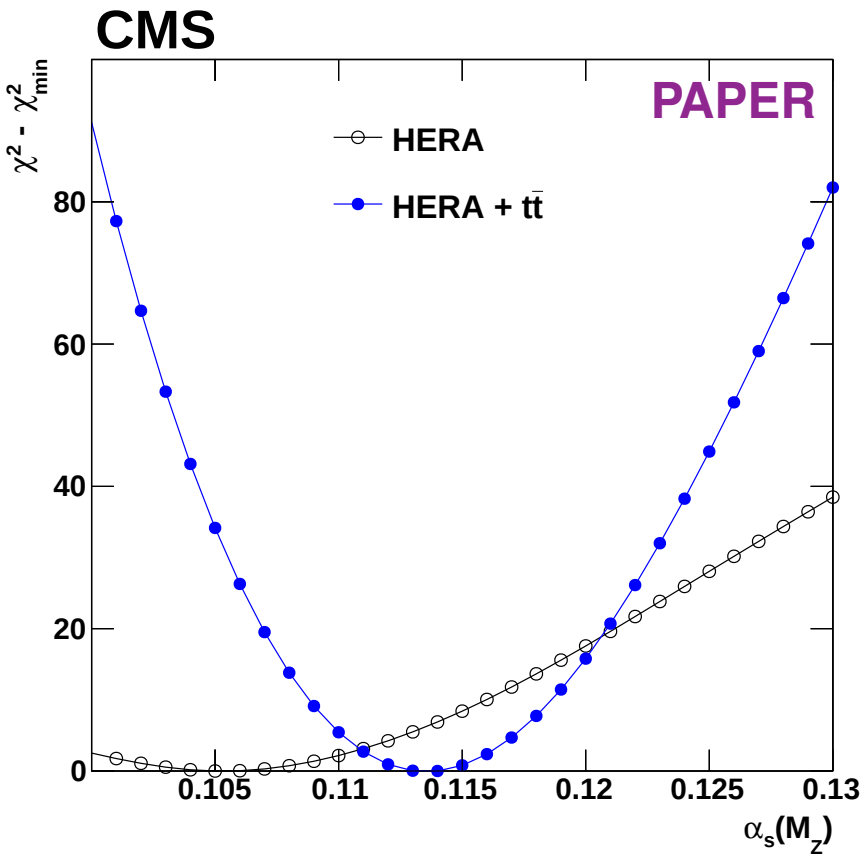

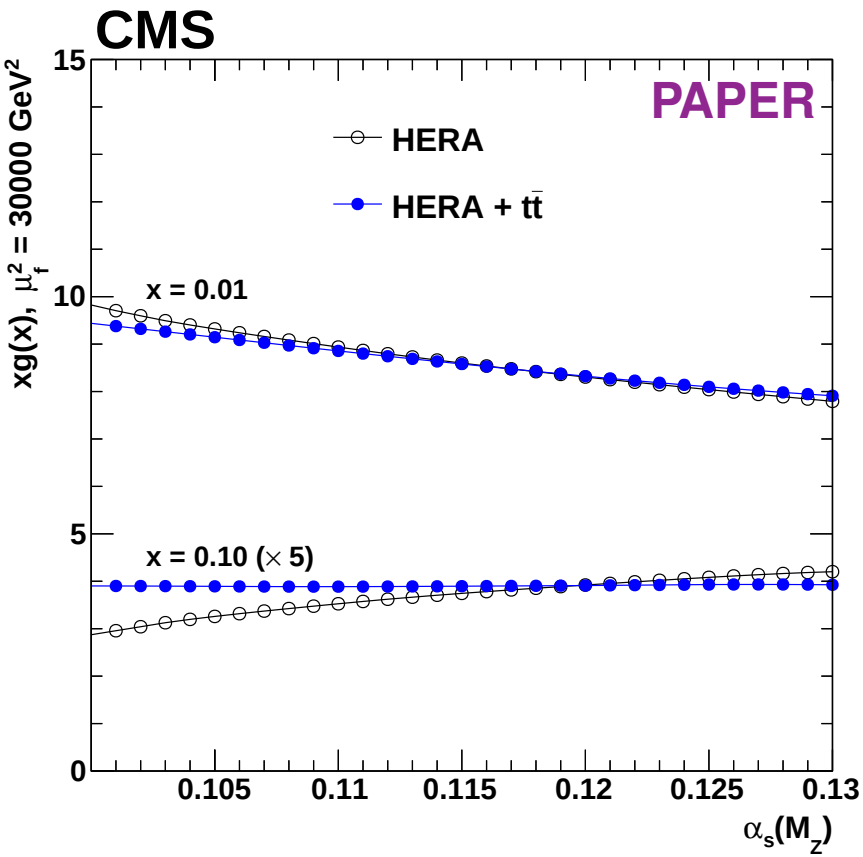

Adding $t\bar{t}$ data:

- constrain α_s (left)
- reduce correlation between α_s and g (right)
  - weak correlation (α_s,m_t) $\rightarrow$ weak correlation (g,m_t)

Simultaneous PDF + α_s + m_t^{pole} fit: Impact on PDFs

PDFs (α_s in HERA-only fit set to $\alpha_s = 0.1135 \pm 0.0016$):

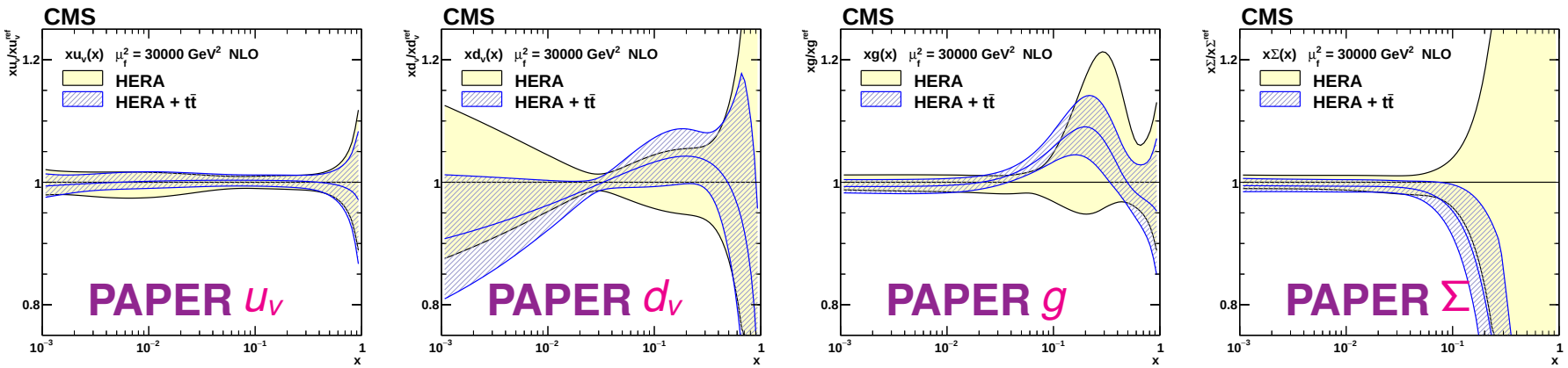

Relative PDF uncertainties (α_s in HERA-only fit set to $\alpha_s = 0.1137 \pm 0.0017$):

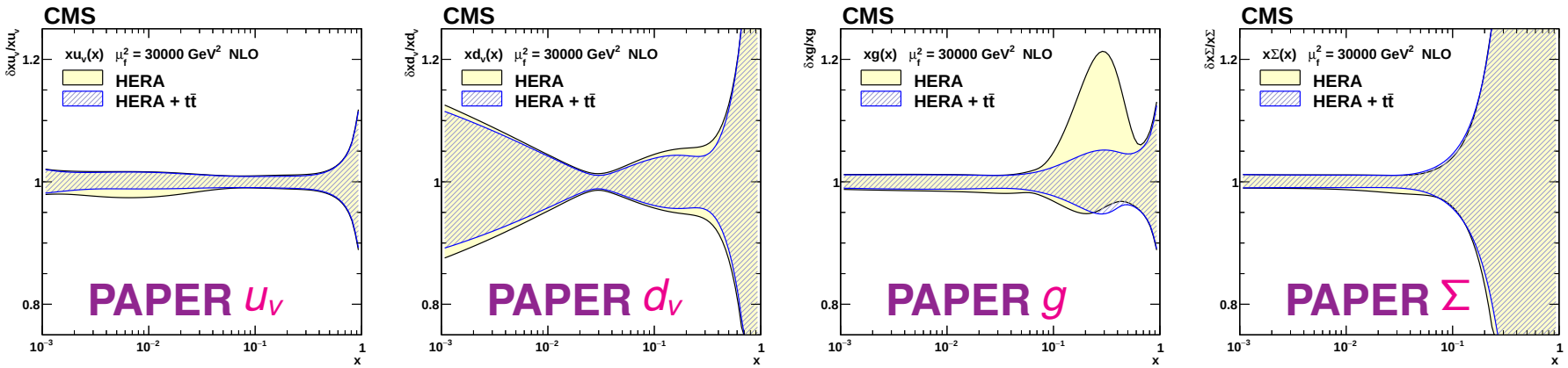

→ reduced g uncertainty at high x

→ smaller impact on other distributions via correlations in the fit

Analysis overview

1. Event selection (same as in 1D $t\bar{t}$ analysis)

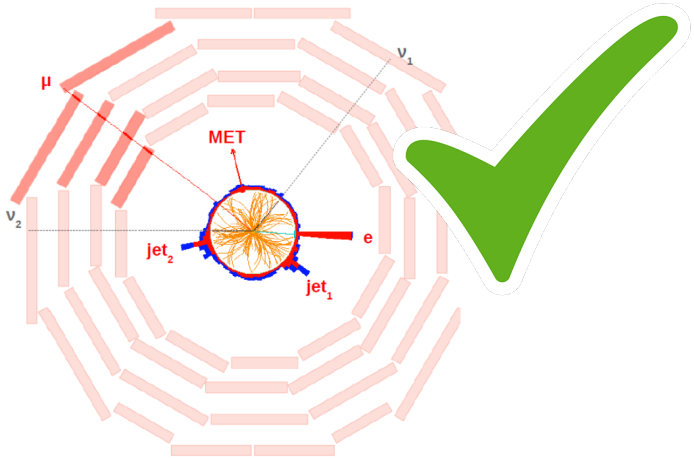

2. Kinematic reconstruction (same as in 1D $t\bar{t}$ analysis + loose)

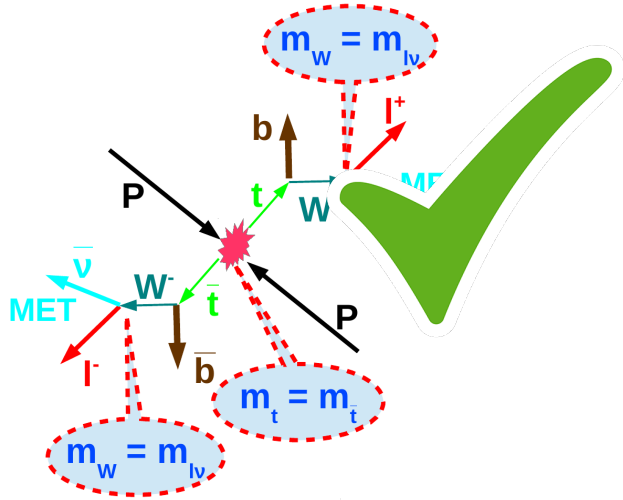

3. Unfolding and results

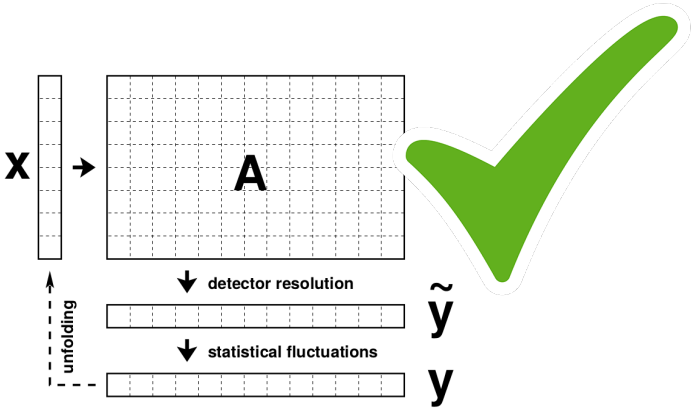

4. Data interpretation

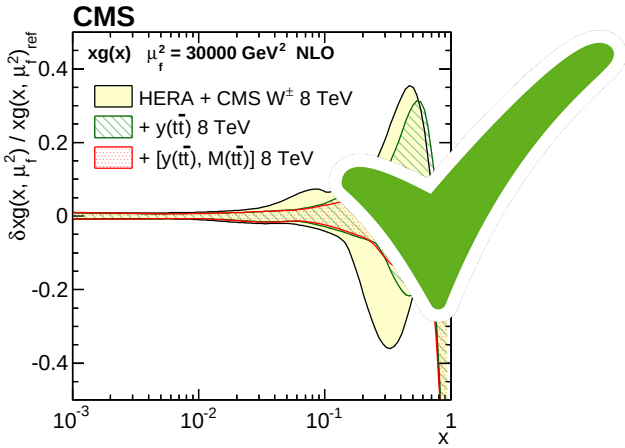

Summary

- Measured 2D and 3D $t\bar{t}$ cross section in dilepton channel using 2016 data
- Quantitative comparison to several MC predictions:
  - data can distinguish between predictions and reveal trends
  - NNLO from theorists is not yet available (last interaction was in April)
    - ★ what is the last chance to include new predictions?
- Used measured 3D cross sections to constrain α_s, m_t^{pole} and PDFs
  - first extraction of such kind using differential $t\bar{t}$ cross sections
  - most precise result on m_t^{pole} from single analysis to date:
    - ★ both exp. and theor. unc. are twice smaller than using total $\sigma(t\bar{t})$ [TOP-17-001]
    - ★ uncertainty on m_t^{pole} is comparable to PDG 2018
  - α_s and m_t^{pole} are extracted simultaneously
- Seek approval of this analysis

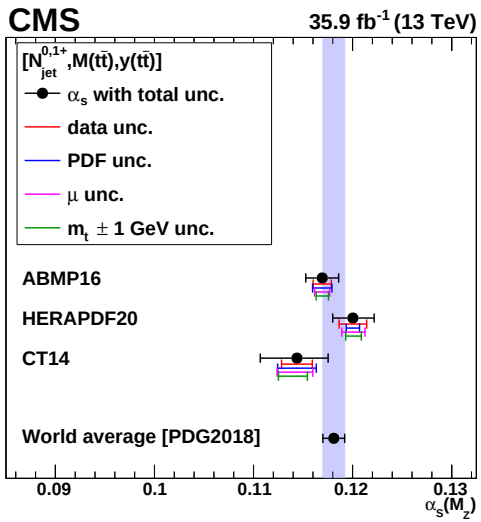

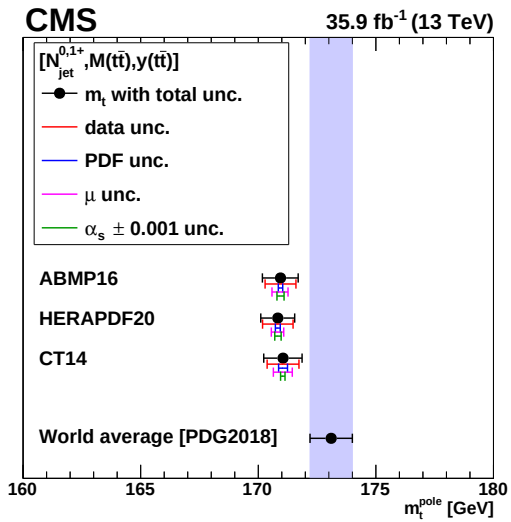

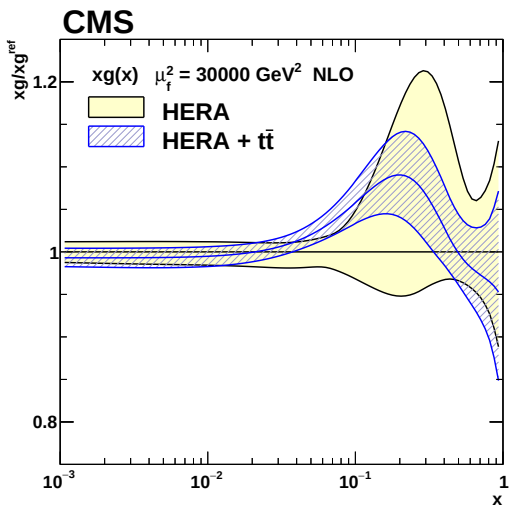

BACKUP

Triggers

(slide from TOP-17-014 preapproval talk)

Table 4: Triggers used in data for the three dilepton channels. The same trigger menu is configured for the use in MC.

channel	run	trigger
$\mu^+\mu^-$	B-G	HLT_Mu17_TrkIsoVVL_Mu8_TrkIsoVVL_v*
	B-G	HLT_Mu17_TrkIsoVVL_TkMu8_TrkIsoVVL_v*
	H	HLT_Mu17_TrkIsoVVL_Mu8_TrkIsoVVL_DZ_v*
	H	HLT_Mu17_TrkIsoVVL_TkMu8_TrkIsoVVL_DZ_v*
	B-H	HLT_IsoMu24_v*
	B-H	HLT_IsoTkMu24_v*
e^+e^-	B-H	HLT_Ele23_Ele12_CaloIdL_TrackIdL_IsoVL_DZ_v*
	B-H	HLT_Ele27_WPTight_Gsf_v*
$\mu^\pm e^\mp$	B-G	HLT_Mu23_TrkIsoVVL_Ele12_CaloIdL_TrackIdL_IsoVL_v*
	B-G	HLT_Mu8_TrkIsoVVL_Ele23_CaloIdL_TrackIdL_IsoVL_v*
	H	HLT_Mu23_TrkIsoVVL_Ele12_CaloIdL_TrackIdL_IsoVL_DZ_v*
	H	HLT_Mu8_TrkIsoVVL_Ele23_CaloIdL_TrackIdL_IsoVL_DZ_v*
	B-H	HLT_Ele27_WPTight_Gsf_v*
	B-H	HLT_IsoMu24_v*
	B-H	HLT_IsoTkMu24_v*

→ Logical “OR” between trigger paths is applied to select events in dilepton channel

→ Using dilepton and single lepton data streams & triggers:

- helps to improve trigger efficiency by ~10%
- same method as in inclusive cross section analysis (by T. Arndt):
  https://indico.cern.ch/event/591629/contributions/2387609/attachments/1382081/2101570/CrossSection1116.pdf

Event yields (table from the AN)

mm	2 leptons	2 jets	E_T^{miss}	b-tag	kin. rec. (loose)
$t\bar{t}$ signal	113221[6.2%]	82177[47.8%]	64896[65.9%]	59820[74.7%]	54900[77.1%] (56767[77.0%])
$t\bar{t}$ other via τ	17014[0.9%]	12284[7.1%]	9944[10.1%]	9138[11.4%]	8571[12.0%] (8722[11.8%])
$t\bar{t}$ other not via τ	1473[0.1%]	1179[0.7%]	863[0.9%]	690[0.9%]	578[0.8%] (597[0.8%])
tW	12816[0.7%]	4938[2.9%]	3883[3.9%]	3339[4.2%]	2273[3.2%] (2505[3.4%])
diboson	17769[1.0%]	1994[1.2%]	1090[1.1%]	352[0.4%]	193[0.3%] (213[0.3%])
W+jets	1508[0.1%]	212[0.1%]	186[0.2%]	163[0.2%]	77[0.1%] (77[0.1%])
Z+jets	1657927[91.0%]	69086[40.2%]	17675[17.9%]	6608[8.2%]	4589[6.4%] (4840[6.6%])
sum MC	1821728[100.0%]	171871[100.0%]	98537[100.0%]	80110[100.0%]	71182[100.0%] (73721[100.0%])
data	2032080	208732	104491	80359	70346 (72835)

em	2 leptons	2 jets	E_T^{miss}	b-tag	kin. rec. (loose)
$t\bar{t}$ signal	199005[57.2%]	145441[78.8%]	145441[78.8%]	134247[81.0%]	124422[82.0%] (127840[81.9%])
$t\bar{t}$ other via τ	30378[8.7%]	22020[11.9%]	22020[11.9%]	20262[12.2%]	19164[12.6%] (19444[12.5%])
$t\bar{t}$ other not via τ	2099[0.6%]	1697[0.9%]	1697[0.9%]	1382[0.8%]	1174[0.8%] (1212[0.8%])
tW	22816[6.6%]	8898[4.8%]	8898[4.8%]	7662[4.6%]	5486[3.6%] (5899[3.8%])
diboson	26640[7.7%]	2074[1.1%]	2074[1.1%]	684[0.4%]	406[0.3%] (444[0.3%])
W+jets	3943[1.1%]	457[0.2%]	457[0.2%]	121[0.1%]	50[0.0%] (100[0.1%])
Z+jets	63280[18.2%]	3883[2.1%]	3883[2.1%]	1366[0.8%]	1053[0.7%] (1081[0.7%])
sum MC	348160[100.0%]	184470[100.0%]	184470[100.0%]	165725[100.0%]	151755[100.0%] (156020[100.0%])
data	353773	184529	184529	164297	150410 (154444)

ee	2 leptons	2 jets	E_T^{miss}	b-tag	kin. rec. (loose)
$t\bar{t}$ signal	55219[7.4%]	40273[50.3%]	31730[68.0%]	29199[76.3%]	26573[78.8%] (27541[78.7%])
$t\bar{t}$ other via τ	7892[1.1%]	5753[7.2%]	4642[10.0%]	4256[11.1%]	3975[11.8%] (4048[11.6%])
$t\bar{t}$ other not via τ	341[0.0%]	274[0.3%]	201[0.4%]	169[0.4%]	144[0.4%] (147[0.4%])
tW	6319[0.9%]	2464[3.1%]	1970[4.2%]	1740[4.5%]	1146[3.4%] (1261[3.6%])
diboson	8171[1.1%]	1033[1.3%]	565[1.2%]	188[0.5%]	96[0.3%] (117[0.3%])
W+jets	1449[0.2%]	161[0.2%]	77[0.2%]	52[0.1%]	25[0.1%] (25[0.1%])
Z+jets	662424[89.3%]	30079[37.6%]	7455[16.0%]	2653[6.9%]	1754[5.2%] (1860[5.3%])
sum MC	741815[100.0%]	80036[100.0%]	46641[100.0%]	38257[100.0%]	33714[100.0%] (35000[100.0%])
data	867766	100137	51336	39984	34890 (36188)

ll	2 leptons	2 jets	E_T^{miss}	b-tag	kin. rec. (loose)
$t\bar{t}$ signal	367445[12.6%]	267891[61.4%]	242067[73.4%]	223267[78.6%]	205895[80.2%] (212147[80.1%])
$t\bar{t}$ other via τ	55284[1.9%]	40058[9.2%]	36607[11.1%]	33655[11.8%]	31710[12.4%] (32213[12.2%])
$t\bar{t}$ other not via τ	3913[0.1%]	3149[0.7%]	2761[0.8%]	2241[0.8%]	1896[0.7%] (1957[0.7%])
tW	41950[1.4%]	16301[3.7%]	14751[4.5%]	12741[4.5%]	8905[3.5%] (9665[3.7%])
diboson	52580[1.8%]	5101[1.2%]	3730[1.1%]	1225[0.4%]	695[0.3%] (774[0.3%])
W+jets	6901[0.2%]	829[0.2%]	719[0.2%]	335[0.1%]	153[0.1%] (203[0.1%])
Z+jets	2383631[81.9%]	103048[23.6%]	29012[8.8%]	10628[3.7%]	7396[2.9%] (7781[2.9%])
sum MC	2911703[100.0%]	436377[100.0%]	329648[100.0%]	284092[100.0%]	256650[100.0%] (264740[100.0%])
data	3253619	493398	340356	284640	255646 (263467)

Reconstructed $M(t\bar{t})$ vs generated $M(t\bar{t})$

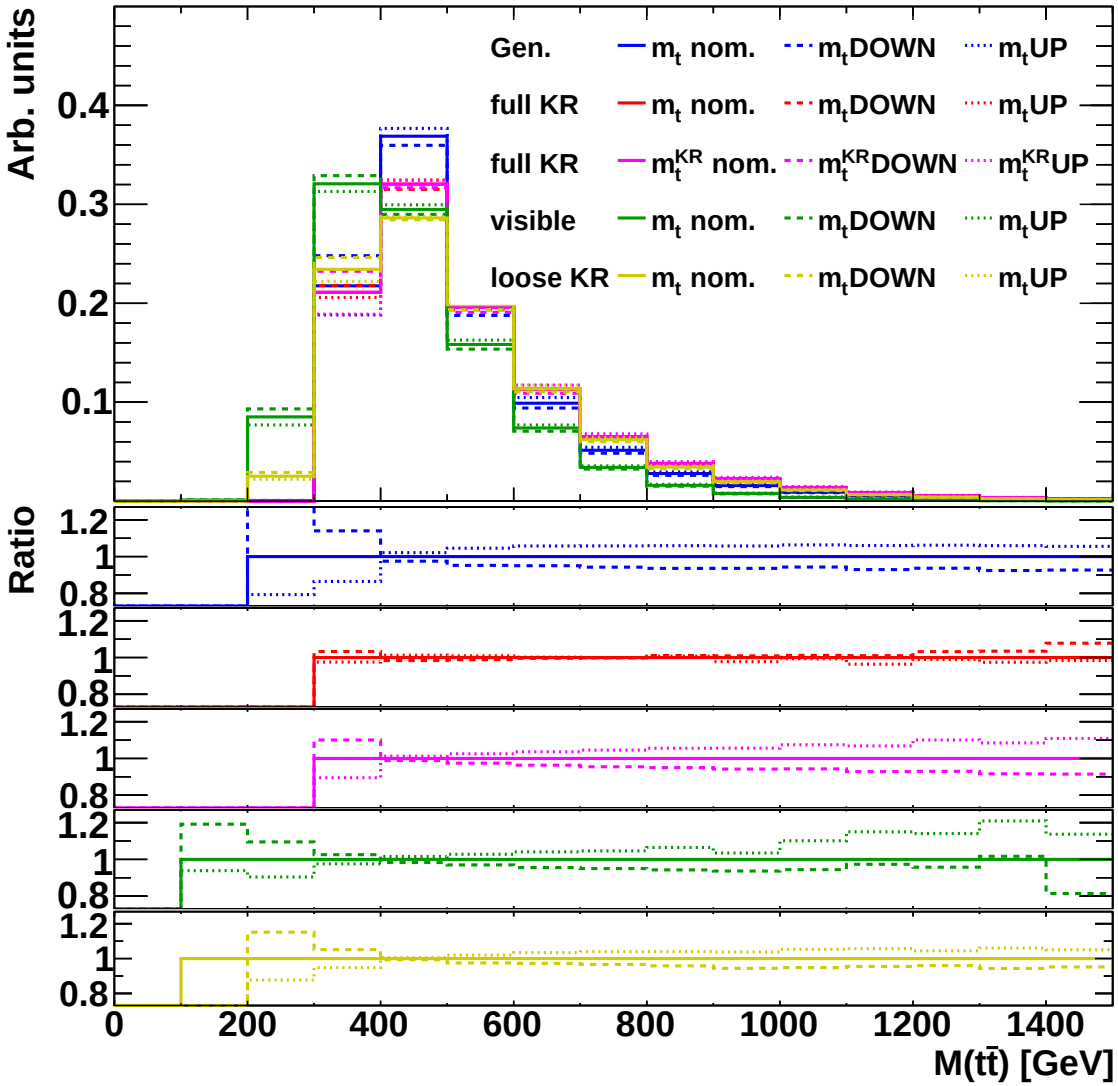

- All distributions are normalised to same area

  $\rightarrow m_t$ variation affects lowest $M(t\bar{t})$ bins, effect at high $M(t\bar{t})$ is via normalisation
- 'full KR': reconstucted $M(t\bar{t})$ is not sensitive to MC m_t, but sensitive to m_t^{KR} constraint
- 'visible':
  $\nu\bar{\nu}_{X,Y} = \mathrm{MET}_{X,Y}$
  $\nu\bar{\nu}_Z = 0$, $\nu\bar{\nu}_E = \mathrm{MET}_E$
- 'loose KR':
  $\nu\bar{\nu}_{X,Y} = \mathrm{MET}_{X,Y}$
  $\nu\bar{\nu}_{Z,E} = l\bar{l}_{Z,E}$
- 'visible' and 'loose KR' provide $M(t\bar{t})$ with unbiased (but smeared) sensitivity to m_t

Simple example: imagine algorithm which always restores same distribution independently of input
$\Rightarrow$ *unfolded distribution == generated distribution, no impact of data*

Choice of $M(lb) < 180$ GeV cut

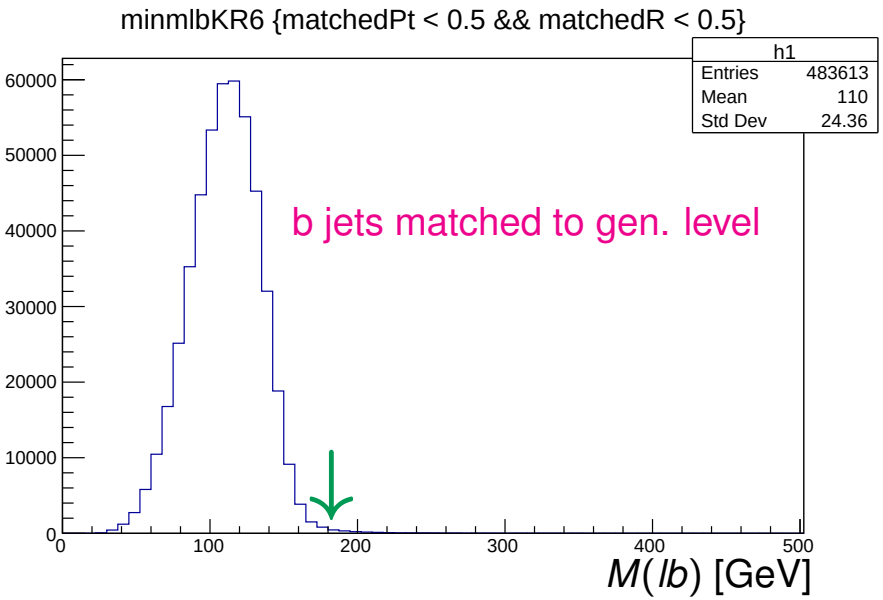

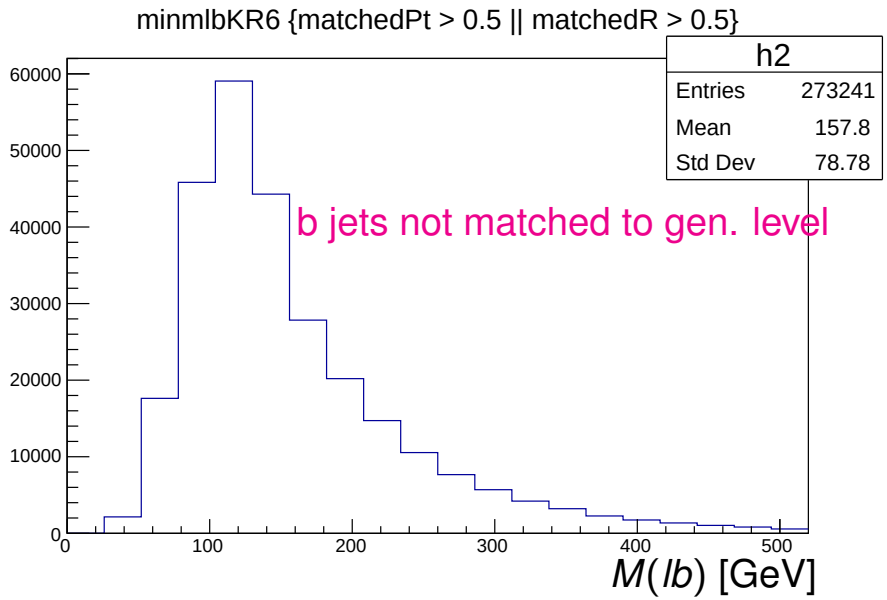

- For each of two jet-lepton assignments, maximum $M(lb)$ of two 'legs' is taken
- Then minimum $M(lb)$ over two jet-lepton assignments is taken
- It is plotted separately in events when b jets matched or not matched to true-level b jets (also accounting for two possible lepton-jet assignments):
  - cut at $M(lb) < M(lb)_{\text{max}} = 180$ GeV reduces combinatorics significantly while not yet introduces dependence of measured $M(t\bar{t})$ cross section on this cut

Performance of kinematic reconstruction

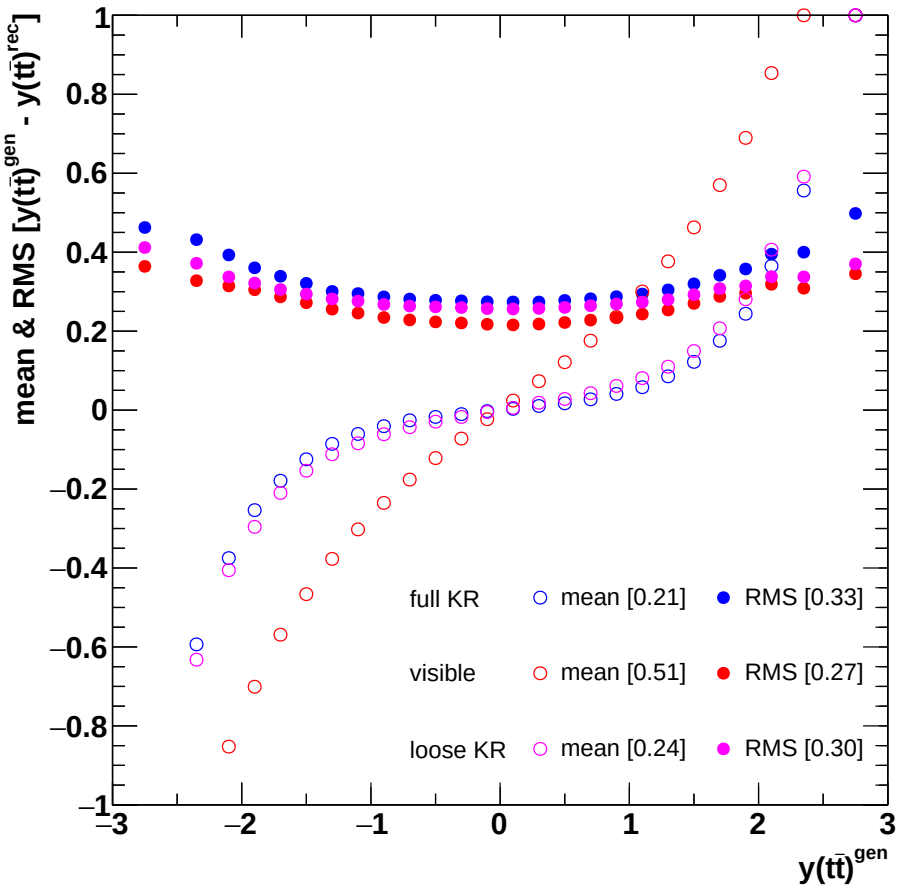

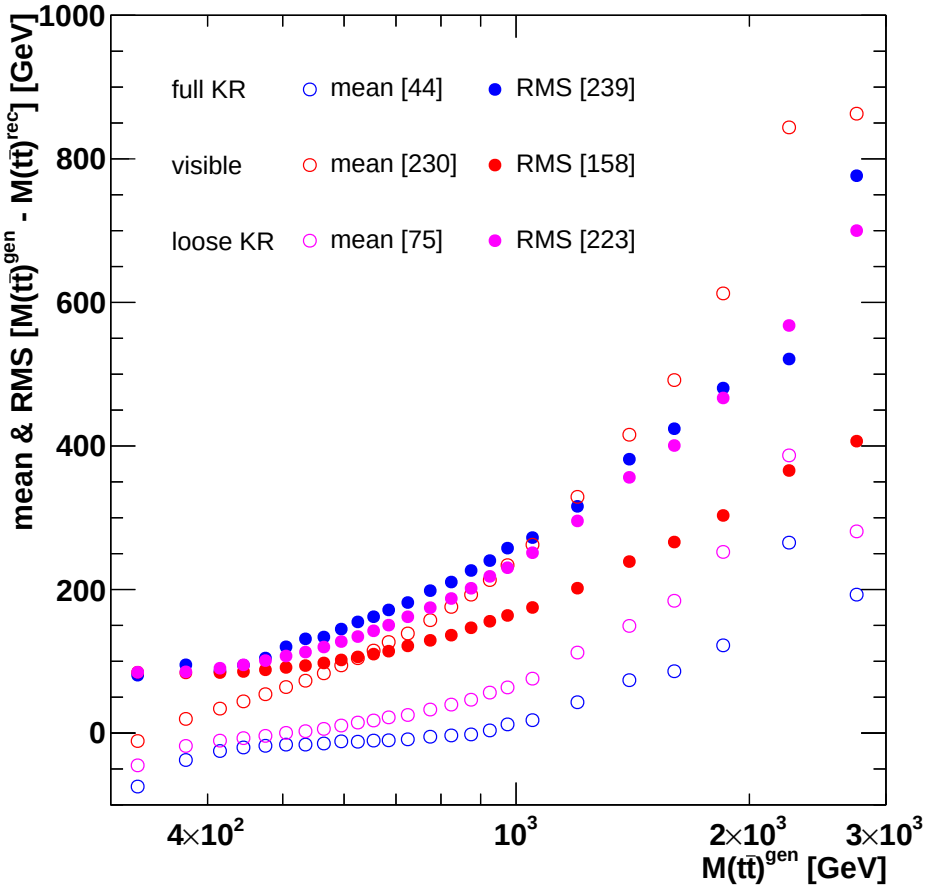

- similar performance of 'loose KR' and 'full KR' ('visible': $p_z(\nu\bar{\nu}) = 0$, not used)

  $\rightarrow$ use 'loose KR' for unfolding of 3D $[N_{\text{jet}}, M(t\bar{t}), y(t\bar{t})]$ to eliminate dependence on MC m_t and use these measured cross sections for PDF+α_s +m_t^{pole} extraction

  $\rightarrow$ use 'full KR' for all other 2D cross sections (allows reconstruction of t, $\bar{t}$)

Performance of loose kinematic reconstruction w/ and w/o $M(lb)$ GeV cut

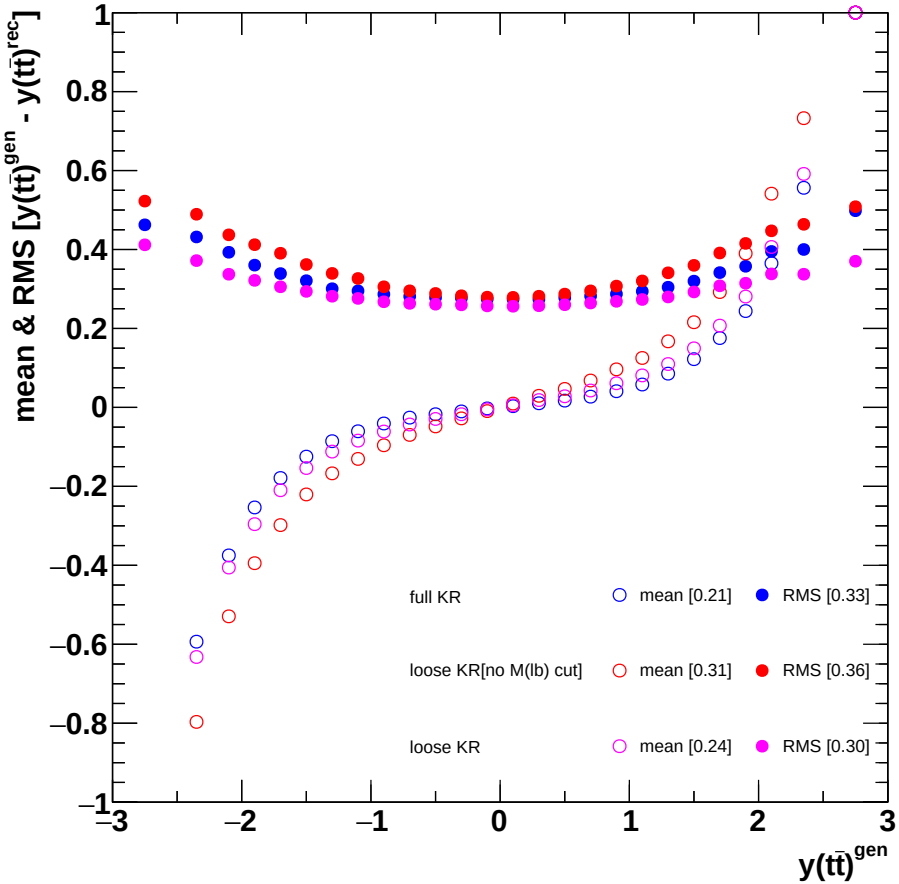

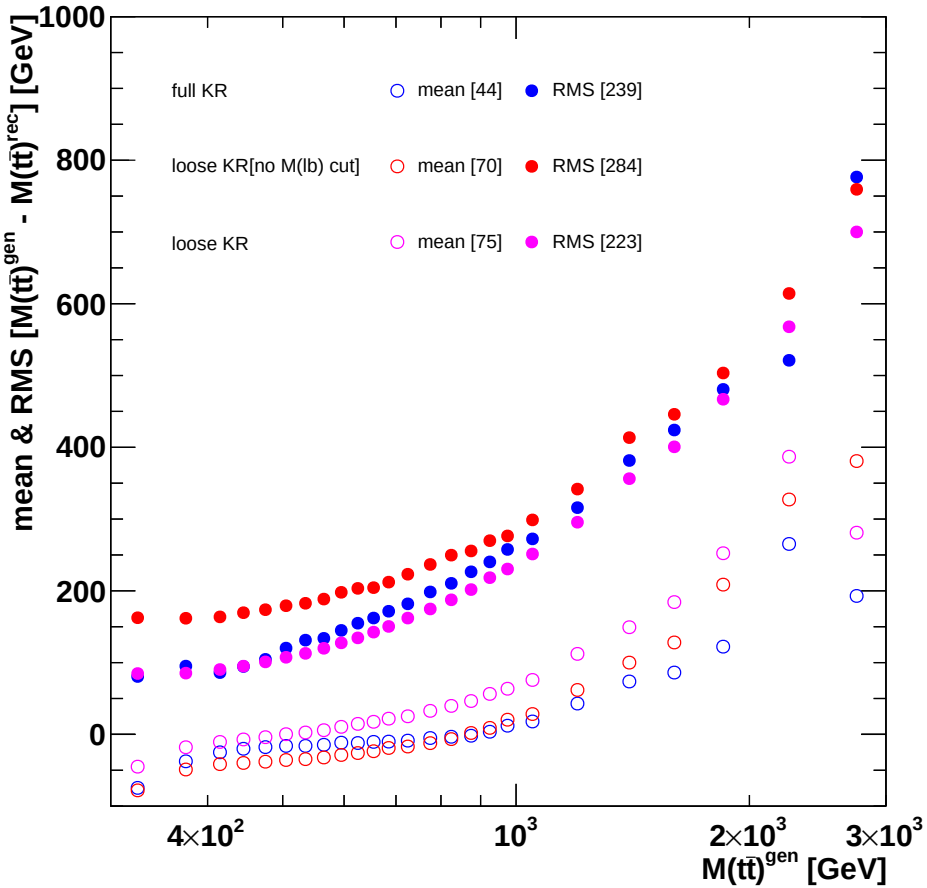

- $M(lb)$ reduces fraction of wrong b jets used in loose KR
  $\rightarrow$ improves resolution significantly, making it similar to full KR

Performance of kinematic reconstruction: $M(t\bar{t})$

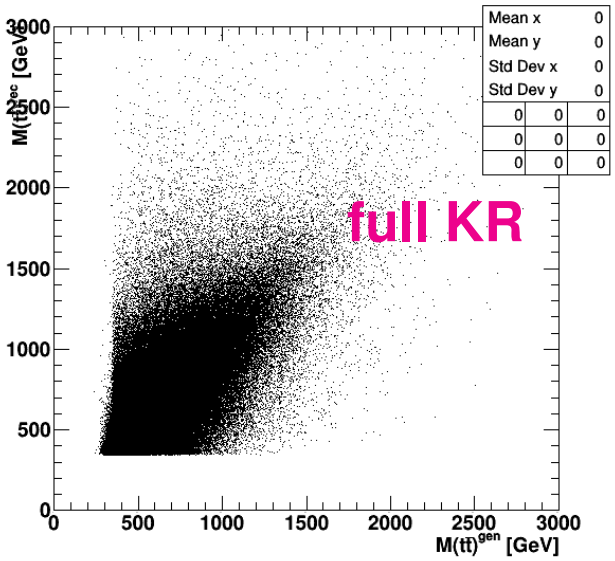

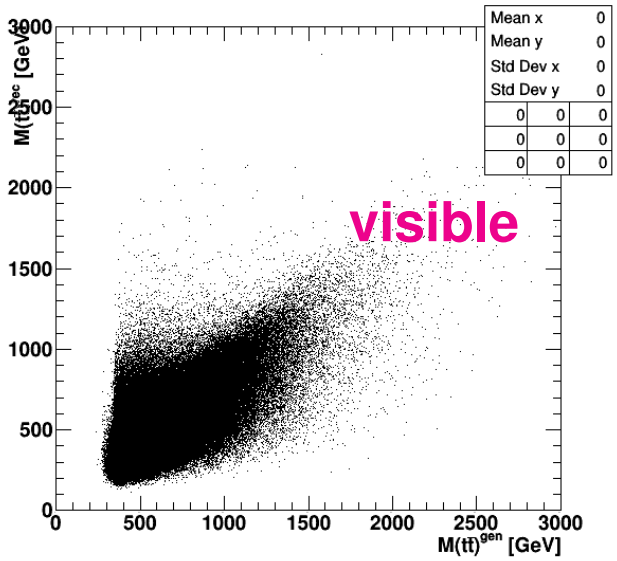

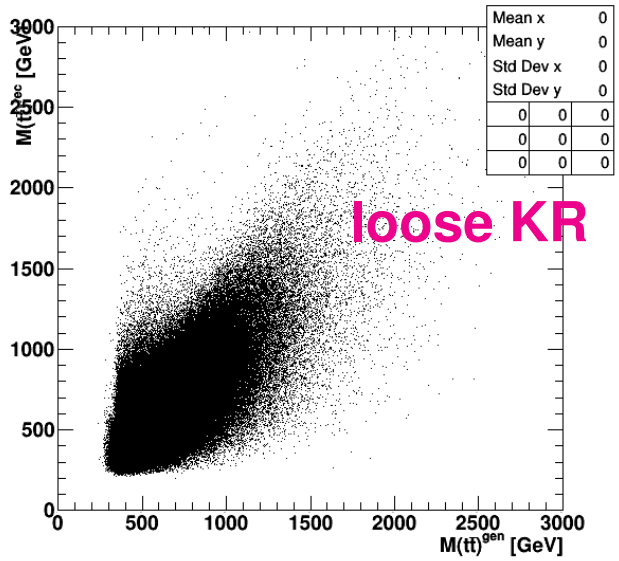

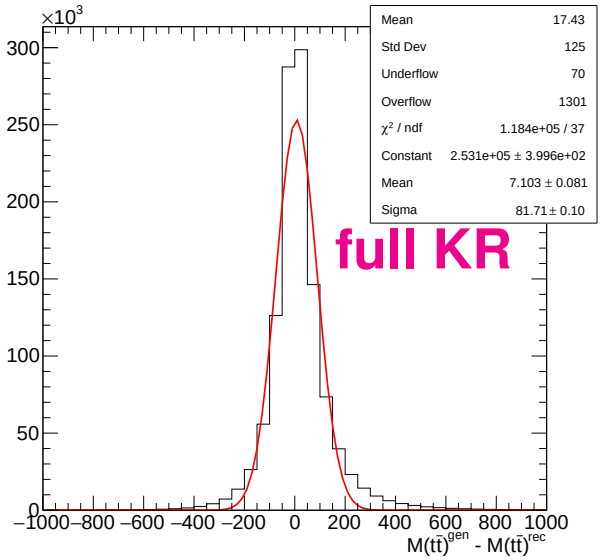

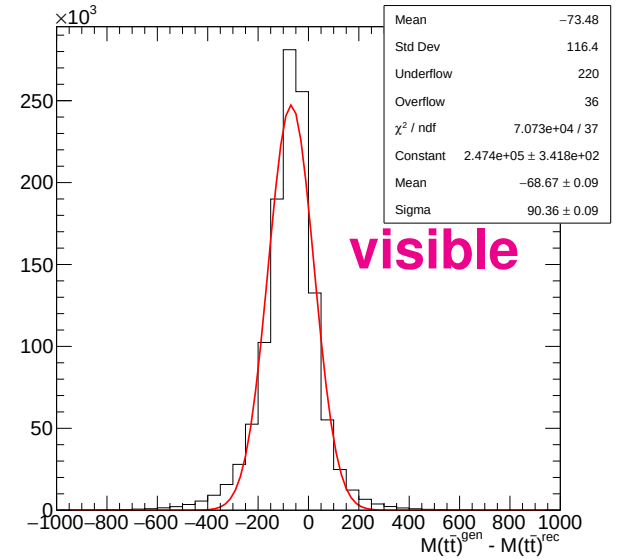

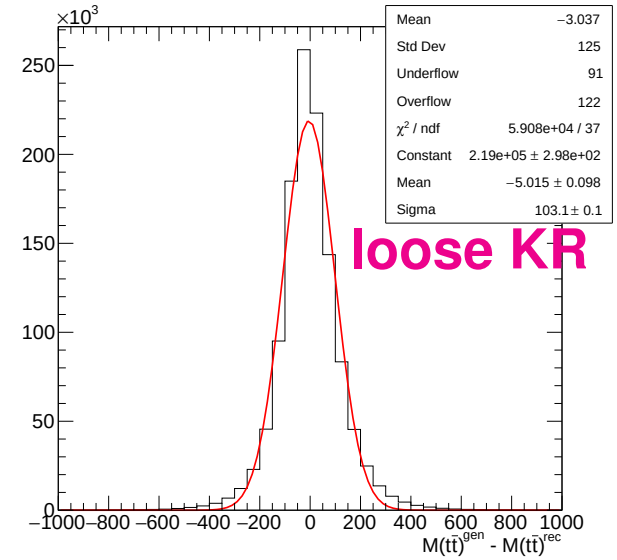

Performance of kinematic reconstruction: $y(t\bar{t})$

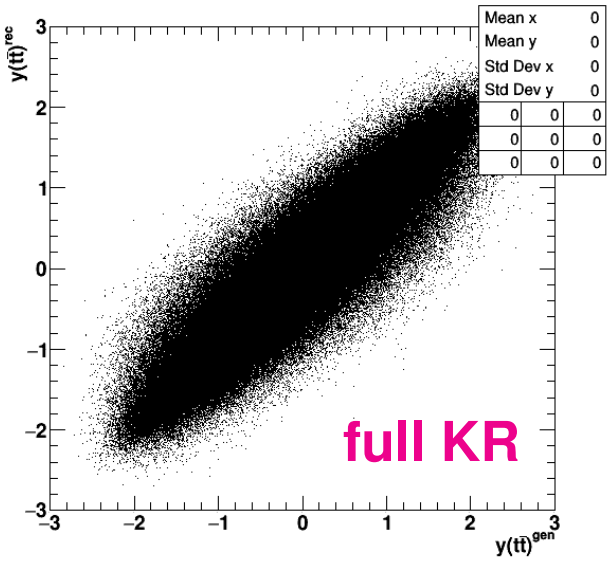

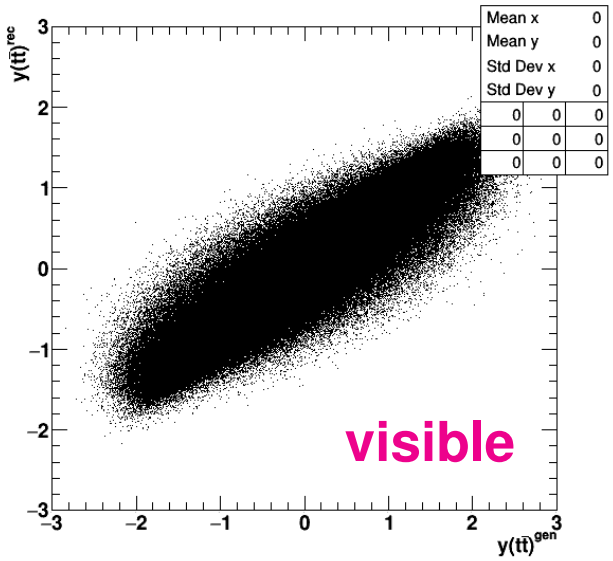

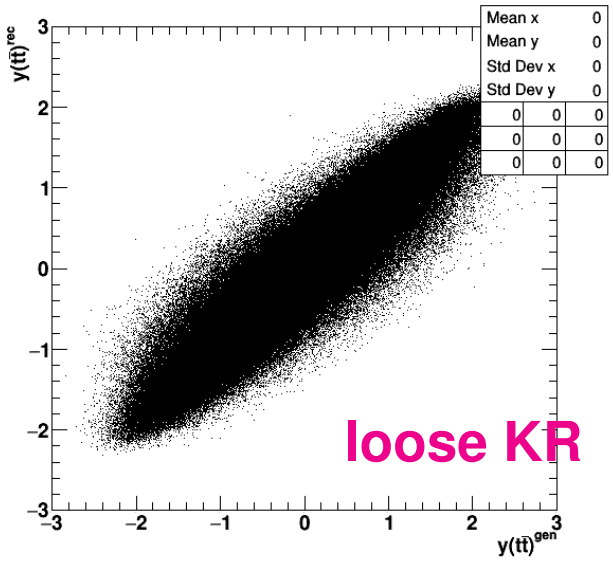

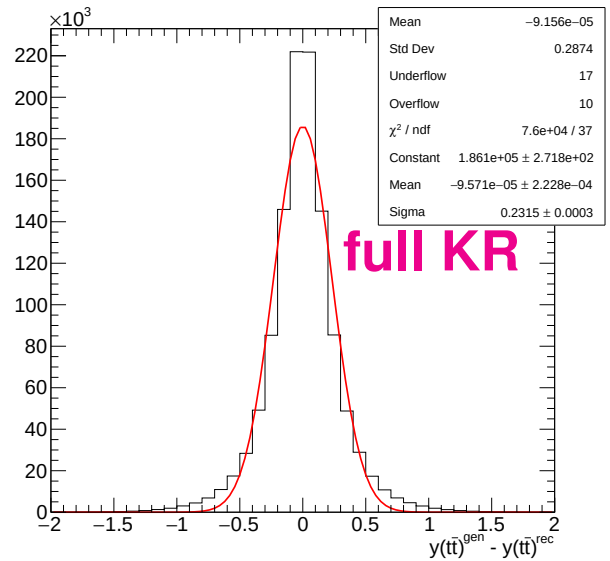

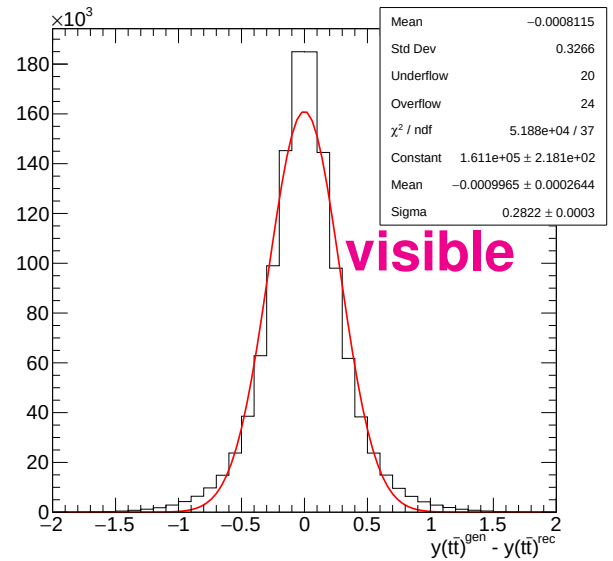

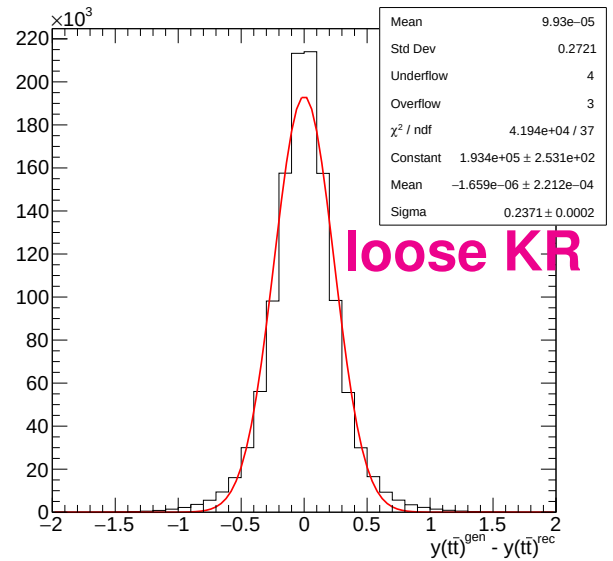

Closure tests: description

Closure tests following arXiv:1611.01972
(S. Schmitt “Data Unfolding Methods in High Energy Physics”):

(0) ‘data test’: $\chi^2 = (\boldsymbol{Ax} - \boldsymbol{y})^T (\boldsymbol{V_{yy}})^{-1} (\mathbf{Ax} - \mathbf{y})$ (folding back)

- expect χ^2-distribution with $\mathrm{dof} = \mathrm{M_y} - \mathrm{M_x}$

(sanity check)

(1) insert $\boldsymbol{y} = \boldsymbol{\mu}^{\mathrm{truth}} = \boldsymbol{Ax}^{\mathrm{truth}}$

- expect $\boldsymbol{x} = \boldsymbol{x}^{\mathrm{truth}}$

(trivial check)

(2) draw $\boldsymbol{y}$ from $\boldsymbol{\mu}^{\mathrm{truth}}$ assuming Poisson statistics, repeat many times getting $\boldsymbol{x}^{\mathrm{avg}} = \langle \boldsymbol{x} \rangle$, $(\boldsymbol{V_{xx}^{\mathrm{avg}}})_{jk} = \langle (x_j - x_j^{\mathrm{avg}})(x_k - x_k^{\mathrm{avg}}) \rangle$:

- expect $\boldsymbol{x}^{\mathrm{avg}} = \boldsymbol{x}^{\mathrm{truth}}$
- expect $\boldsymbol{V_{xx}^{\mathrm{avg}}} = \langle \boldsymbol{V_{xx}} \rangle$

(test statistical properties: how good is estimator)

(3) draw $\boldsymbol{y}$ from modified $\boldsymbol{\mu}^{\mathrm{mod}} = \boldsymbol{Ax}^{\mathrm{mod}}$:

- expect $\boldsymbol{x} = \boldsymbol{x}^{\mathrm{mod}}$

(test absence of systematic bias caused by differences between MC and truth)

Summary of unfolding closure tests

Full description and results in appendix, only summary is shown here:

Test \Unfolding	bin-by-bin	Unregularised	Regularised
Data test	n/a	passed	passed
Truth test	passed	passed	passed
Toy test	smallest unc., bias within unc.	largest unc., no bias	moderate unc., no bias
Reweighting test	always fails	always passed	passed if reweighting $\lesssim 25\%$

- Have chosen regularised unfolding which offers reasonable trade-off between variance and bias
  - bias is well covered for MC with up to $\sim 25\%$ mismodelled cross sections
- StatCom questionnaire filled

Closure test (0) (example for $[M(t\bar{t}), y(t\bar{t})]$)

Regularised unfolding $[M(t\bar{t}), y(t\bar{t})]$

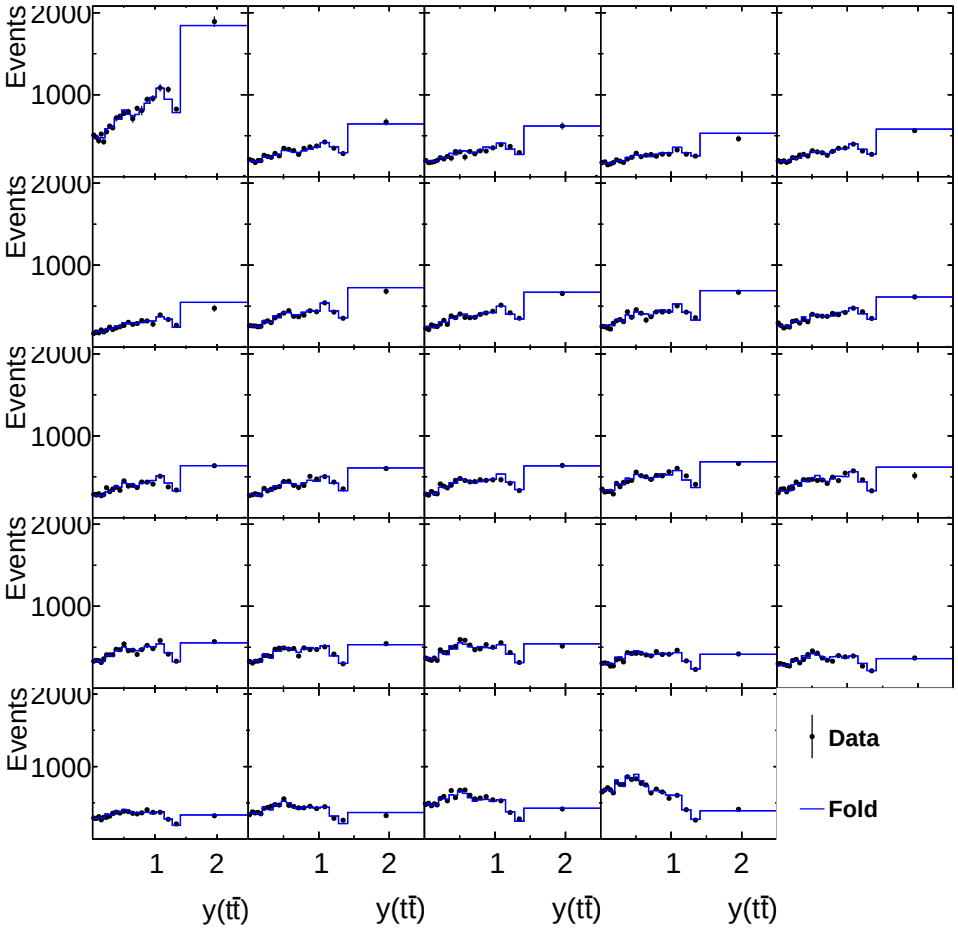

Ratio

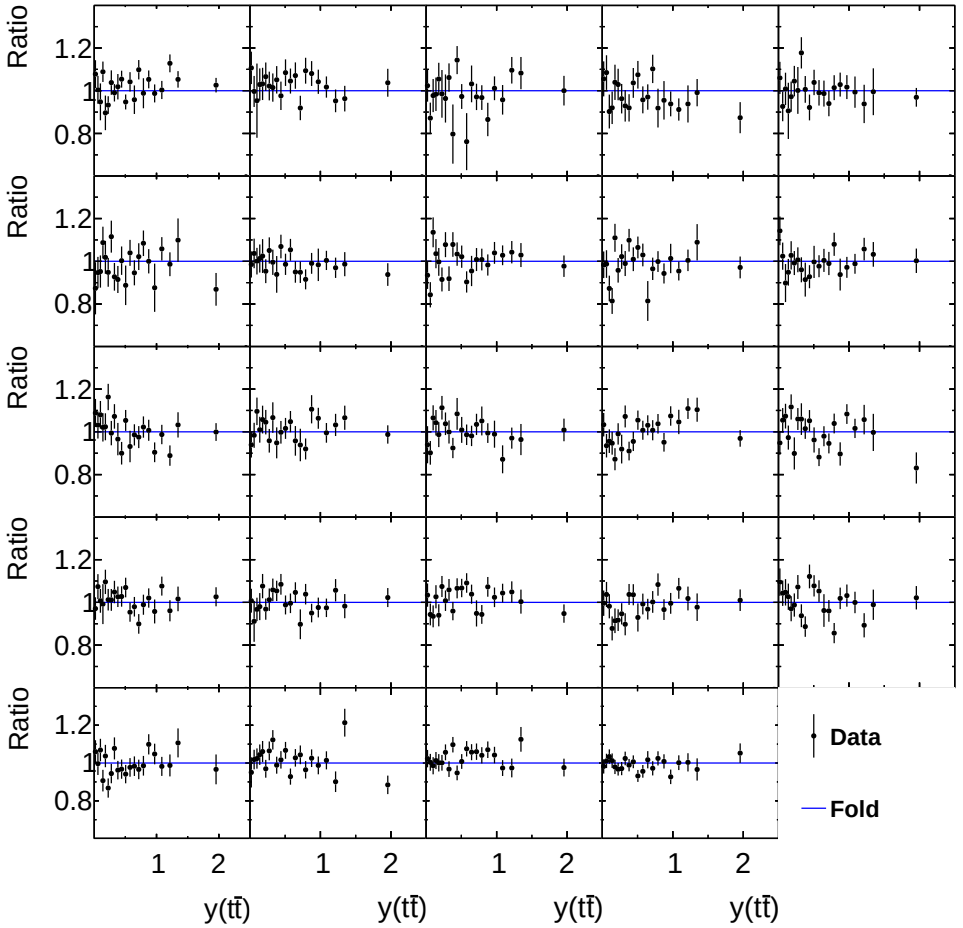

$\chi^2/\mathrm{dof} = 574.2/487$ (+8.6 from $\mathcal{L}_2$)

Closure test (1) (example for $[M(t\bar{t}), y(t\bar{t})]$)

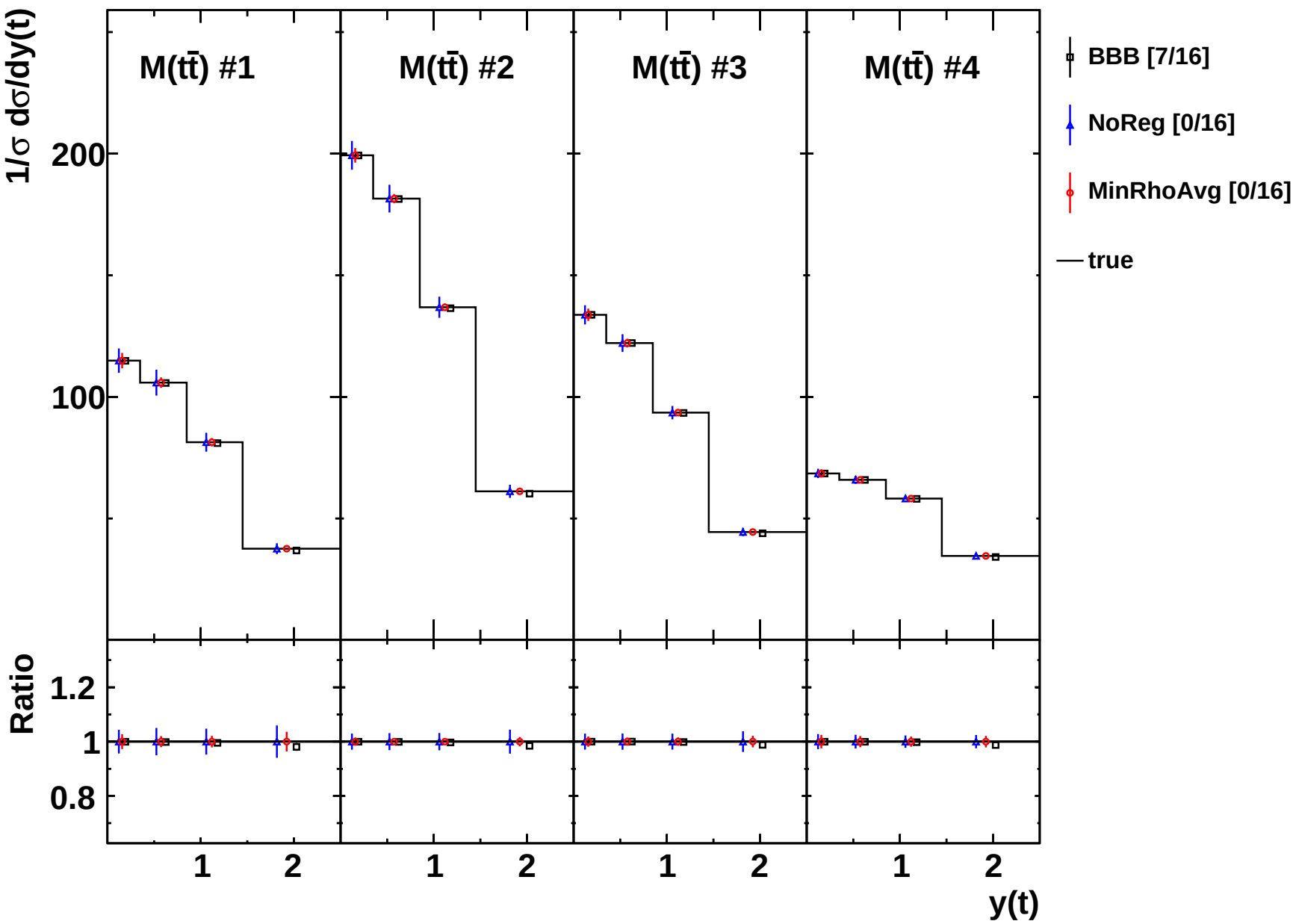

Closure test (2) (example for $[M(t\bar{t}), y(t\bar{t})]$)

- 1000 toy detector-level distributions ($\boldsymbol{y}$) drawn from nominal MC ($\boldsymbol{x}^{\text{truth}}$) assuming data Poisson uncertainties
- perform unfolding for each toy distribution
- obtain $\boldsymbol{x}^{\text{avg}}$, $\boldsymbol{V}_{\boldsymbol{xx}}^{\text{avg}}$ by averaging over all toys

Look at:

- residuals $\boldsymbol{x} - \boldsymbol{x}^{\text{truth}}$ (in bins and total):
  - expect 0 mean ($\boldsymbol{x}^{\text{avg}} = \boldsymbol{x}^{\text{truth}}$)
  - aim for minimum RMS (smallest uncertainties Δx)
- pulls $\left(\boldsymbol{x} - \boldsymbol{x}^{\text{truth}}\right) / \Delta \boldsymbol{x}$ (in bins and total):
  - expect 0 mean
  - expect 1 RMS
- $\boldsymbol{V}_{\boldsymbol{xx}}^{\text{avg}}$ vs $\langle \boldsymbol{V}_{\boldsymbol{xx}} \rangle$ (plots provided in backup):
  - expect agreement
- χ^2 of $\boldsymbol{x}$ vs $\boldsymbol{x}^{\text{truth}}$ (accounts for bin-to-bin correlations, plots in backup):
  - expect χ^2 distribution for $\text{dof} = M_x$

Closure test (2): residuals (example for $[M(t\bar{t}), y(t\bar{t})]$)

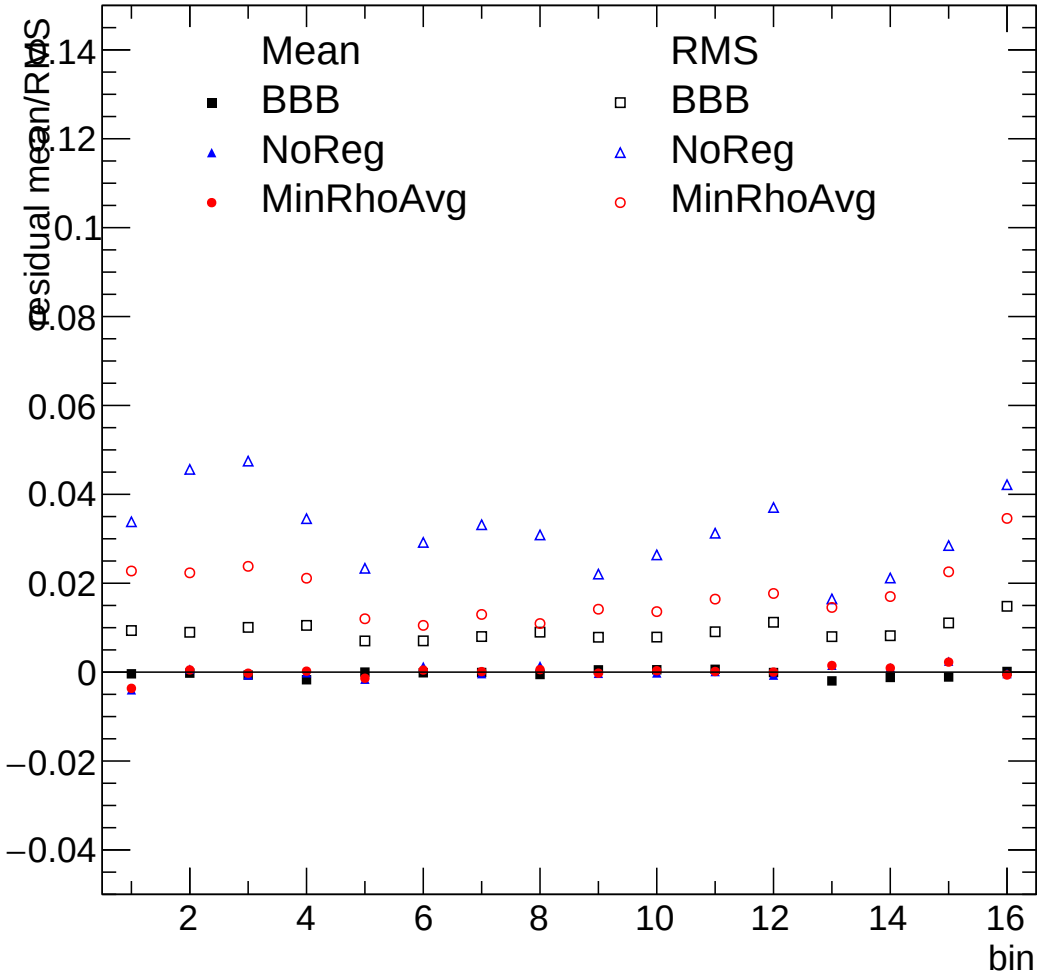

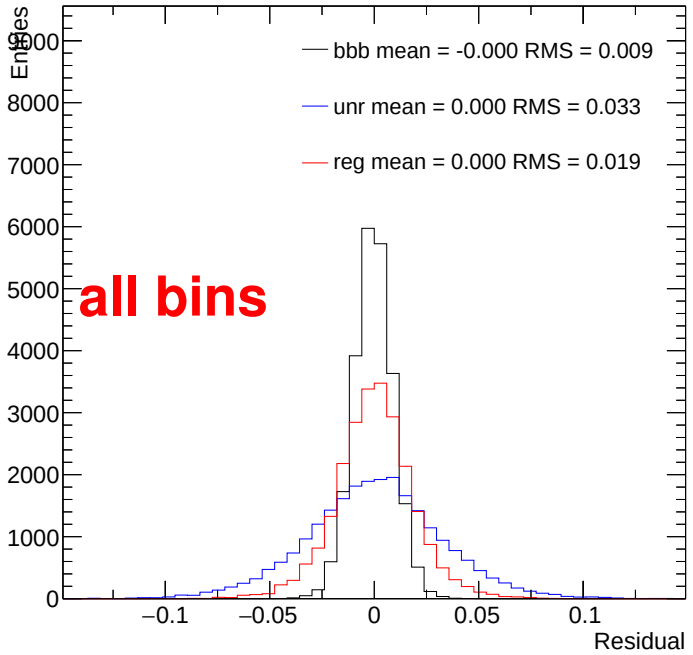

- Smallest uncertainties ‘BBB’, then reg. unfolding, then unreg. unfolding
- Largest biases for ‘BBB’, however within uncertainties
- Unreg. and reg. unfolding: no sizable biases

Closure test (2): pulls and χ^2 (example for $[M(t\bar{t}), y(t\bar{t})]$)

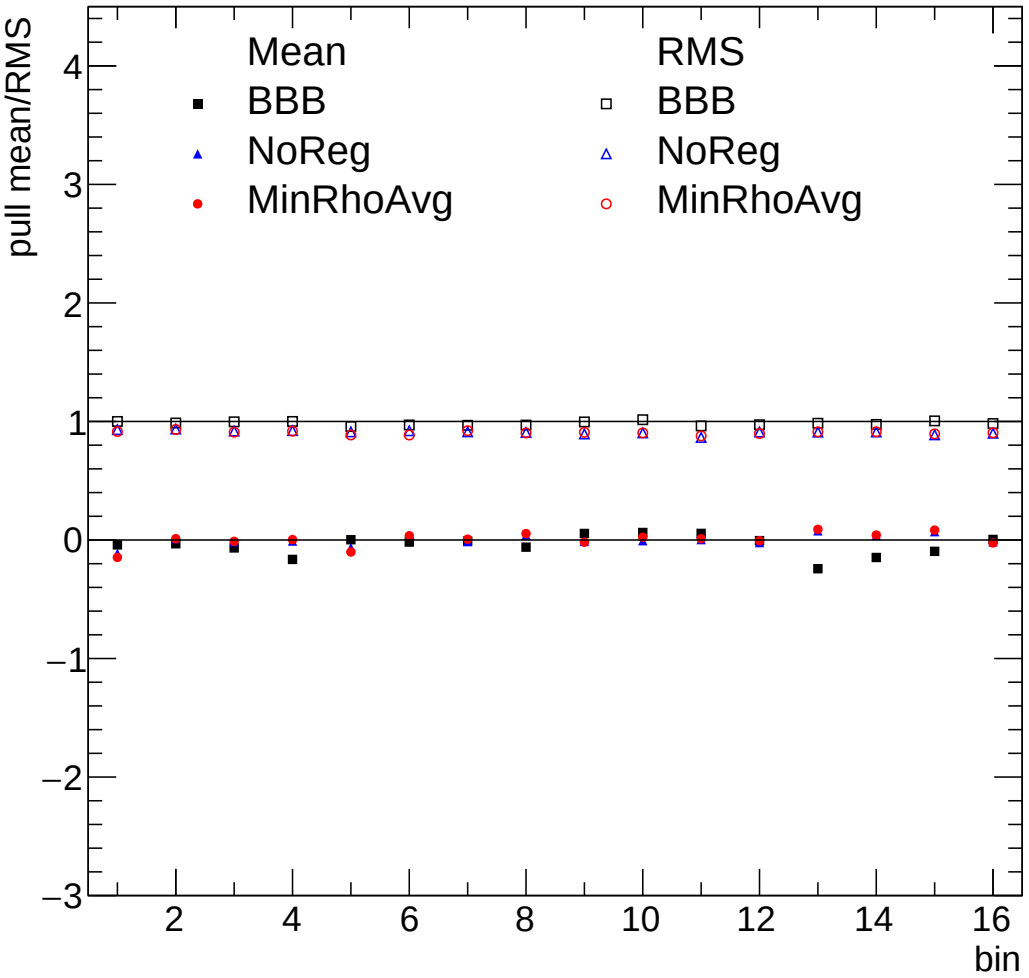

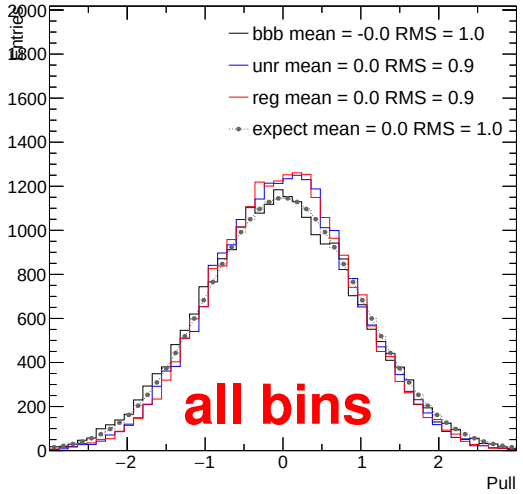

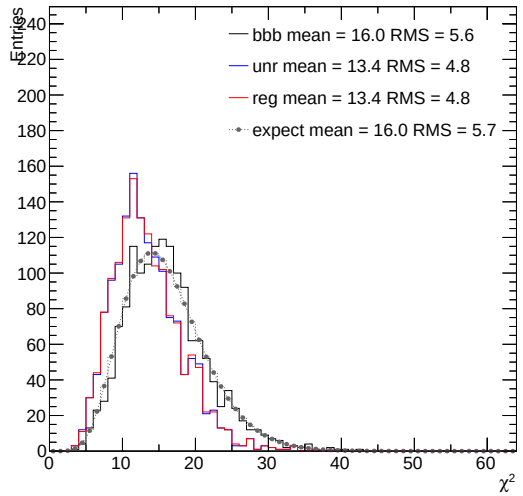

- All algorithms perform well within uncertainties
- However, 'BBB' produces visible bias (still within uncertainties)

Closure test (3) (example for $[M(t\bar{t}), y(t\bar{t})]$)

- Manually modify MC x-section by reweighting as function of $M(t\bar{t})$, $y(t\bar{t})$
- Function used:

$$w = Ax^B(1-x)^C(1+Dx+Ex^2), x = \frac{y - y_{\text{min}}}{y_{\text{max}} - y_{\text{min}}}$$

  with $A \ldots E$ free parameters
  (but preserving normalisation of the total x-section)
- Unfolding performed using response matrix and bias vector from unmodified MC
- Several tests performed which differ by the amplitude of reweighting

Closure test (3): moderate reweighting ($\lesssim 5\%$) $[M(t\bar{t}), y(t\bar{t})]$

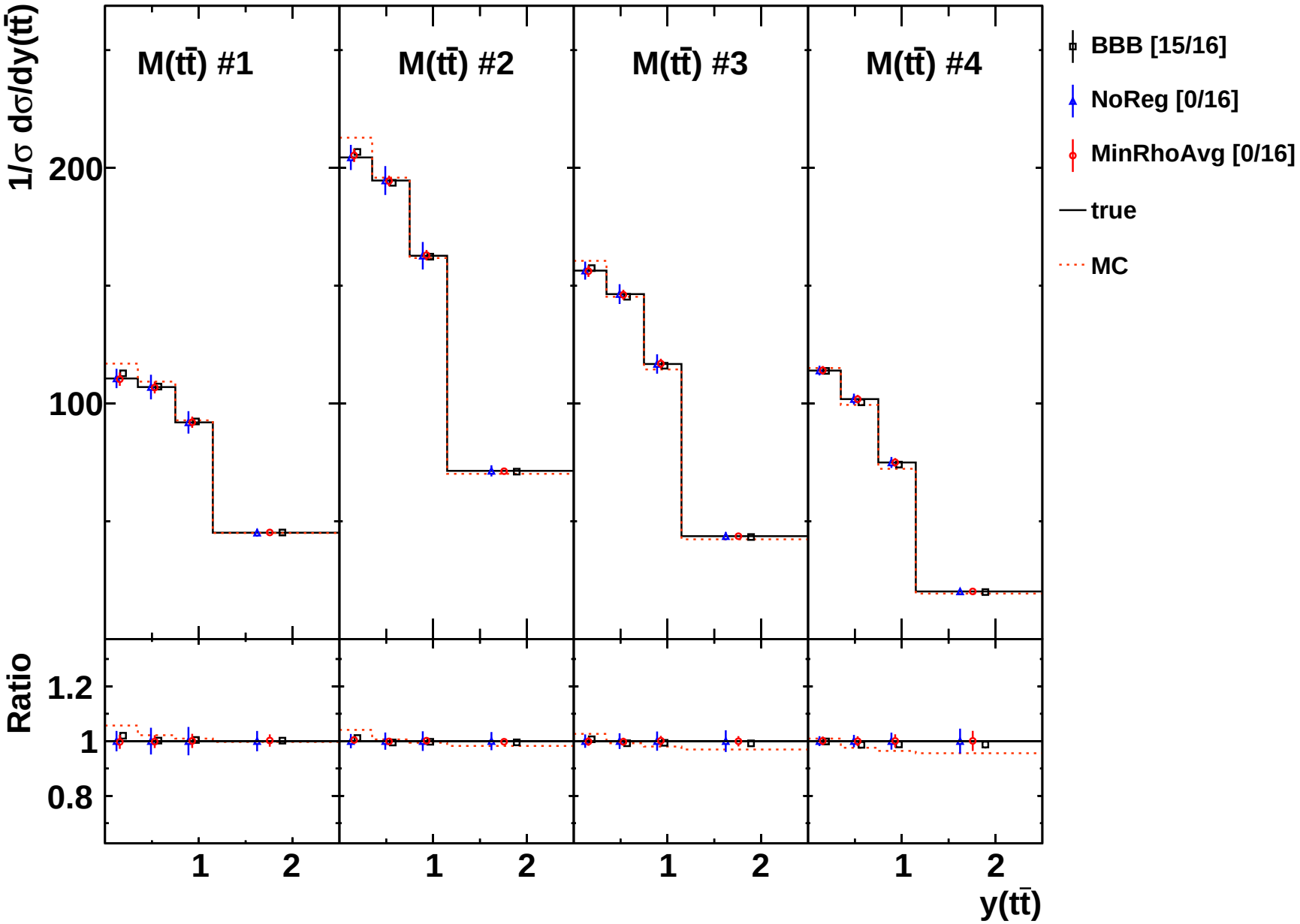

Closure test (3): moderate reweighting ($\lesssim 25\%$) $[M(t\bar{t}), y(t\bar{t})]$

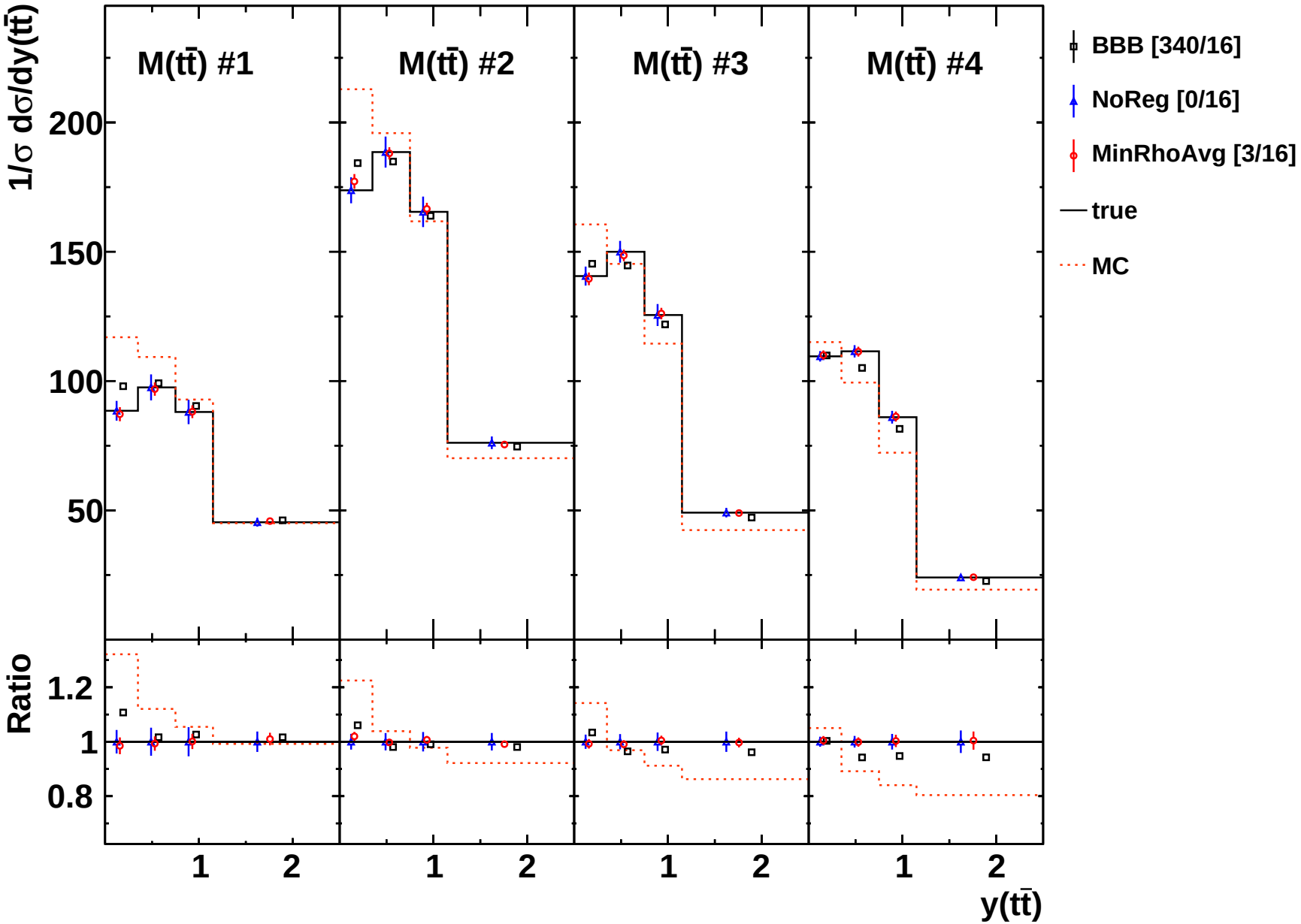

Closure test (3): moderate reweighting ($\lesssim 50\%$) $[M(t\bar{t}), y(t\bar{t})]$

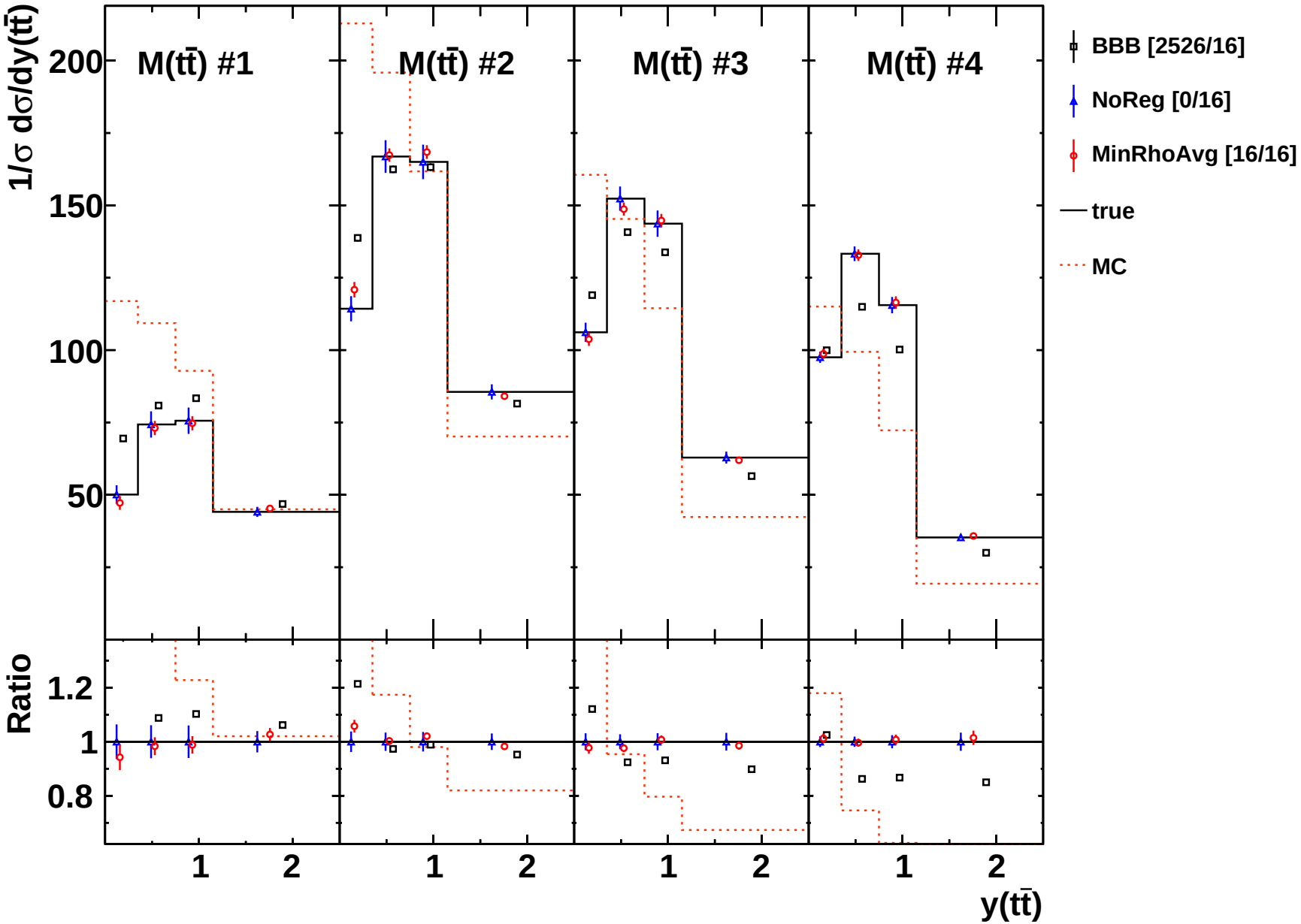

Closure test (3): moderate reweighting ($\lesssim 100\%$) $[M(t\bar{t}), y(t\bar{t})]$

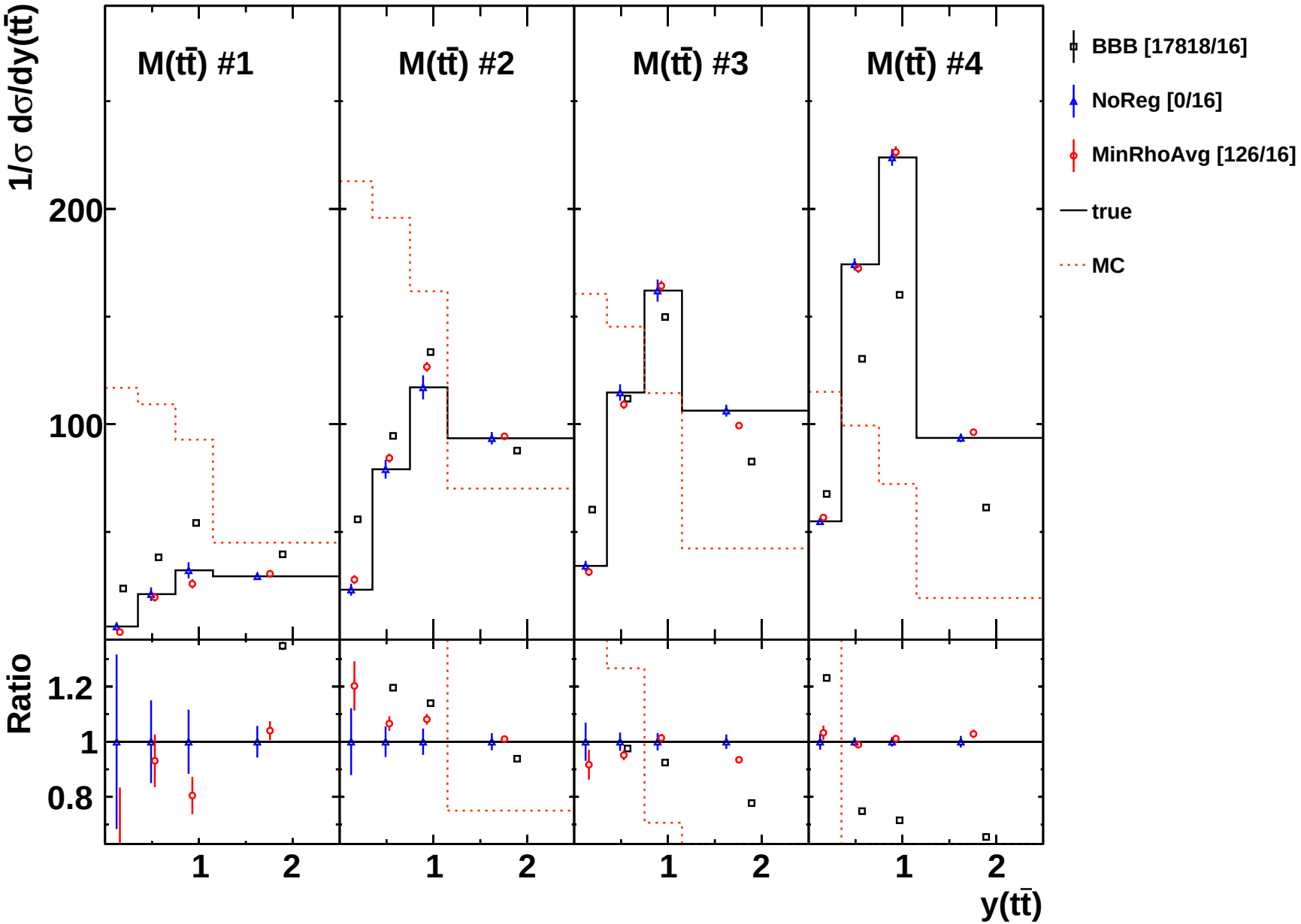

Data uncertainties: 2D x-sections

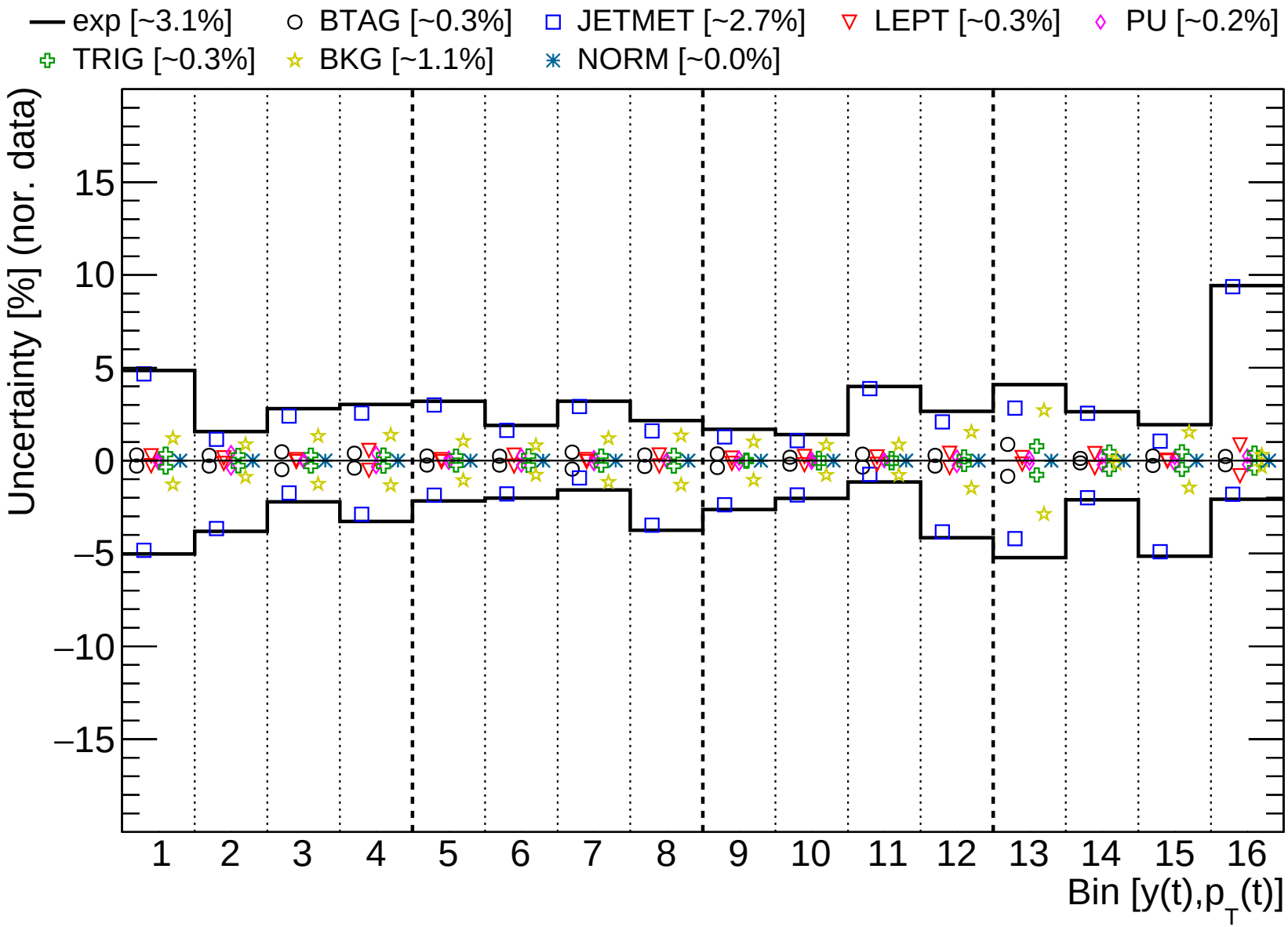

Data uncertainties: 2D x-sections

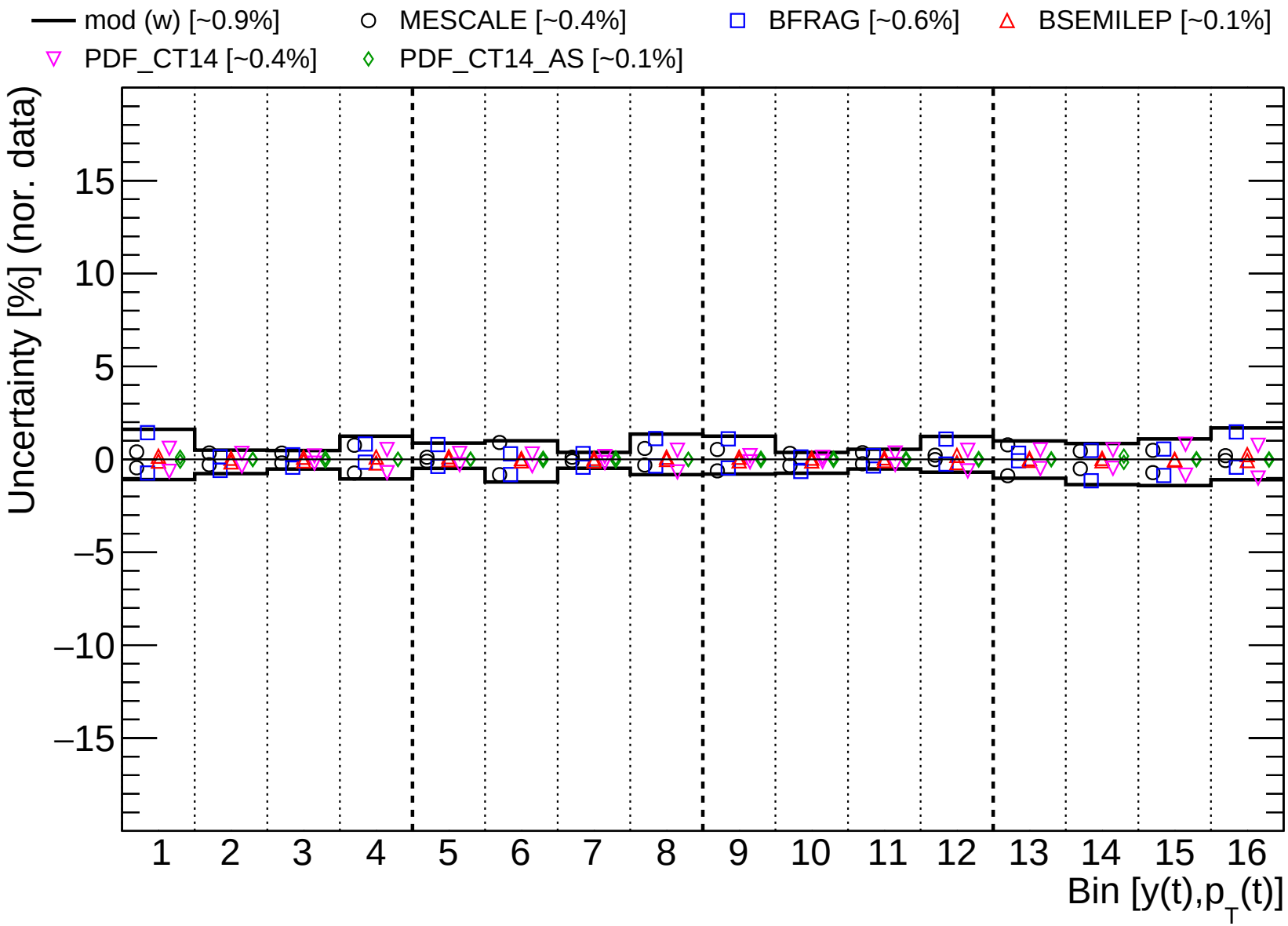

Data uncertainties: 2D x-sections

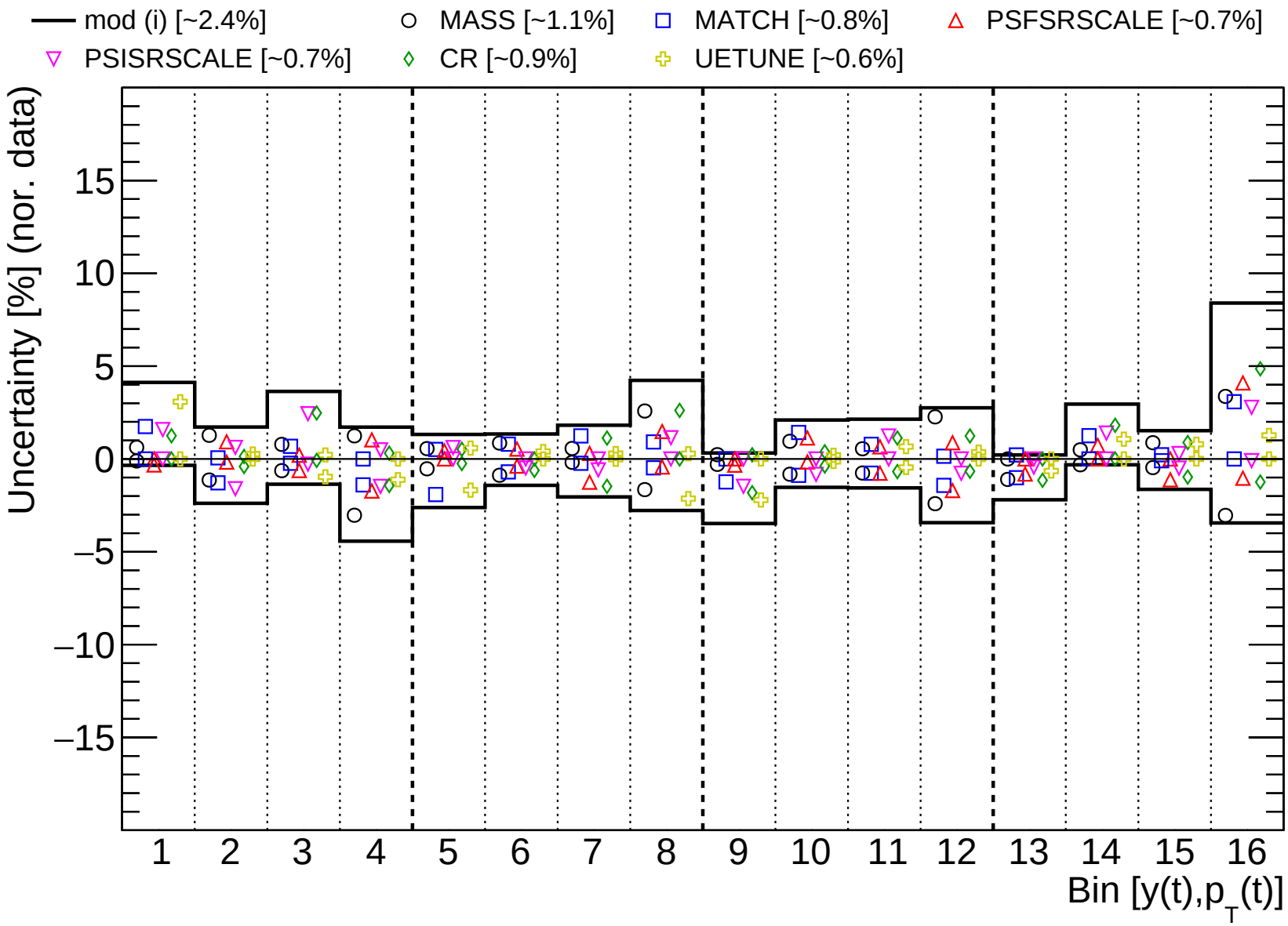

Data uncertainties: 3D x-sections

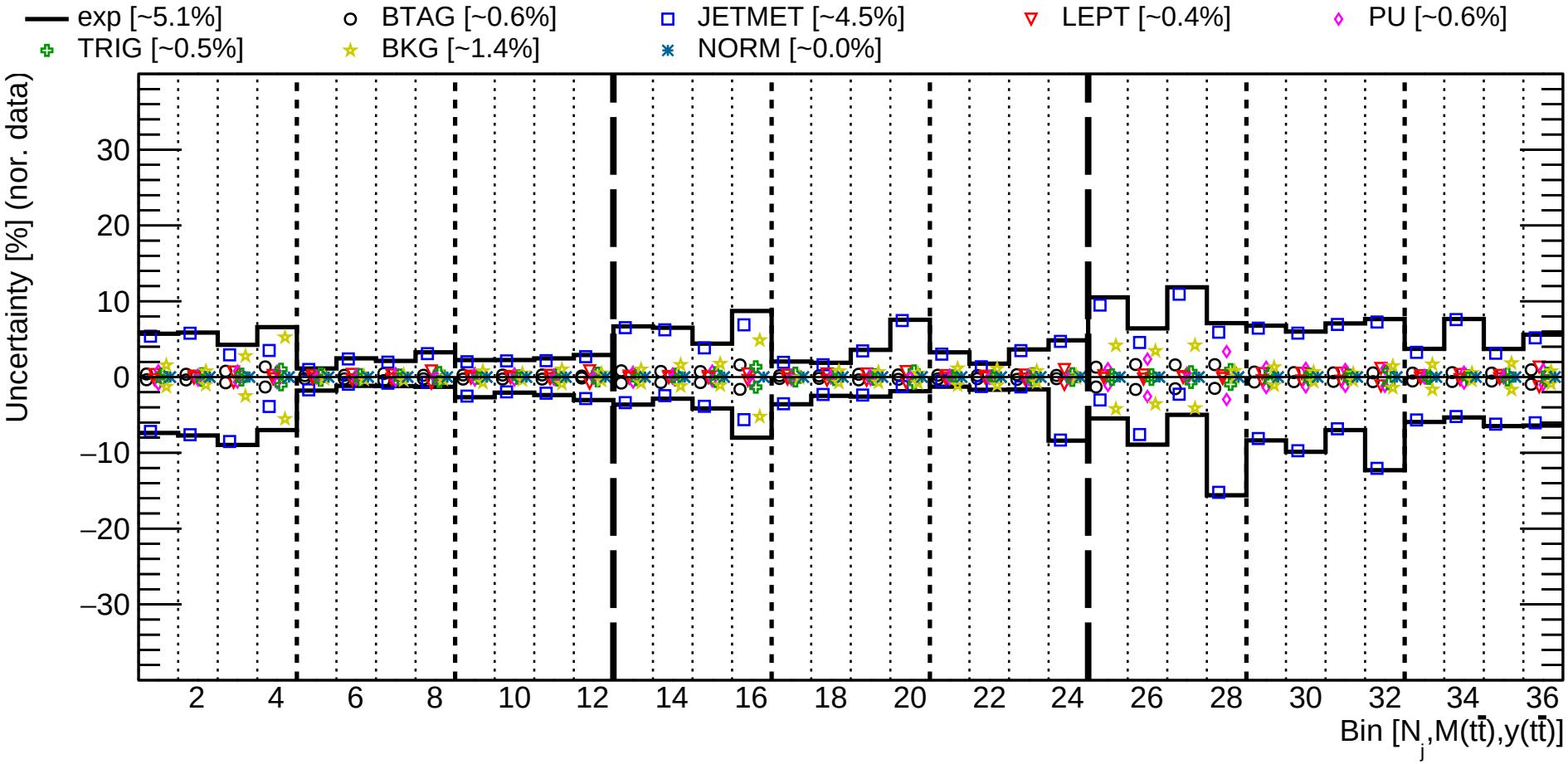

Data uncertainties: 3D x-sections

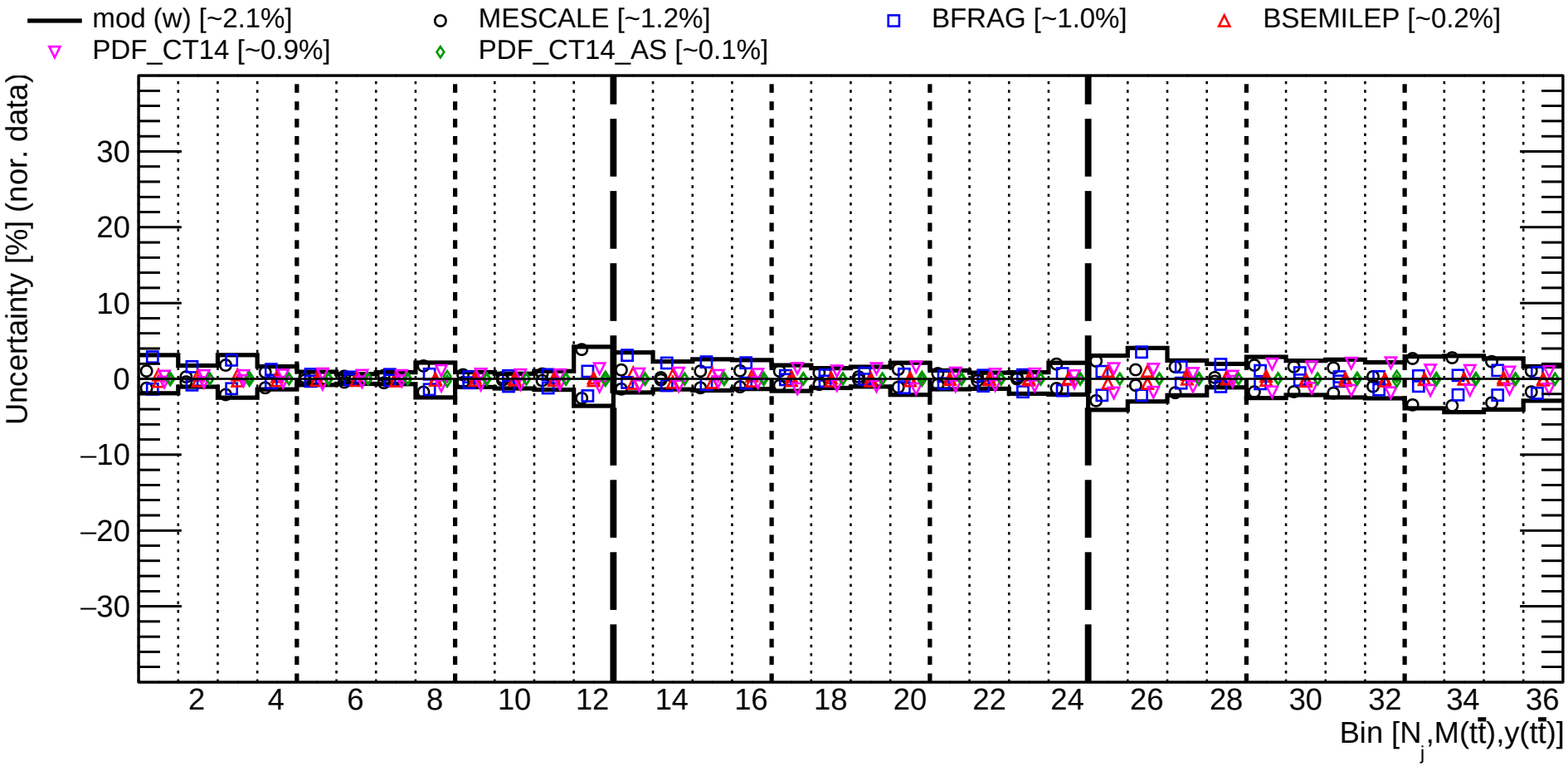

Data uncertainties: 3D x-sections

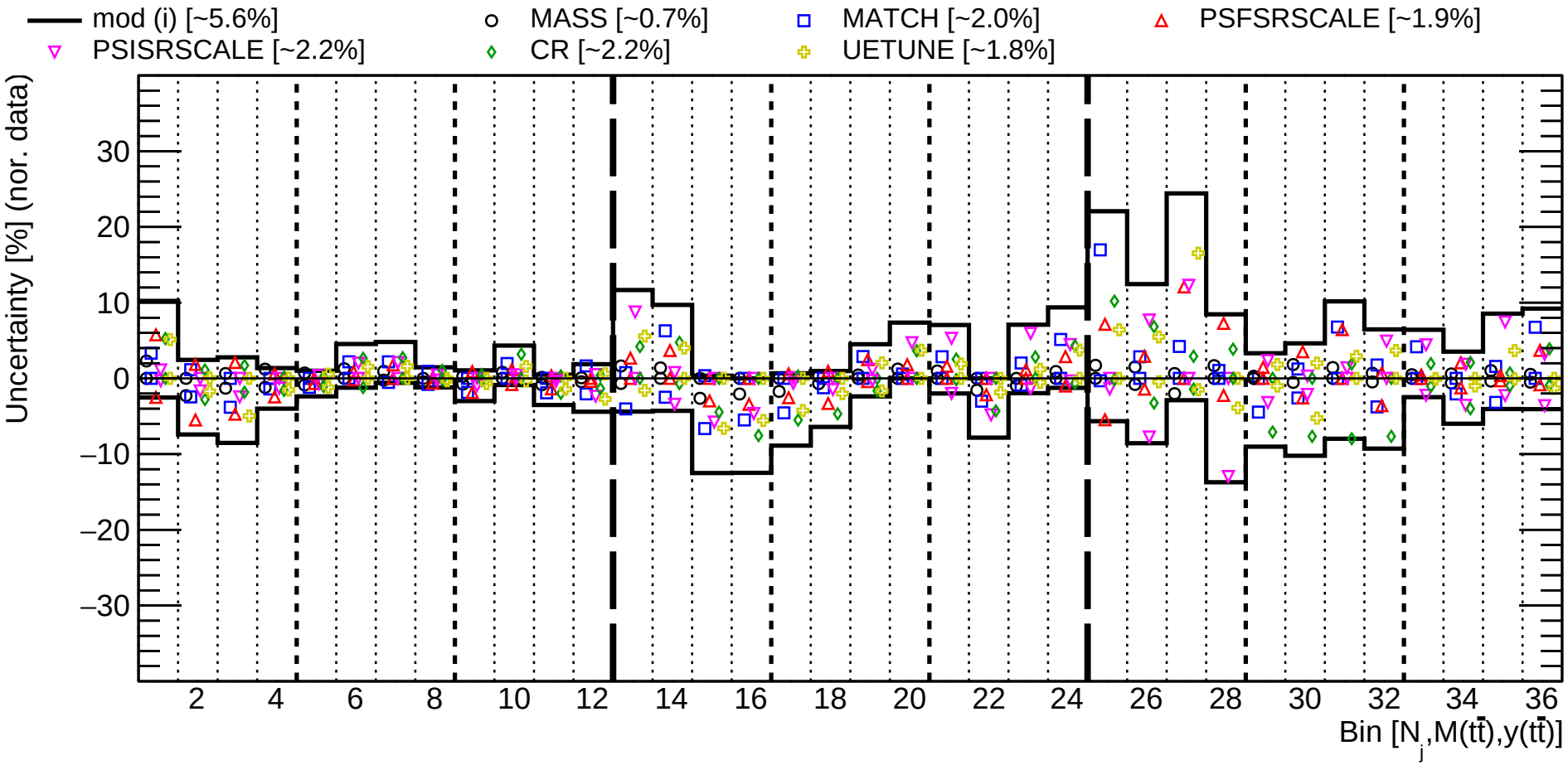

Comparison of data vs MC χ^2 values with TOP-14-013

Cross section variables	dof	*chi*^{2}		
		'POW-PYT'	'POW-HER'	'FXFX-PYT'
$[y(t),p_T(t)]$	15	57 [58]	18[14]	35
$[M(t\bar{t}),y(t)]$	15	26[20]	18[13]	36
$[M(t\bar{t}),y(t\bar{t})]$	15	28[21]	17[15]	23
$[M(t\bar{t}),\Delta\eta(t,\bar{t})]$	11	66[33]	68[20]	124
$[M(t\bar{t}),\Delta\phi(t,\bar{t})]$	15	14[21]	18[10]	10
$[M(t\bar{t}),p_T(t\bar{t})]$	15	21[83]	22[30]	29
$[M(t\bar{t}),p_T(t)]$	15	77	34	68
$[N_{\text{jet}}^{0,1+},M(t\bar{t}),y(t\bar{t})]$	23	34	31	34
$[N_{\text{jet}}^{0,1,2+},M(t\bar{t}),y(t\bar{t})]$	35	50	66	63

TOP-14-013 (2012 data) vs TOP-18-004(2016 data):

- POWHEG+PYTHIA6 (Z2* tune) vs POWHEG+PYTHIA8 (CUETP8M2T4 tune) in 2016
- POWHEG+HERWIG6 (AUET2 tune) vs POWHEG+HERWIG++ (EE5C tune) in 2016

List of discovered features/bugs in MadGraph5_aMC@NLO

- https://bugs.launchpad.net/mg5amcnlo/+bug/1737367
- https://bugs.launchpad.net/mg5amcnlo/+bug/1737368
- https://bugs.launchpad.net/mg5amcnlo/+bug/1752981
- https://bugs.launchpad.net/mg5amcnlo/+bug/1758683
- + many more features and improvements were just implemented locally to provide smooth running on a cluster

Definition of extra jets (not from top decay)

- NLO predictions for inclusive $t\bar{t}$, $t\bar{t}$ + 1 jet and $t\bar{t}$ + 2 jets computed and compared to data using MadGraph5_aMC@NLO + aMCfast + ApplGrid + xFitter
- particle-level jet definition used in measurement, further corrected to parton level using separate MC POWHEGV2 + PYTHIA8 simulations
  - $p_T(j) > 30$ GeV, $|\eta(j)| < 2.4$
  - 'Particle level': particle jets (no ν) required to be isolated within $\Delta R > 0.4$ from l and b from $t\bar{t}$
  - Parton level: standalone POWHEGV2 + PYTHIA8 generated without
    (1) top decays: $C_{\text{def}} = \sigma_{\text{no l,b from } t\bar{t}} \,/\, \sigma_{\text{no } t\bar{t}}$
    (2) hadronisation: $C_{\text{had}} = \sigma_{\text{with had.}} \,/\, \sigma_{\text{no had.}}$
    (3) MPI: $C_{\text{MPI}} = \sigma_{\text{with MPI}} \,/\, \sigma_{\text{no MPI}}$
- $C_{\text{NP}} = \sigma_{\text{no l,b from } t\bar{t}} / \sigma_{\text{no } t\bar{t}\text{,had.,MPI}}$ $[C_{\text{NP}} \approx C_{\text{def}} \times C_{\text{had}} \times C_{\text{MPI}}]$
- theoretical predictions = $\text{NLO} \times \text{C}_{\text{NP}}$
- similar procedure used in jet measurements (although without excluding decay products)

NP corrections

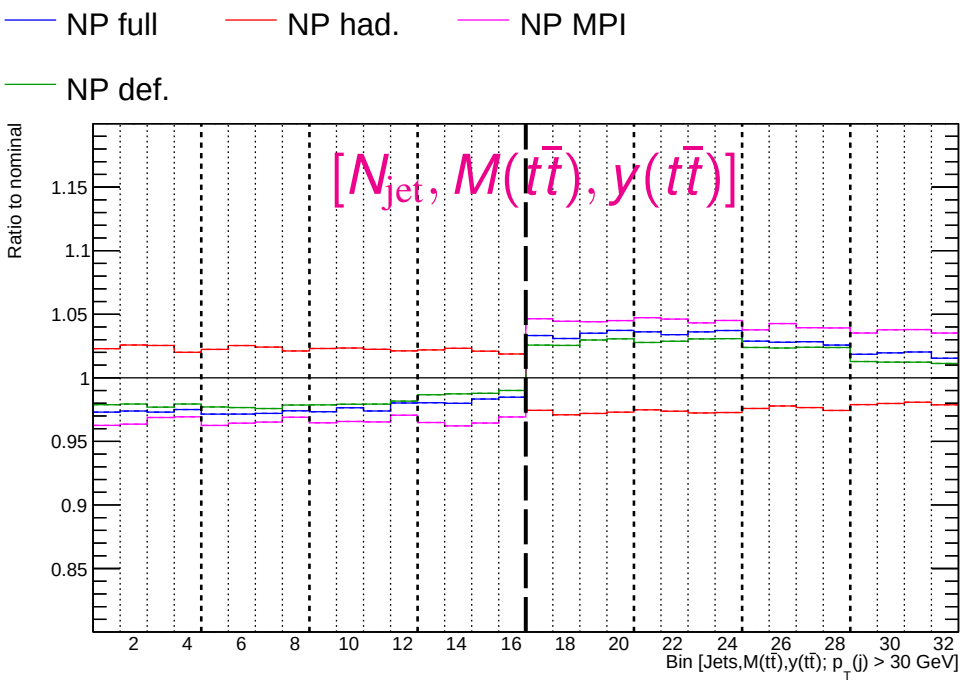

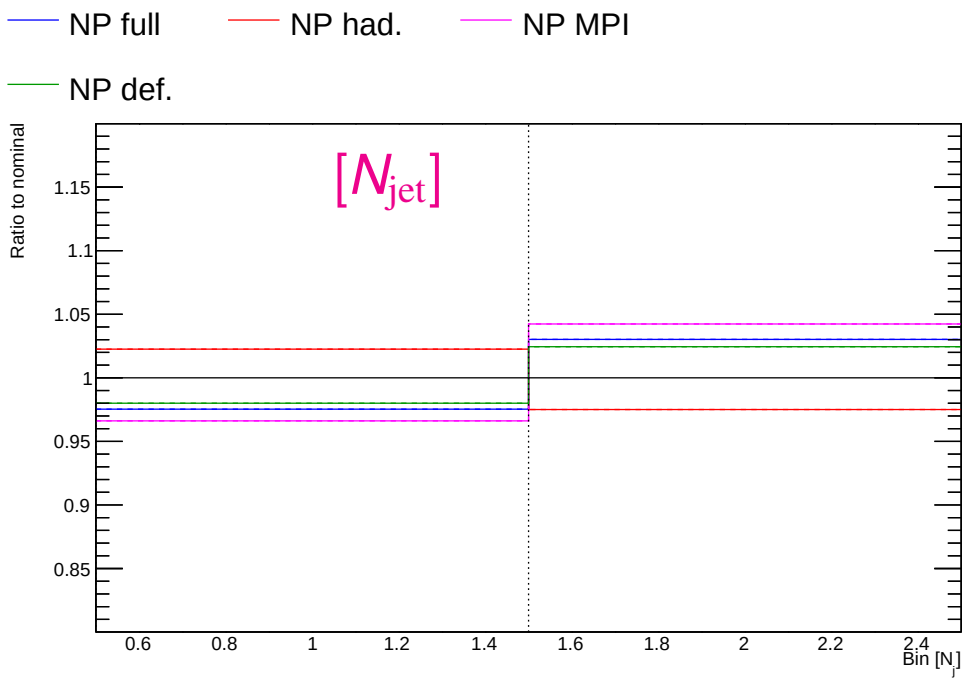

- depend on N_{jet}, almost no $M(t\bar{t})$ $y(t\bar{t})$ dependence
- NP corrections: $\lesssim 5\%$
  - C_{MPI}: $\uparrow$ jets
  - C_{had}: $\downarrow$ jets
  - C_{def}: $\uparrow$ jets [correction to exclude top decay products]
- negligible uncertainties due to underlying event, hadronisation modelelling, PS and scale variations as estimated using alternative MC (backup)

Uncertainties of NP corrections

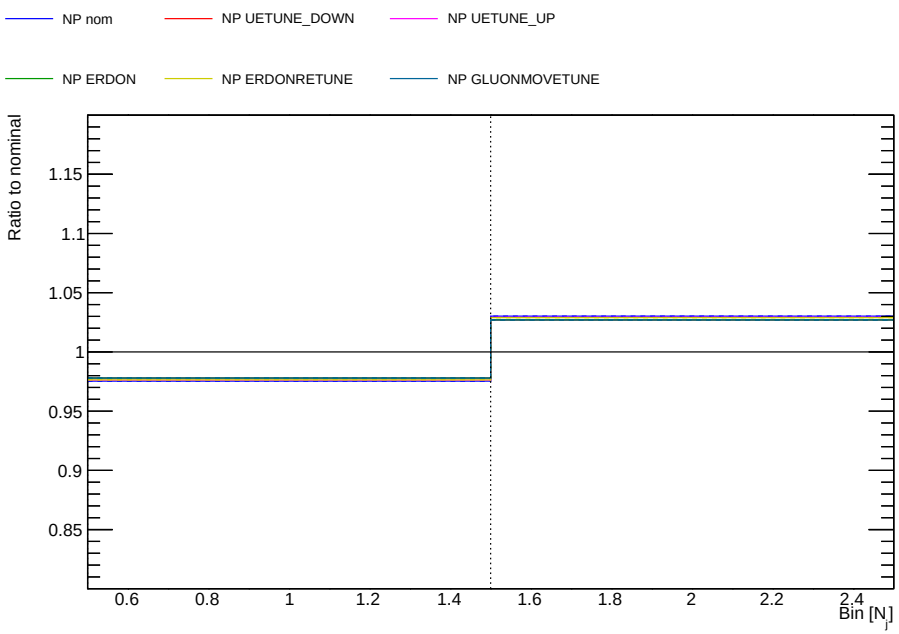

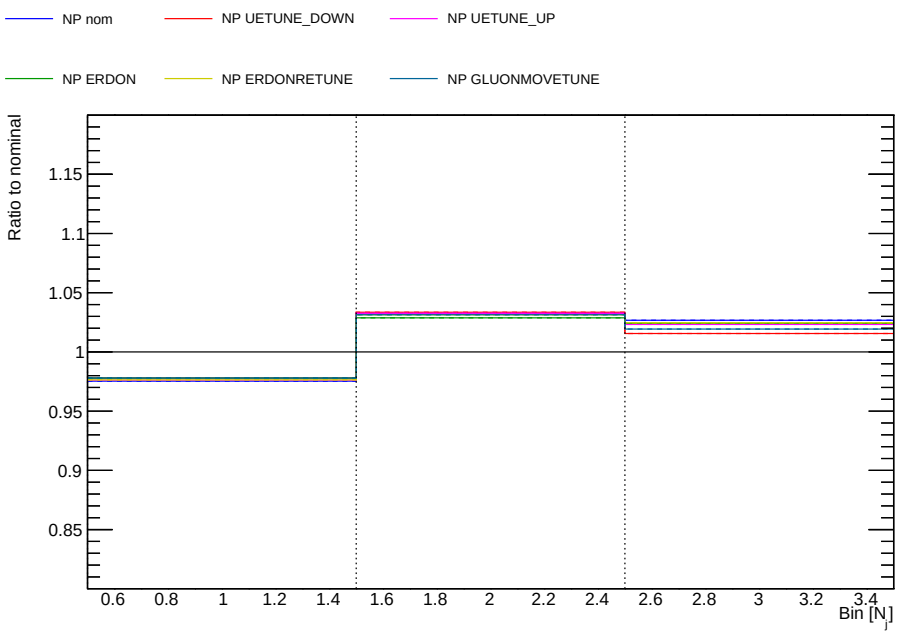

Data and theory uncertainties (3 N_{jet} bins)

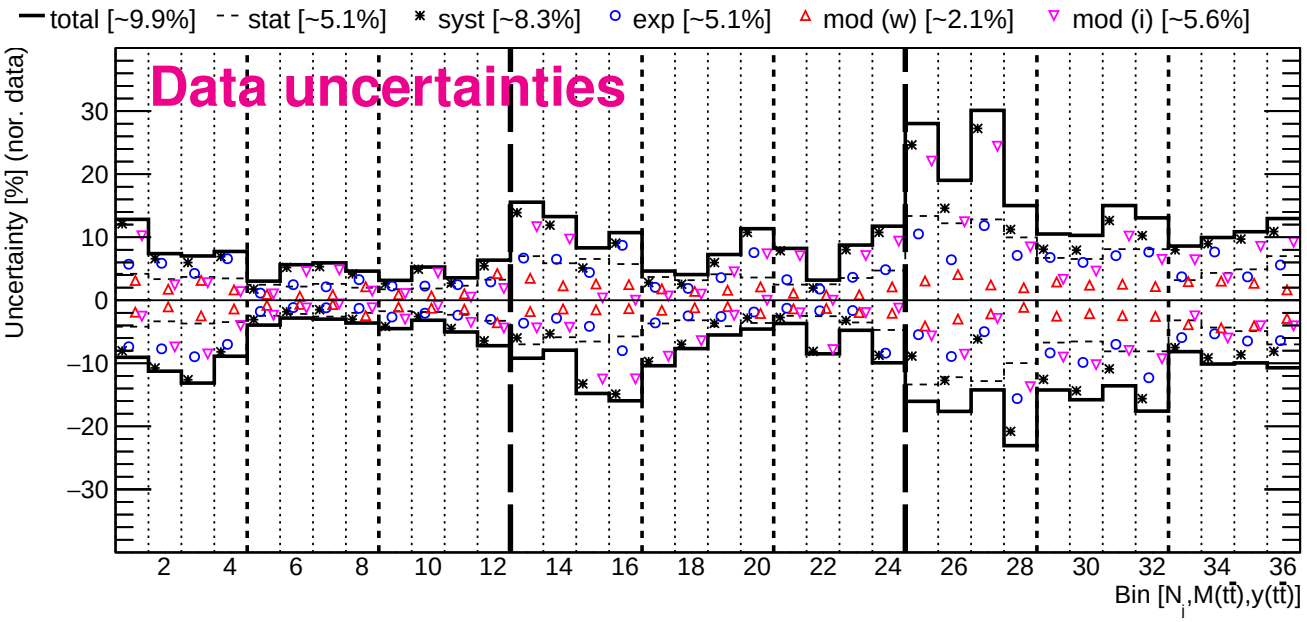

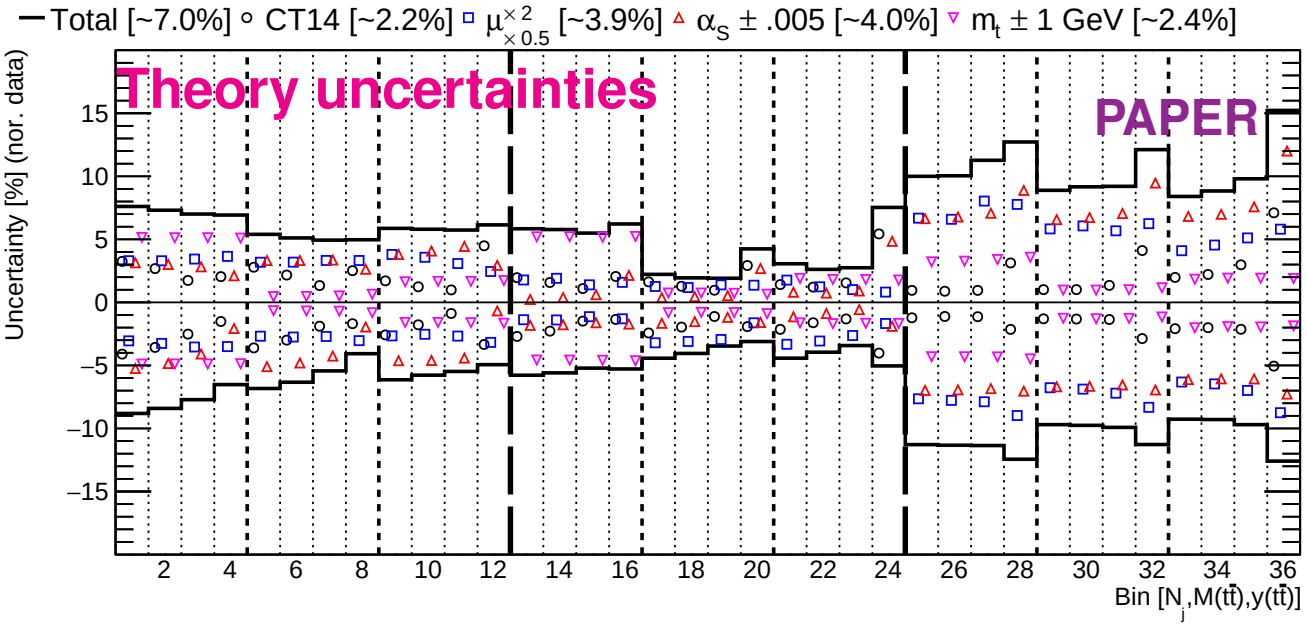

- Larger scale uncertainties

→ use as cross check only

Study of scale choice for NLO calculations

- μ_r, μ_f scales are important for both central values and their uncertainties

  $\rightarrow$ direct effect on e.g extracted α_s
- many possible choices for differential $t\bar{t}$, $t\bar{t}+$ jets calculations:
  - $\mu = m_t$
  - $\mu = H = \sqrt{m_t^2 + p_T^2(t)} + \sqrt{m_t^2 + p_T^2(\bar{t})}$
  - $\mu = H' = \sum_i \sqrt{m_i^2 + p_{T,i}^2}, \quad i =$ all partons
  - $\mu = H'' = \sum_i \sqrt{m_i^2 + p_{T,i}^2}, \quad i = t, \bar{t}$, jets
- scales can be chosen:
  - fastest apparent convergence (FAC): minimise higher order corrections
  - principle of minimal sensitivity (PMS): minimise unc. when varying scale
- Mitov et al. [1606.03350] advocates $\mu = H/4$ for $t\bar{t}$ production and all distributions except $p_T(t)$ based on FAC and NNLO, NNLL
- but in our analysis we have also $t\bar{t}$ + jets: only NLO avail., FAC is not applicable
- for normalised cross sections scale choice is important for N_{jet}
  - a few % for N_{jet} distribution
  - $\sim$ 1% for other distributions (e.g. $M(t\bar{t})$, $y(t\bar{t})$)

Study of scale choice for NLO calculations

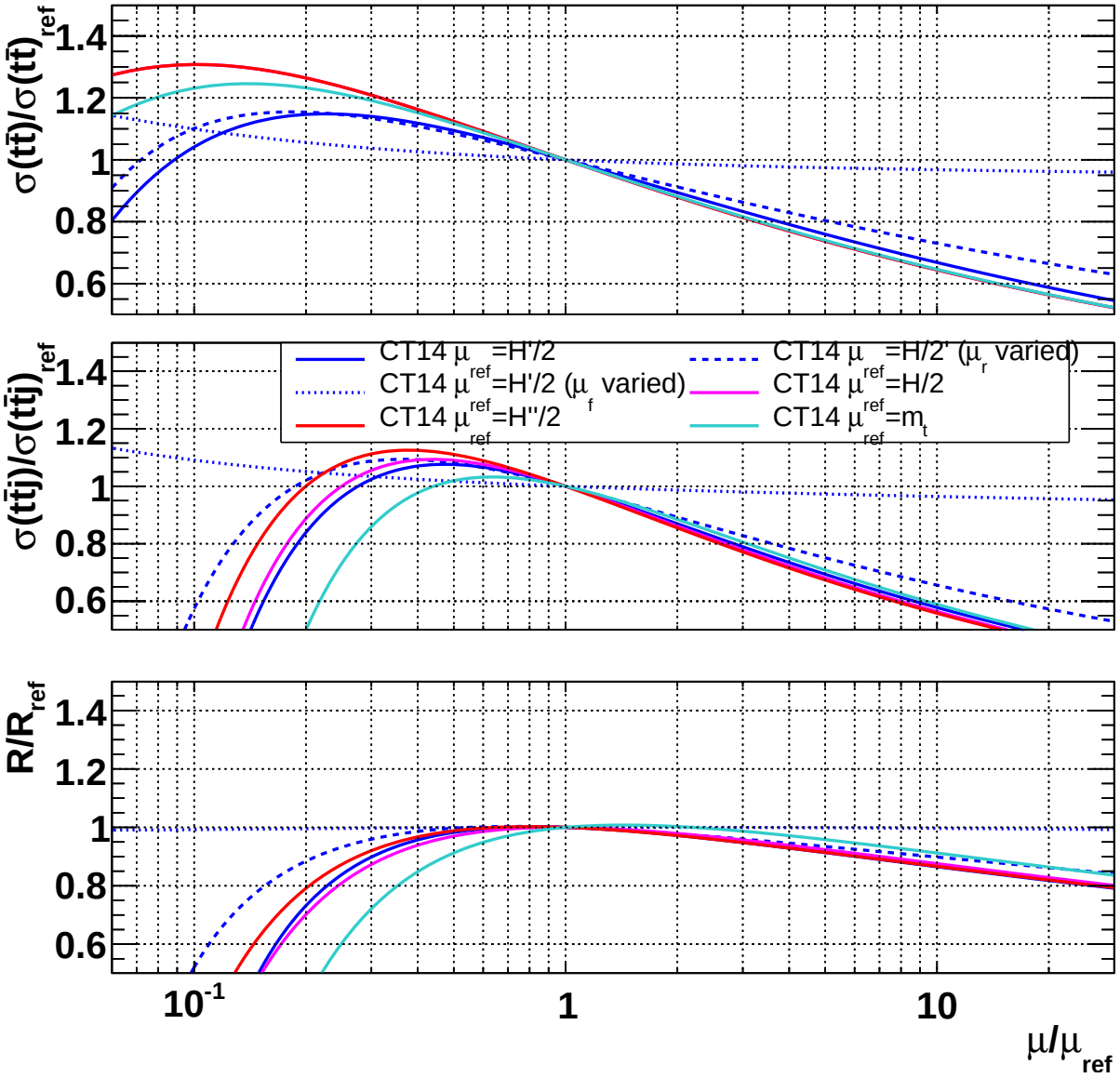

- ratios cross 1 by construction
- partial cancellation of scale dependence for $R = \sigma(t\bar{t}j)/\sigma(t\bar{t})$
- H, H' and H'' are similar
- $H/4$ is bad for $t\bar{t}j$

  $\rightarrow$ use $H'/2$ based on PMS (as before)
- dominant unc. are from simultaneous μ_r and μ_f variation
- side remark: choice $\mu = H'$ maximises R, but this is default scale choice in MC, which often predicts higher N_{jet} than data

Study of scale choice for NLO calculations

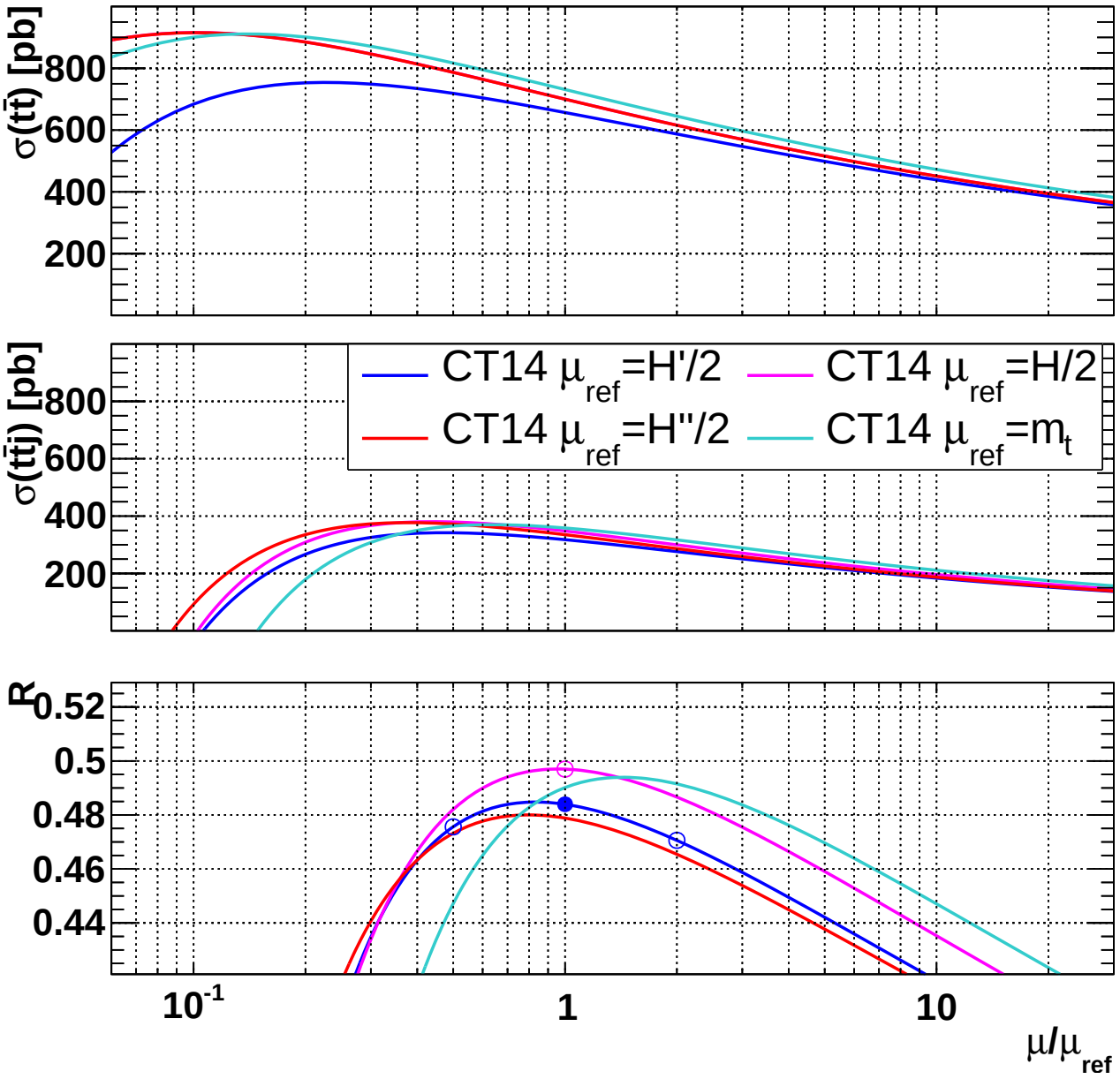

- propose nominal $\mu = H'/2$
- variation $H'/4 < \mu < H'$ and $\mu = H/2$ as unc.

  $\rightarrow$ a few % unc.

Impact of scale variations on α_s extraction

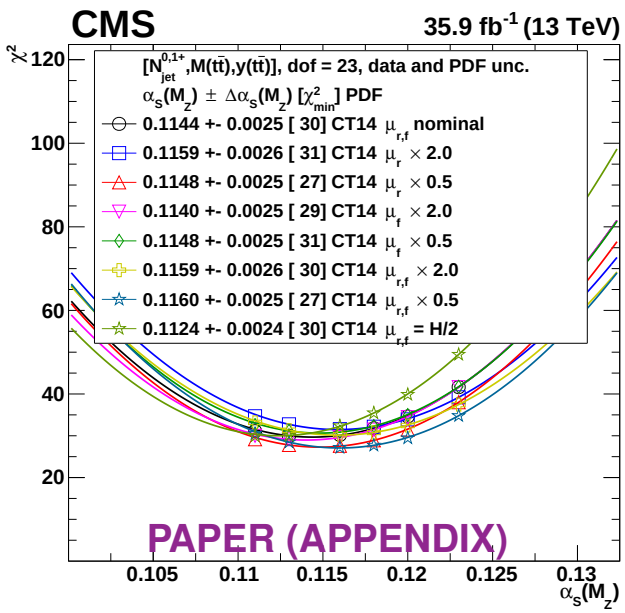

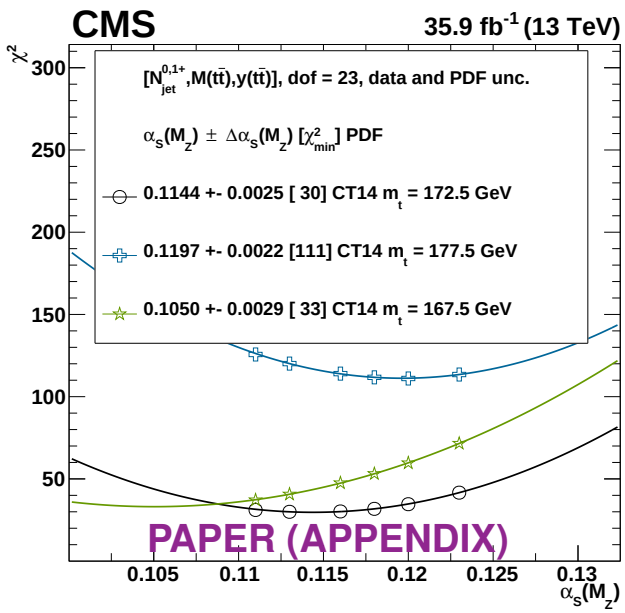

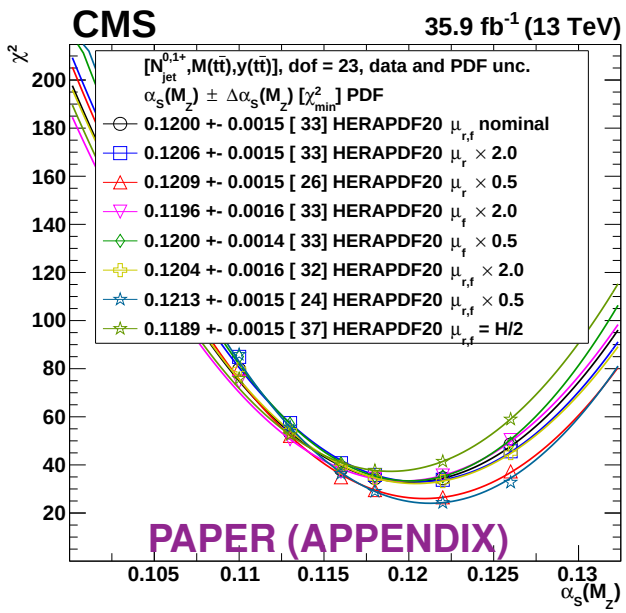

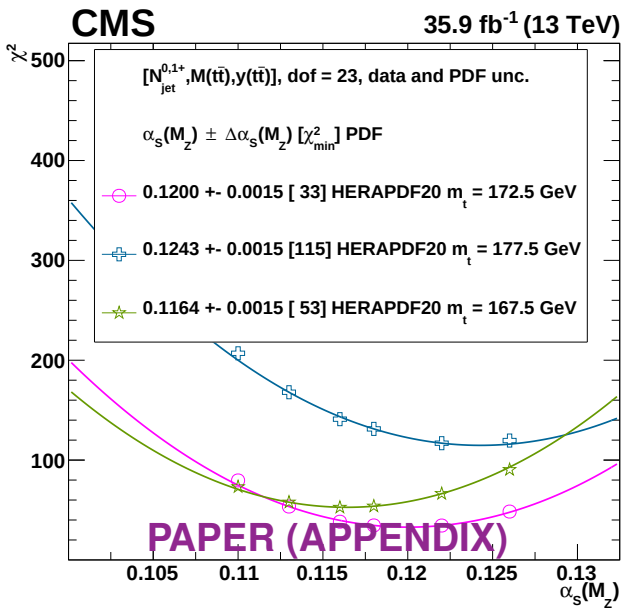

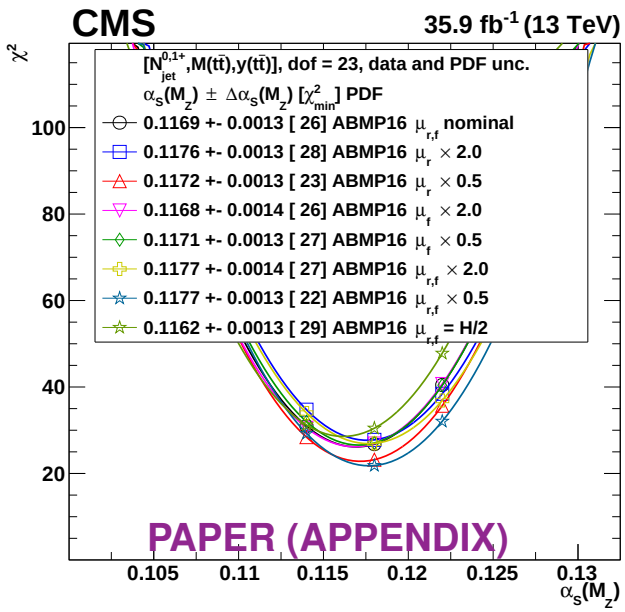

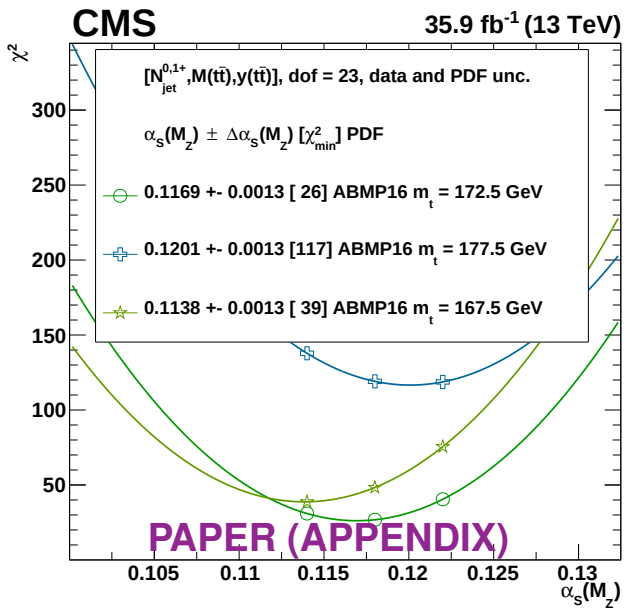

Impact of scale variations on m_t^{pole} extraction

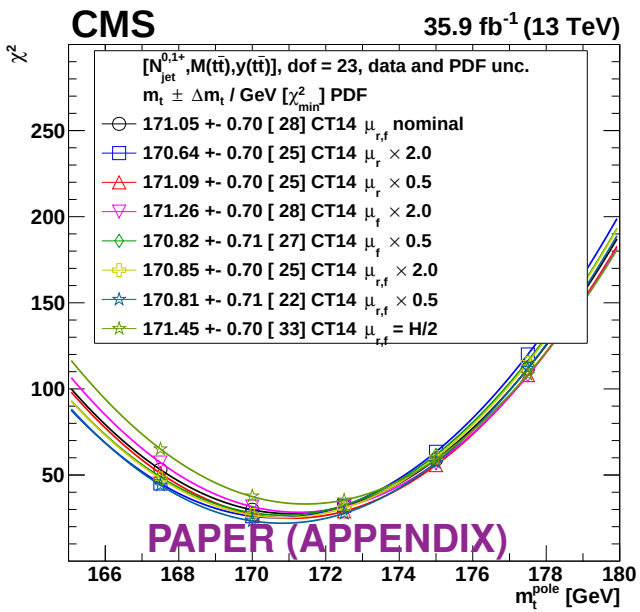

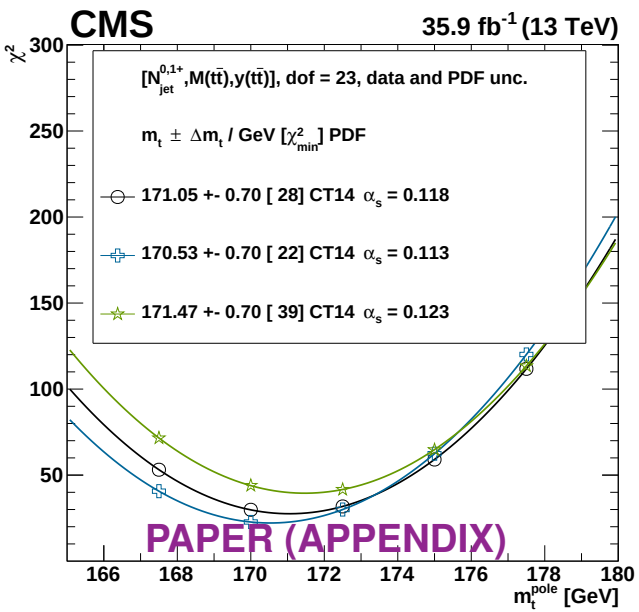

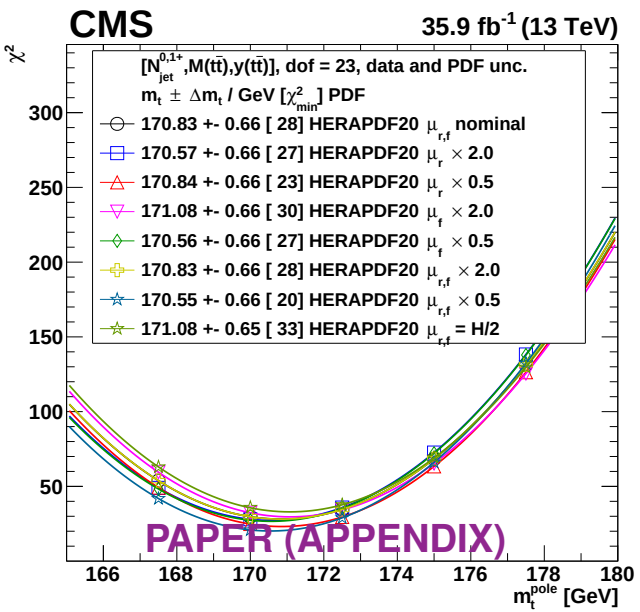

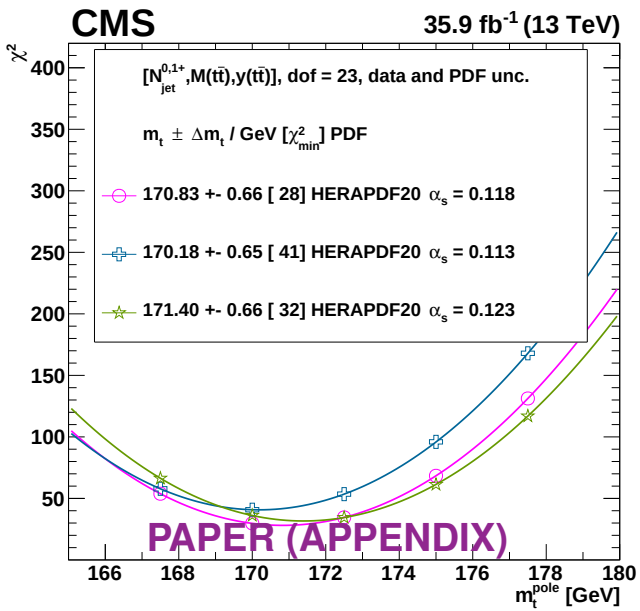

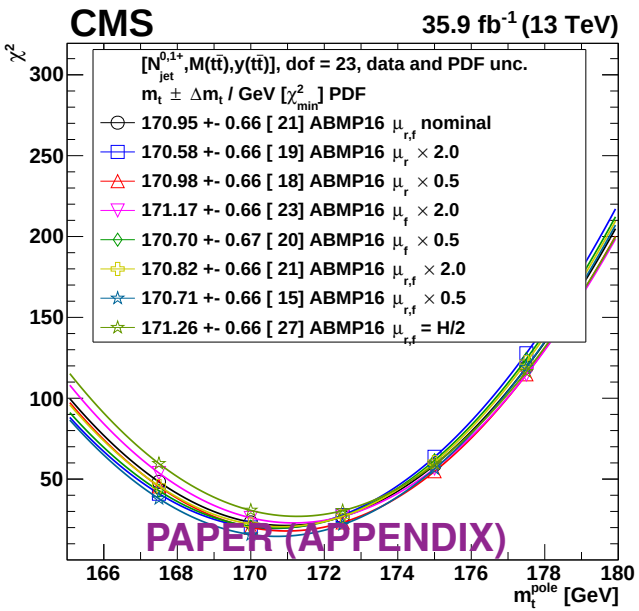

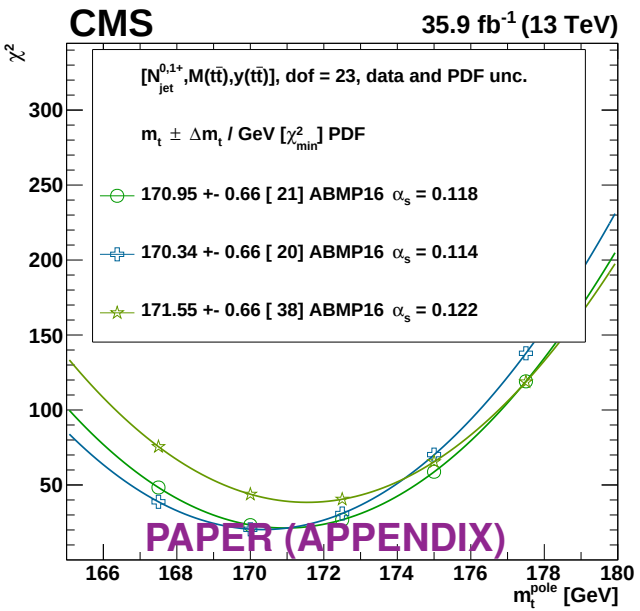

α_s and m_t^{pole} from $[N_{\text{jet}}, mtt, y(t\bar{t})]$ with 3 N_{jet} bins

PAPER (APPENDIX)

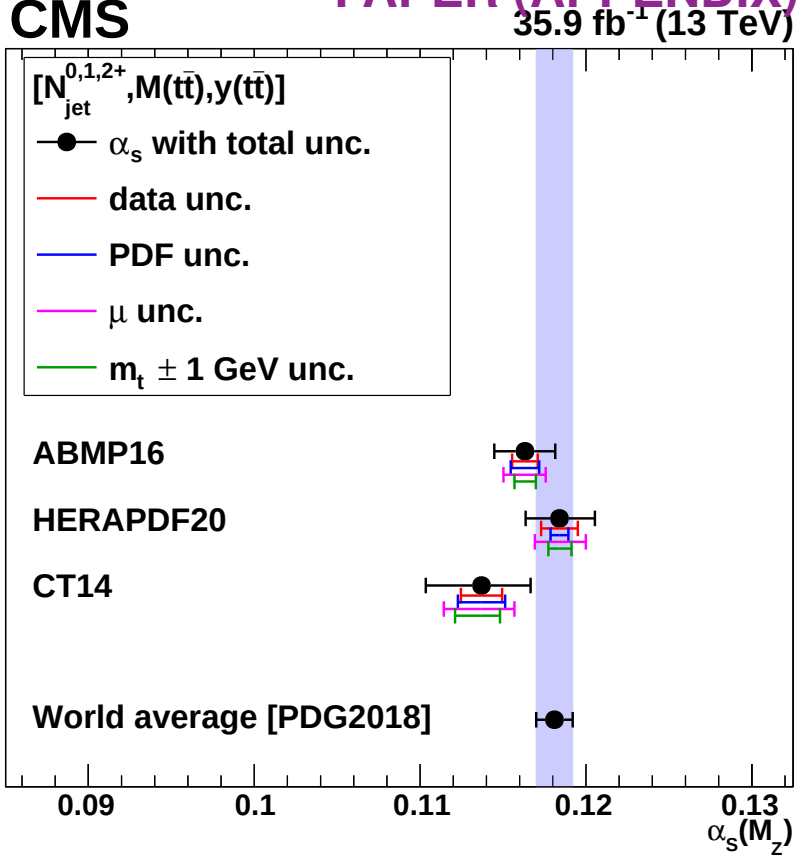

PAPER (APPENDIX)

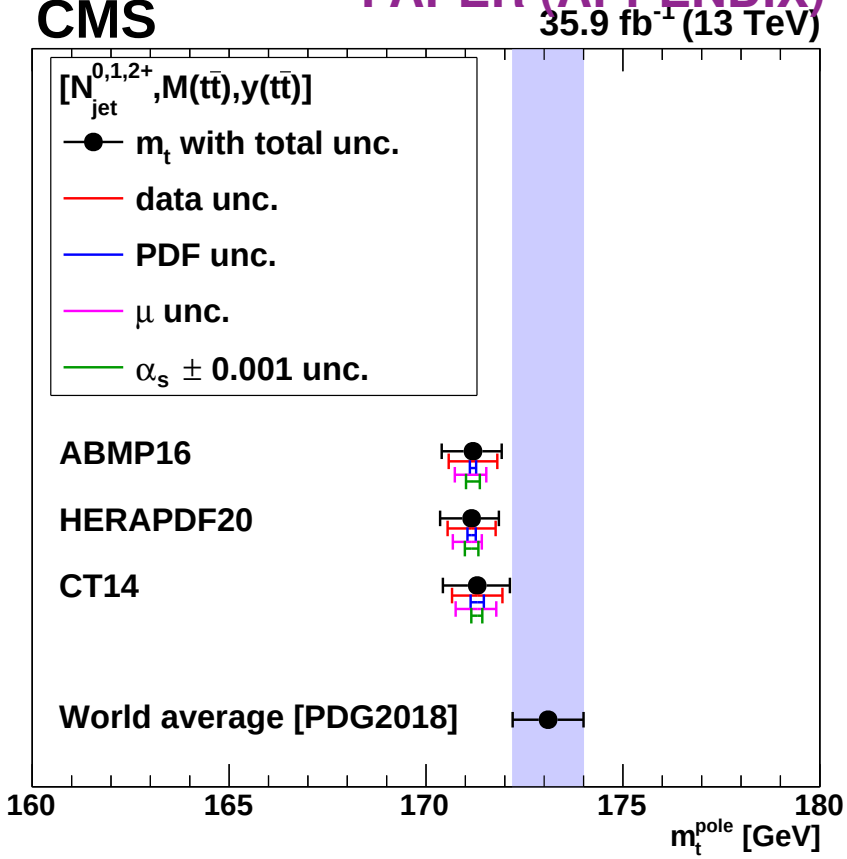

α_s and m_t^{pole} from $[p_T(t\bar{t}), mtt, y(t\bar{t})]$ with 2 $p_T(t\bar{t})$ bins

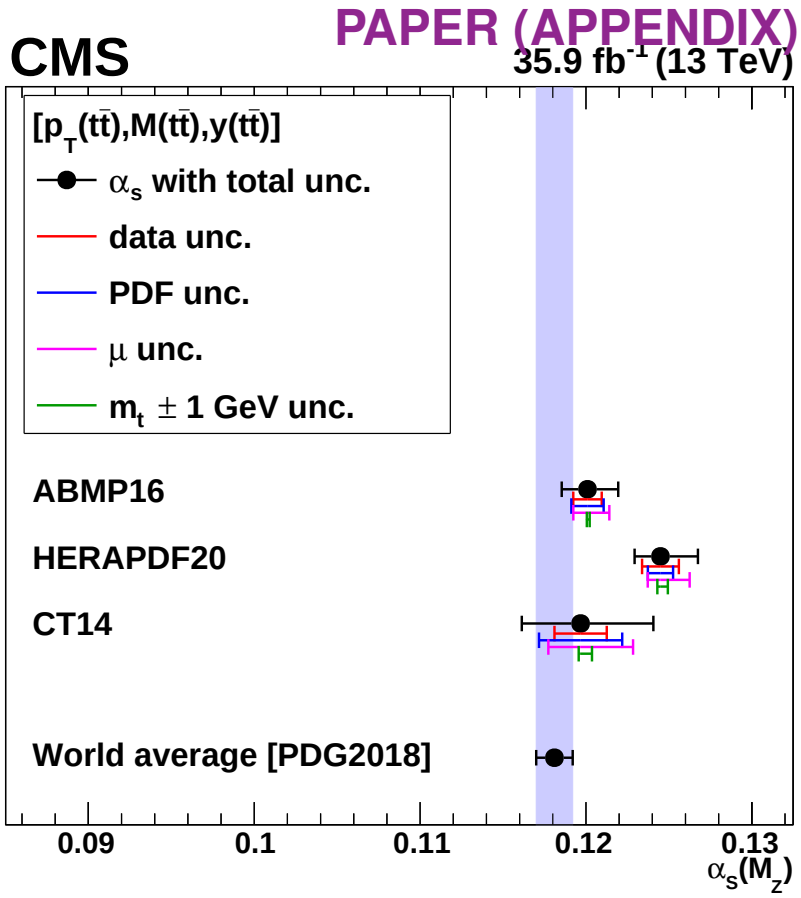

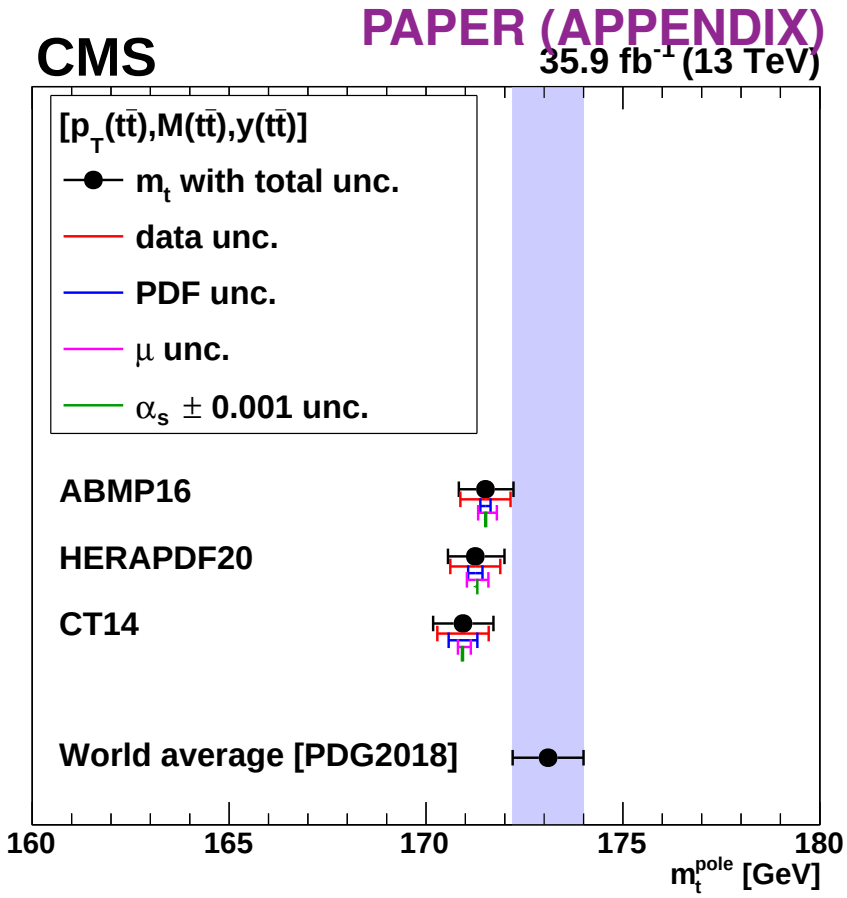

α_s and m_t^{pole} from single-differential cross sections

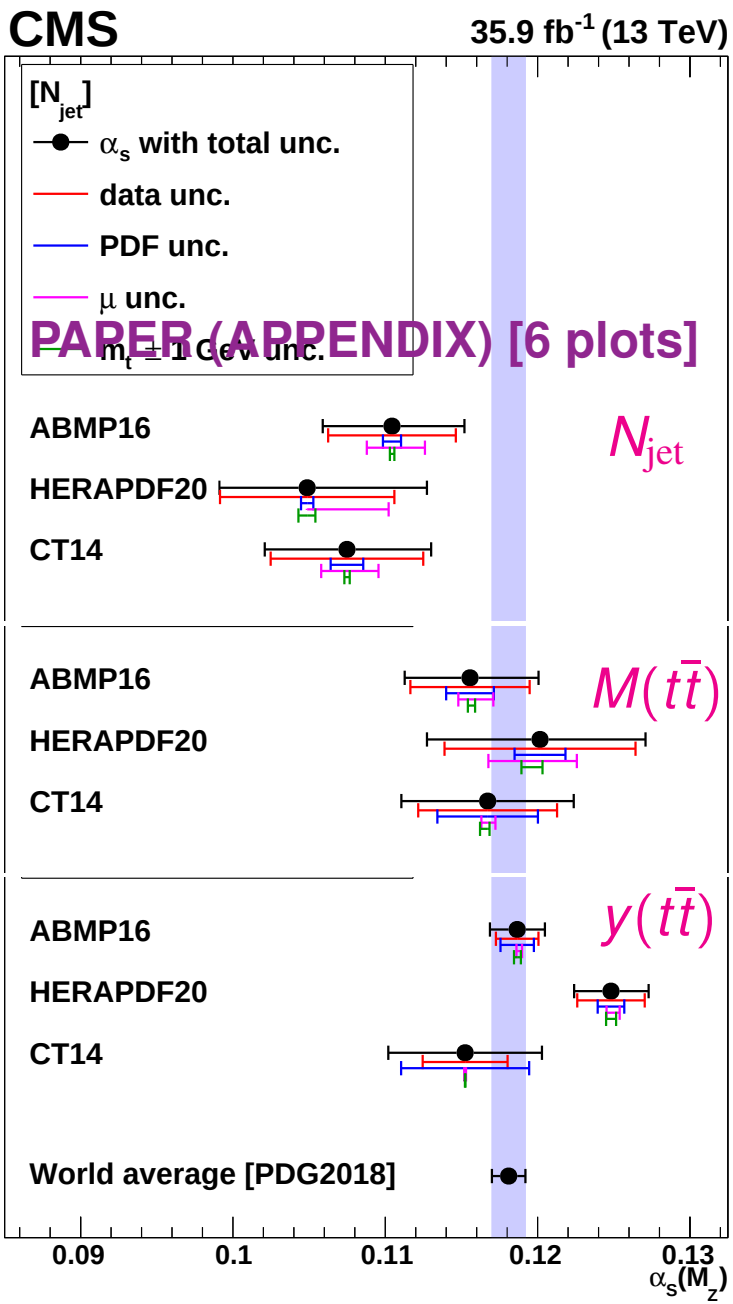

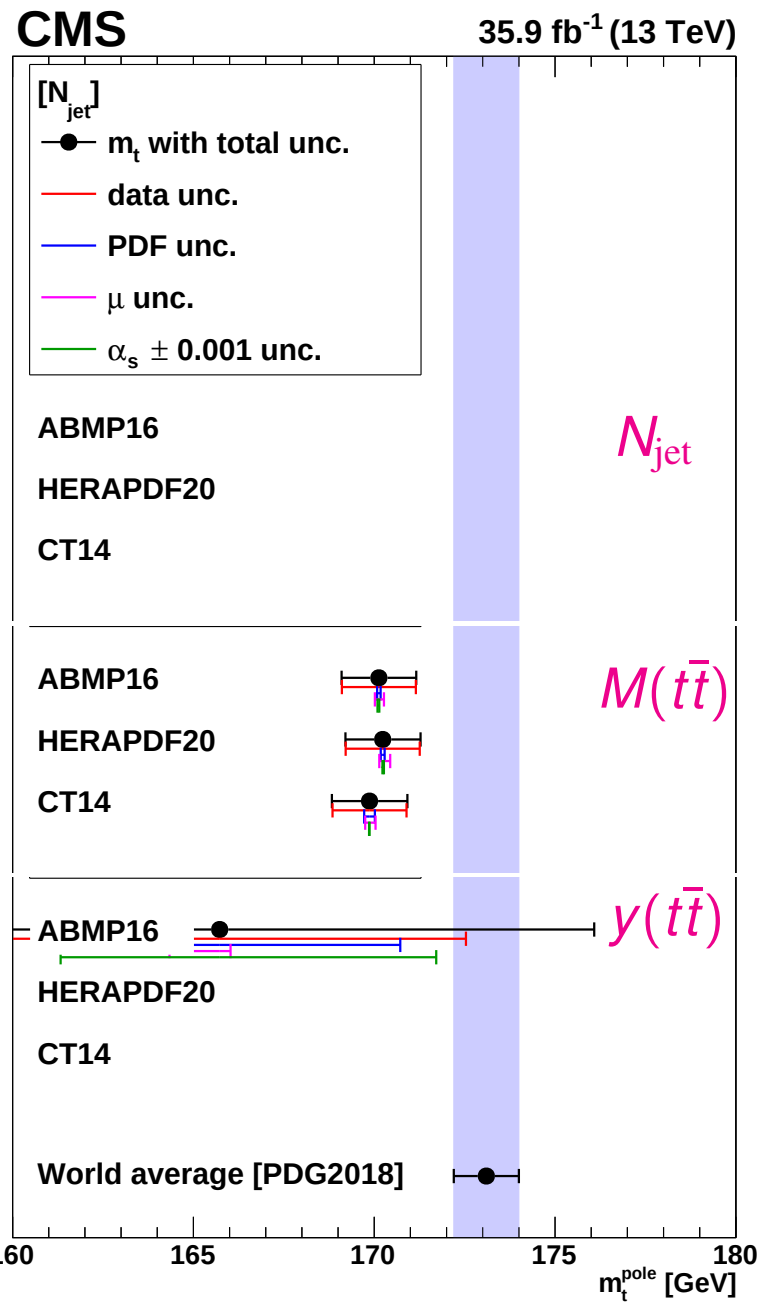

PAPER (APPENDIX) [6 plots]

Simultaneous PDF+α_s + m_t^{pole} fit: settings

- followed standard approach: using HERA DIS data only, or HERA + $t\bar{t}$ data to demonstrate added value from $t\bar{t}$ on PDF and α_s determination
- settings follow HERAPDF2.0 fit (very similar to TOP-14-013), use xFitter-2.0.0
- input data: combined HERA DIS [1506.06042] + $t\bar{t}$
- RTOPT, $M_c = 1.47$ GeV, $M_b = 4.5$ GeV, $Q^2_{\text{min}} = 3.5^{+1.5}_{-1.0}$ GeV^2
- predictions fot $t\bar{t}$ data via MadGraph5_aMC@NLO + aMCfast + ApplGrid, $\mu_r = \mu_f = H_t/4$, $H_t = \sqrt{m_t^2 + (p_T(t))^2} + \sqrt{m_t^2 + (p_T(\bar{t}))^2}$ varied by factor 2
  - dependence on α_s and scales written in ApplGrid tables
  - dependence on m_t^{pole} derived by linear interpolation between tables generated with different values of m_t^{pole} (new feature for xFitter)
  - kinematic range probed by $t\bar{t}$: $x = (M(t\bar{t})/\sqrt{s})\exp[\pm y(t\bar{t})] \Rightarrow 0.01 \lesssim x \lesssim 0.1$
- 15-parameter form (backup) determined using parametrisation scan (one extra g parameter required by $t\bar{t}$ data) at $Q_0^2 = 1.9$ GeV^2, $f_s = 0.4 \pm 0.1$
- DGLAP NLO PDF evolution via QCDNUM-17.01.14
- PDF uncertainties: fit ($\Delta\chi^2 = 1$ via HESSE, cross checked with MC replica method), model and parametrisation; in addition for α_s and m_t^{pole} scale uncertainties for $t\bar{t}$ are considered

Simultaneous PDF, α_s and m_t^{pole} fit: PDF parametrisation

Determined using parametrisation scan:

$$
\begin{aligned}
x_g(x) &= A_g x^{B_g} (1-x)^{C_g} (1 + E_g x^2) - A'_g x^{B'_g} (1-x)^{C'_g}, \\
x_{u_v}(x) &= A_{u_v} x^{B_{u_v}} (1-x)^{C_{u_v}} (1 + D_{u_v} x), \\
x_{d_v}(x) &= A_{d_v} x^{B_{d_v}} (1-x)^{C_{d_v}}, \\
x\overline{U}(x) &= A_{\overline{U}} x^{B_{\overline{U}}} (1-x)^{C_{\overline{U}}} (1 + D_{\overline{U}} x), \\
x\overline{D}(x) &= A_{\overline{D}} x^{B_{\overline{D}}} (1-x)^{C_{\overline{D}}},
\end{aligned}
$$

Data	15p	$A'_g = 0$	$E_g = 0$	$D_{u_v} = 0$	$D_{\overline{U}} = 0$	D_g	E_{u_v}	D_{d_v}	E_{d_v}	$E_{\overline{U}}$	$D_{\overline{D}}$	$E_{\overline{D}}$
HERA DIS	1342.2	1344.0	1342.7*	1404.1	1390.3*	1337.7*	1340.0	1342.0	1341.3*	1342.1*	1342.2	1342.0*
HERA DIS + $t\bar{t}$	1368.9	1373.4	1373.0	1432.5	1433.2	1358.1*	1367.5	1368.5	1368.3	1368.7	1368.9	1368.5

* minima with an error matrix which is not positive-definite as reported by HESSE

- additional gluon parameyter (E_g) required by new $t\bar{t}$ data
- PDF parametrisation uncertainties given by $A'_g = 0$ (13p) and $E_g = 0$ (14p), and $Q_0^2 = 1.9 \pm 0.3$ GeV^2 variation

PDFs uncertainties

PDFs (α_s in HERA-only fit set to $\alpha_s = 0.1137 \pm 0.0017$):

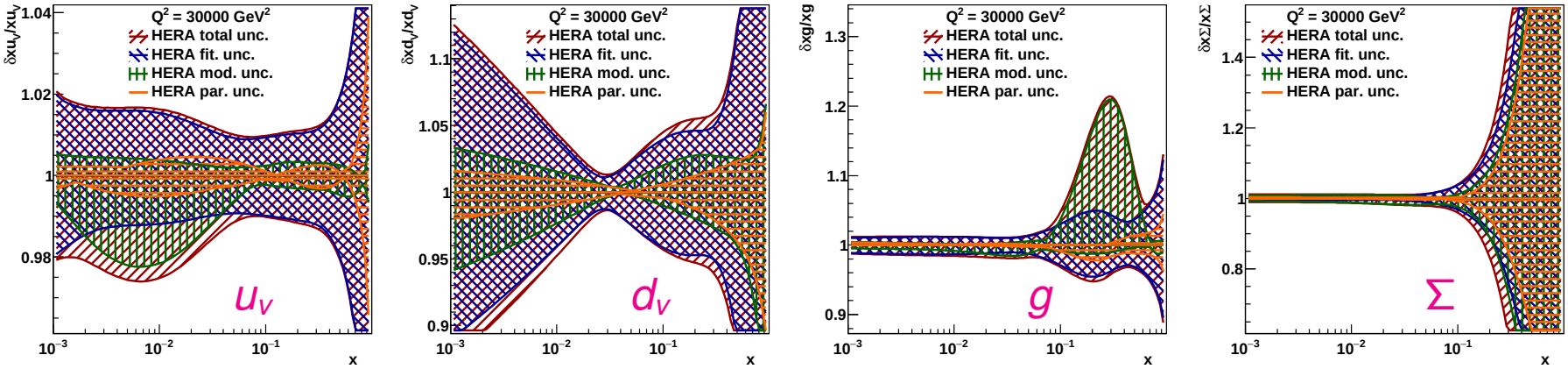

Relative PDF uncertainties (α_s in HERA-only fit set to $\alpha_s = 0.1137 \pm 0.0017$):

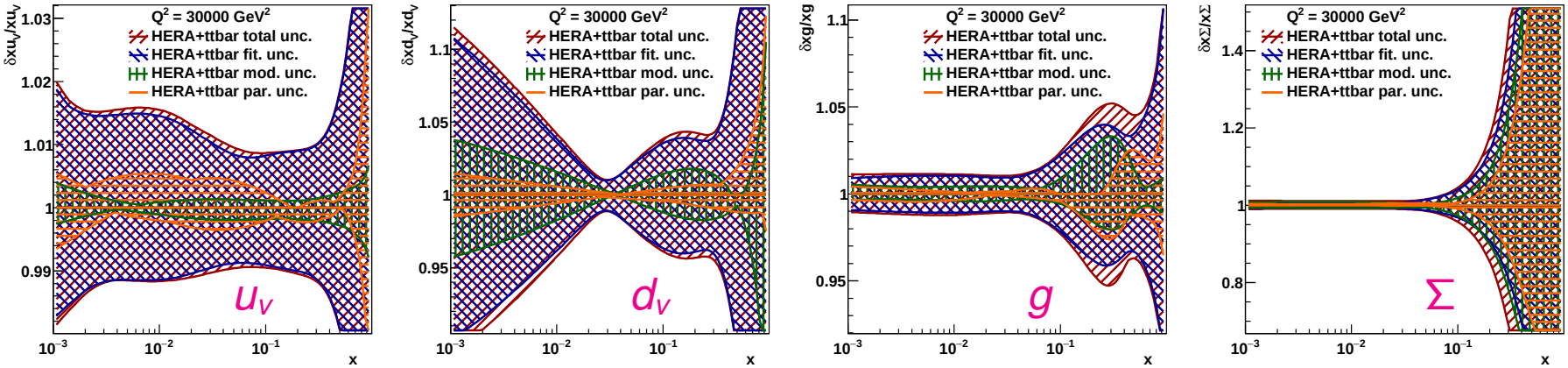

Impact on PDF fit uncertainties

Relative PDF fit uncertainties (α_s in HERA-only fit set to $\alpha_s = 0.1137 \pm 0.0017$):

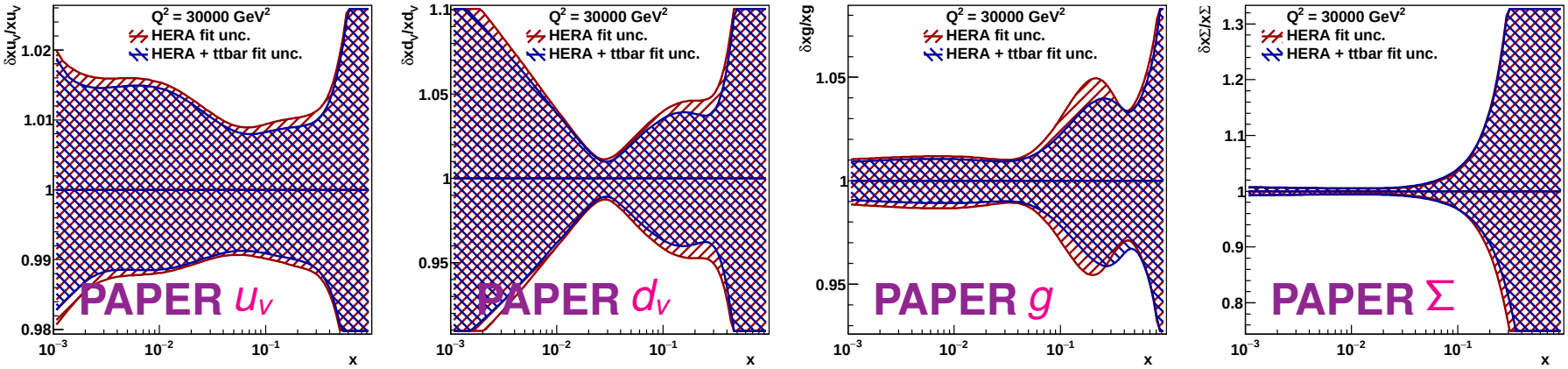

MC replica method vs HESSE

PDFs with fit uncertainties (free α_s in both HERA-only and HERA+$t\bar{t}$ fits):

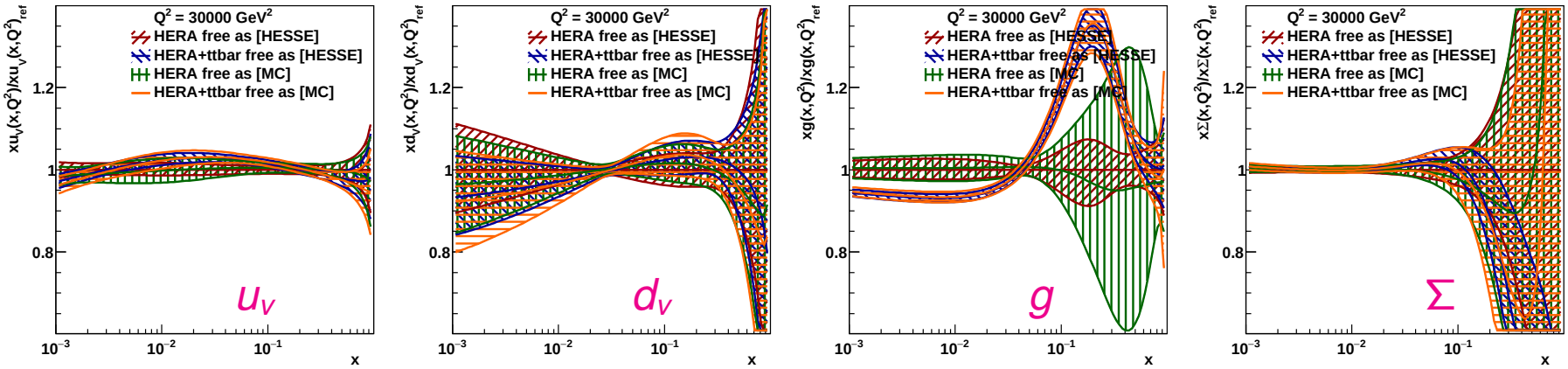

Relative PDF fit uncertainties (free α_s in both HERA-only and HERA+$t\bar{t}$ fits):

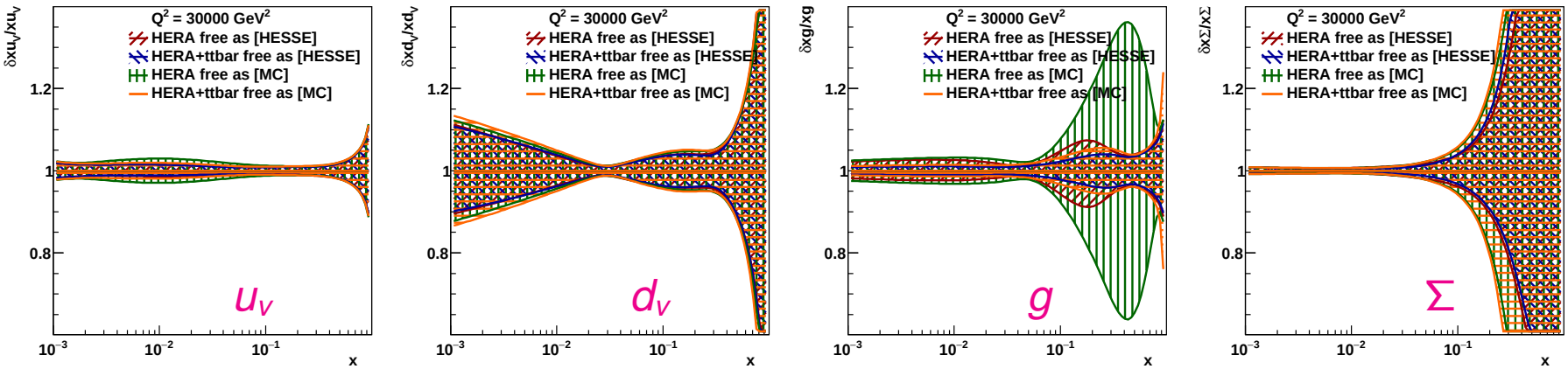

Simultaneous PDF+α_s +m_t fit correlation matrix

PARAMETER CORRELATION COEFFICIENTS

NO.	GLOBAL	2	3	5	7	8	12	13	14	22	23	33	34	41	42	43	101
2	0.99912	1.000	0.428	0.255	-0.807	-0.527	-0.034	-0.145	0.054	-0.055	-0.103	-0.128	-0.010	-0.148	-0.189	-0.128	0.225
3	0.99918	0.428	1.000	0.889	-0.157	-0.001	-0.030	0.151	0.038	-0.078	-0.062	0.219	0.307	-0.205	-0.192	-0.204	-0.179
5	0.99841	0.255	0.889	1.000	-0.048	0.046	-0.006	0.120	0.027	0.054	0.047	0.270	0.201	-0.094	-0.095	-0.023	-0.048
7	0.99948	-0.807	-0.157	-0.048	1.000	0.915	0.021	-0.040	-0.018	-0.013	-0.024	-0.065	-0.028	-0.062	-0.077	-0.029	0.076
8	0.99790	-0.527	-0.001	0.046	0.915	1.000	0.008	-0.126	0.001	-0.037	-0.073	-0.194	-0.123	-0.059	-0.099	-0.058	0.185
12	0.99960	-0.034	-0.030	-0.006	0.021	0.008	1.000	0.485	-0.987	0.074	0.085	-0.339	-0.544	0.160	0.093	0.038	0.054
13	0.96558	-0.145	0.151	0.120	-0.040	-0.126	0.485	1.000	-0.450	-0.029	0.022	0.240	-0.051	0.245	0.276	0.117	-0.486
14	0.99957	0.054	0.038	0.027	-0.018	0.001	-0.987	-0.450	1.000	-0.058	-0.084	0.385	0.587	-0.184	-0.132	-0.043	0.031
22	0.99258	-0.055	-0.078	0.054	-0.013	-0.037	0.074	-0.029	-0.058	1.000	0.927	0.065	0.087	0.161	0.143	0.678	-0.039
23	0.98586	-0.103	-0.062	0.047	-0.024	-0.073	0.085	0.022	-0.084	0.927	1.000	0.151	0.089	0.194	0.199	0.584	-0.197
33	0.98840	-0.128	0.219	0.270	-0.065	-0.194	-0.339	0.240	0.385	0.065	0.151	1.000	0.710	-0.106	-0.012	-0.247	-0.193
34	0.99294	-0.010	0.307	0.201	-0.028	-0.123	-0.544	-0.051	0.587	0.087	0.089	0.710	1.000	-0.570	-0.471	-0.202	-0.106
41	0.98786	-0.148	-0.205	-0.094	-0.062	-0.059	0.160	0.245	-0.184	0.161	0.194	-0.106	-0.570	1.000	0.966	0.430	-0.334
42	0.98730	-0.189	-0.192	-0.095	-0.077	-0.099	0.093	0.276	-0.132	0.143	0.199	-0.012	-0.471	0.966	1.000	0.423	-0.456
43	0.99414	-0.128	-0.204	-0.023	-0.029	-0.058	0.038	0.117	-0.043	0.678	0.584	-0.247	-0.202	0.430	0.423	1.000	-0.285
101	0.99734	0.225	-0.179	-0.048	0.076	0.185	0.054	-0.486	0.031	-0.039	-0.197	-0.193	-0.106	-0.334	-0.456	-0.285	1.000
102	0.33372	0.061	-0.025	-0.026	0.010	0.023	0.026	-0.120	0.002	-0.075	-0.114	0.006	0.037	-0.126	-0.156	-0.196	0.289
		1.000															

PARAMETER DEFINITIONS:

NO.	NAME	VALUE	STEP SIZE	LIMITS
2	'Bg'	0.23513E-01	0.76033E-01	no limits
3	'Cg'	11.596	1.6156	no limits
5	'Eg'	16.635	11.488	no limits
7	'Aprig'	0.14341	0.23367	no limits
8	'Bprig'	-0.34025	0.12610	no limits
9	'Cprig'	25.000	constant	
12	'Buv'	0.42937	0.72265E-01	no limits
13	'Cuv'	4.0973	0.62384E-01	no limits
14	'Duv'	17.363	7.0458	no limits
15	'Euv'	0.0000	constant	
22	'Bdv'	1.0211	0.91748E-01	no limits
23	'Cdv'	4.8639	0.40719	no limits
33	'CUbar'	15.641	0.72284	no limits
34	'DUbar'	41.022	4.6933	no limits
41	'ADbar'	0.16695	0.97660E-02	no limits
42	'BDbar'	-0.17258	0.72850E-02	no limits
43	'CDbar'	7.5390	2.3609	no limits

PARAMETER DEFINITIONS:

NO.	NAME	VALUE	STEP SIZE	LIMITS
101	'alphas'	0.11354	0.10000E-03	no limits
102	'mtFit'	170.51	0.10000	no limits

- weak correlation between m_t (102) and g parameters (2, 3, 5, 7, 8)
- (weaker than between α_s (101) and g parameters, or m_t and α_s)

MC replica method vs HESSE

Parameter	HERA [HESSE]	HERA+ttbar [HESSE]	HERA [MC]	HERA+ttbar [MC]
'Bg'	-0.119 ± 0.058	0.021 ± 0.047	-0.066 ± 0.072	0.011 ± 0.045
'Cg'	14.9 ± 1.3	11.4 ± 1.2	13.1 ± 2.3	11.2 ± 1.5
'Eg'	-1.9 ± 7.1	15.0 ± 6.2	1 ± 15	14.6 ± 3.7
'Aprig'	2.30 ± 0.73	0.148 ± 0.056	0.81 ± 0.90	0.151 ± 0.051
'Bprig'	-0.216 ± 0.048	-0.341 ± 0.046	-0.24 ± 0.13	-0.347 ± 0.045
'Buv'	0.390 ± 0.025	0.430 ± 0.028	0.405 ± 0.044	0.434 ± 0.044
'Cuv'	4.205 ± 0.066	4.093 ± 0.059	4.229 ± 0.068	4.111 ± 0.067
'Duv'	17.9 ± 2.5	17.3 ± 2.5	18.0 ± 4.6	17.9 ± 4.6
'Bdv'	0.915 ± 0.072	1.013 ± 0.078	0.963 ± 0.088	1.028 ± 0.093
'Cdv'	4.84 ± 0.35	4.81 ± 0.36	5.03 ± 0.40	4.93 ± 0.40
'CUbar'	15.44 ± 0.69	15.63 ± 0.64	15.5 ± 1.0	15.81 ± 0.74
'DUbar'	48.3 ± 5.6	41.1 ± 4.0	46.3 ± 6.9	41.6 ± 5.1
'ADbar'	0.1648 ± 0.0099	0.1666 ± 0.0093	0.170 ± 0.013	0.170 ± 0.011
'BDbar'	-0.1701 ± 0.0074	-0.1729 ± 0.0070	-0.1680 ± 0.0092	-0.1712 ± 0.0083
'CDbar'	6.0 ± 1.1	7.3 ± 1.4	6.9 ± 1.7	8.4 ± 3.0
'alphas'	0.1053 ± 0.0027	0.1137 ± 0.0017	0.1059 ± 0.0037	0.1137 ± 0.0024
'mtFit'	n/a	170.07 ± 0.69	n/a	170.14 ± 0.91
Fit status	converged	converged	MC-replica	MC-replica
Uncertainties	iterate	iterate	mean$\pm$rms	mean$\pm$rms

- When using MC replica method, data points are fluctuated according to their unc., and data uncertainties are increased by factor $\sqrt{2}$ (important for HERA unc. treated multiplicative)
- Consistent results obtained using HESSE and MC methods